

APPENDIX C: GROUNDWATER MODELLING

1. The Groundwater Model

1.1 Background

A MODFLOW-based groundwater model was used for the original Environmental Impact Statement (EIS) (HLA Envirosiences, 2001), whereas MODFLOW-SURFACT model was employed for the Pikes Gully (PG) Longwall/Miniwall (LW/MW) 5 to 9 SMP investigations (Aquaterra, 2008). The use of MODFLOW-SURFACT allows a better simulation of groundwater-surface water interaction and transitions between saturated and unsaturated flow. The current groundwater model (the Model) was derived from the initial HLA Envirosiences model, but includes a number of significant improvements. It allowed for a more realistic representation of the cracking and hydraulic conductivity increases, which occur above longwall panels. The Model incorporates more layers, unsaturated flow conditions and variable hydraulic parameters over time.

One of the key differences between the current Model and the model used in the 2001 EIS assessment is that pre-mining groundwater heads within the various strata are more realistically represented. In particular, the Model better represents the general upwards pressure gradient that is known to have existed within the Permian across the study area prior to the commencement of ACP mining. This was not fully represented within the 2001 modelling.

More recently, the Model was further improved to assess the potential impacts from a revised mining plan and the diversion of Bowmans Creek (Aquaterra, 2009c). It includes realistic representations of other mines in the area, in particular the Ravensworth Underground Mine (RUM), the Narama Mine, and the Ashton Coal Project (ACP) North East Open Cut (NEOC) and proposed South East Open Cut (SEOC). In doing so, the upgraded Model takes into account the potential cumulative impacts of these mines in the area.

With further minor modifications, the Model has been used as the basis for the groundwater modelling component of this Upper Liddell (ULD) Seam Extraction Plan Groundwater Impact Assessment.

1.2 Modelling Software

A three-dimensional finite difference model has been used, based on the MODFLOW code (McDonald and Harbaugh, 1988) in conjunction with SURFACT (Version 3). Model simulations involved the variably-saturated flow conditions using the van Genuchten function as an unsaturated flow modelling option provided by the MODFLOW-SURFACT BCF4 package. This is the most significant modification to the model used for the Bowmans Creek Diversion project where the pseudo soil function in SURFACT was used. This most recent change was made as the van Genuchten function (for simulation of unsaturated flow) more accurately simulates the recharge processes and flow through the unsaturated zone. It also allows for the presentation of the vertical distribution of pressure heads (as sections), which are increasingly being required by the regulators (NSW Office of Water (NoW)) and their third party technical reviewers.

The modelling has been undertaken running under the Groundwater Vistas (Version 5.16) graphical user interface.

The Model was set up to simulate groundwater conditions over a 132km² area. Due to the strong influence of other mining activities in the area, the model has explicitly included other operations as described in **Section 1.1** above.

1.3 Conceptual Model Design

The conceptual site model (CSM) is a simplified representation of the real system, identifying the most important geological units and hydrogeological processes, while acknowledging that the real system is hydrologically and geologically more complex. The CSM forms the basis for the computational groundwater flow model. The key features of the CSM used for this assessment are described below, with its domain illustrated in **Figures C1** and **C2**.

Geology and Hydrogeology

The local geology has been represented by 15 model layers. These are largely defined by the main coal seams and the interburden intervals. The top layer (Layer 1) represents the weathered regolith and the areas of river/creek alluvium. The overburden above the PG Seam has been divided into six layers to allow for hydrogeological representation of the overlying Lemington Seams, Bayswater Seams and associated interburden/overburden units, and the impact of longwall mining on the whole overburden sequence. A typical Model cross section (representing the line A-A' on **Figure C1**) is shown in **Figure C2**. A summary description of the model layers is as follows:

- Layer 1: Bowmans Creek, Glennies Creek and Hunter River alluvium, colluvium, weathered Permian overburden (regolith) and Ravensworth spoil (backfill in the old Ravensworth Mine open cut).
- Layers 2, 3, 4, 5, 6 and 7: PG Seam overburden – this has been split into a number of layers to allow the simulation of fracturing to be assigned progressively to different heights above the coal seam during mining impact assessment. These layers include the full range of coal measures lithologies, including Lemington coal seams (1 to 19), and in the far western part of the area, the Bayswater 1 and 2 seams.
- Layer 8: Pikes Gully Seam.
- Layer 9: Pikes Gully – Upper Liddell interburden.
- Layer 10: Upper Liddell Seam.
- Layer 11: Upper Liddell – Upper Lower Liddell interburden.
- Layer 12: Upper Lower Liddell Seam.
- Layer 13: Upper Lower Liddell – Lower Barrett interburden.
- Layer 14: Lower Barrett Seam.
- Layer 15: Basal layer – coal measures below Lower Barrett.

The Model geometry is largely defined by our understanding of the physical features. The boundaries of river alluvium have been defined using the findings of previous studies and investigations for nearby projects (including site visits, aerial reconnaissance, core samples and geochemistry) and layer thicknesses are set up in accordance with drilling results. The deeper layers (Layer 8 downwards) have been defined according to the Ashton Coal Operations Pty Limited (ACOL) coal resource models, with thicknesses described in **Table C1**. For the overburden, thicknesses have been defined to allow for different 'zones' of hydraulic impacts caused by longwall subsidence.

The hydraulic conductivity and storage of the Model layers have been assigned in accordance with hydraulic testing results. Layer thicknesses and the final calibrated values of horizontal and vertical hydraulic conductivity and storage that have been used within the Model are shown in **Table C1**.

Table C1 Layer Thicknesses and Hydraulic Parameters*

Layer	Geological Unit	Thickness (m)	In Situ Kh (m/d)	In Situ Kv (m/d)	Confined Storage (Ss)	Unconfined Storage (Sy)
1	Bowmans Creek Alluvium	Variable, based on drilling results	0.5	5×10^{-6}	5×10^{-4}	0.05
	Regolith (weathered Permian)	10 (Nominal thickness)	0.1	5×10^{-6}	5×10^{-4}	0.001
	Glennies Creek Alluvium	Variable, based on drilling results	Variable, see Appendix E	5×10^{-6}	5×10^{-4}	0.05
	Hunter River Alluvium	Variable, based on 15m maximum depth and valley geometry	45	5×10^{-6}	5×10^{-4}	0.05
	Ravensworth spoil	Based on Bayswater Seam floor levels	0.02	5×10^{-6}	5×10^{-4}	0.001
2	PG overburden	Residual thickness between L1 and L3 (thickness variable due to dip on strata)	0.005	5×10^{-5}	3×10^{-4}	0.001
3	PG overburden	20	0.005	5×10^{-5}	3×10^{-4}	0.001
4	PG overburden	30	0.005	5×10^{-5}	3×10^{-4}	0.001
5	PG overburden	30	0.005	5×10^{-5}	3×10^{-4}	0.001
6	PG overburden	40	0.005	5×10^{-5}	3×10^{-4}	0.001
7	PG overburden	30	0.005	5×10^{-5}	3×10^{-4}	0.001
8	PG Seam	2	0.08	8×10^{-4}	3×10^{-4}	0.001
9	PG – ULD interburden	35 – 40	0.001	1×10^{-5}	3×10^{-4}	0.001
10	ULD Seam	2	0.02	2×10^{-4}	3×10^{-4}	0.001
11	ULD-ULLD interburden	30	0.001	1×10^{-5}	3×10^{-4}	0.001
12	ULLD Seam	2	0.02	2×10^{-4}	3×10^{-4}	0.001
13	ULLD – Lower Barrett interburden	40	0.001	1×10^{-5}	3×10^{-4}	0.001
14	Lower Barrett Seam	2	0.02	2×10^{-4}	3×10^{-4}	0.001

* These values represent general rock mass properties. Some other values are contained within the Model to represent specific features. These are described where appropriate, in the text within this Appendix.

1.4 Groundwater Flow Pattern

The observed groundwater heads prior to underground mining at the ACP or RUM have been used to calibrate the steady state Model and ensure that the regional flow pattern is well represented. In particular, care has been taken to ensure that the Model reflects the current understanding of the hydrogeological environment, recharge/discharge behaviour and regional flow patterns. The groundwater elevations in the deeper Permian layers are controlled by the heights of the elevated recharge zones. This results in an upward gradient from deeper to shallower layers and artesian conditions in some parts of the Bowmans Creek valley. Modelled groundwater heads in the alluvium/regolith (Model Layer 1) and the PG Seam (Model Layer 8) prior to underground mining by ACOL are shown in **Figure C3**.

Flow within valley alluvium is largely dominated by local recharge through rainfall infiltration and connectivity with the creeks and rivers, which allows baseflow to occur as the primary discharge mechanism. The amount of baseflow contribution to the watercourses varies according to recharge quantity and the hydraulic conductivity of the

alluvium, and is small in magnitude throughout the ACP area. Flow within the alluvium is generally along the valleys and convergent towards the watercourses.

The deeper regional flow pattern around the ACP on the western side of the Camberwell anticline is generally towards the southwest. This has been well represented through the set up of recharge areas, watercourses and boundary conditions contained within the Model, including the presence of the Ravensworth open cut mine. Because the target seams subcrop within the western limb of the anticline, the hydrogeology of the Model area to the east of the anticline has almost no influence area around the Mine.

1.5 Surface Drainage and River Baseflow

Glennies Creek, Bowmans Creek and the Hunter River are represented in the Model using the river cell package to allow for stream-aquifer interaction. Creek bed / riverbed elevations have been based on both topography and their water levels at monitoring points to represent creek/river stage heights in the absence of any recorded field data. Where river/creek stage elevations have been available, these have been checked against the stages contained in the model. The creek bed elevation has been assumed to be 1m below the stage elevation.

The effect of watercourse bed sediments and geometry upon the hydraulic interaction between the creek/river and their alluvial aquifers is controlled by the streambed conductance parameter. This has been set to 25m²/d for smaller cells in Glennies Creek and Bowmans Creek, to up to 100m²/d for the bed of the Hunter River.

Baseflow contribution to river and creek features represents one of the primary natural groundwater discharge processes for the alluvium (the other main discharge process applicable to this area is evapotranspiration). When groundwater levels within the alluvium are higher than the stage elevations, the river/creek 'gains' water as dictated by the relative levels and the streambed conductance. When groundwater levels are lower than the river/creek stage they may lose water by seepage to adjacent or underlying aquifers, again in accordance with the relative levels and bed conductance. The river/creek is then considered to be 'losing' water to form groundwater recharge in those areas. The ACP Model for the underground mine is designed to allow both processes (i.e. 'gaining' baseflow discharge and 'losing' groundwater recharge) to occur.

Where ephemeral streams are present within the area, these have been represented within the Model as drain cells. These simply drain water from the Model once groundwater levels are higher than the drain bed level.

Because the PG Seam is known to outcrop within or alongside the channel of Glennies Creek, east of the underground mine, a specific modelling approach has been used to represent this connection. A very high value of horizontal and vertical hydraulic conductivity (10m/d) has been used in the alluvium, which ensures connection between the PG Seam and the Glennies Creek alluvium. A zone of enhanced horizontal hydraulic conductivity was identified in this area during test pumping, probably a result of in-situ stress relief that is caused by the shallow cover depth.

1.6 Recharge

The demarcation of recharge zones applied to the Model is shown in **Figure C4**.

Recharge input to the Model primarily follows that incorporated in the previous modelling work (HLA Envirosciences, 2001; Aquaterra, 2008); albeit with some modifications made to improve steady state calibration and model stability. Recharge is modelled so it is applied to the highest active layer. Overall recharge rates have been maintained at an average of 0.17% of annual rainfall, as detailed within the EIS (HLA Envirosciences, 2001). For areas where the Hunter River and Bowmans Creek alluvium is present,

recharge to the water table is set to 0.8% of the average annual rainfall, while a recharge rate of 0.6% is applied in areas where the Glennies Creek alluvium and the Ravensworth open cut pit backfill is present. These values are based around a 'standard' 0.5% to 1% of annual rainfall recharge for alluvium in this area and have been modified to local conditions as part of the model calibration process.

Outside of the alluvium and backfill areas, the recharge rate is set to 0.2% of average annual rainfall, except where the basal model layers subcrop along the axis of the Camberwell syncline, where the rate has been halved due to the highly impermeable nature of the strata. Because of the monitoring evidence that indicates that recharge to the coal seams occurs in subcrop areas, a higher recharge rate of 0.4% of annual rainfall has been applied to the area of subcrop for the Lemington Seams in the hillside above the proposed mine workings. As this is a subcrop area, localised increases in vertical hydraulic conductivity have also been applied in overlying 'dummy' layers to ensure that recharged water is able to enter the relevant subcropping coal seams.

Evaporation is simulated using the Evapotranspiration (EVT) package of MODFLOW. The EVT parameter values adopted are a constant rate of 250mm/yr with an extinction depth of 1.5m, which allows evapotranspiration to be active in areas of low topography and a shallow water table. This generally occurs along surface watercourses such as Bowmans Creek, Glennies Creek and the Hunter River floodplain.

1.7 Model Domain and Boundary Conditions

The domain and boundaries of the Model are indicated in **Figure C1**. Layer 1 groundwater levels are largely controlled by recharge (from rainfall) and discharge (to the creeks and river). For the remaining layers groundwater levels are controlled by lateral and downward leakage and the Model boundary conditions. The Model predominately has 'no flow' boundaries to represent the general lack of movement in the deep Permian strata. However, the presence of other mines and regional dewatering can influence these deeper groundwater conditions. It is therefore important to adequately represent the presence of other mines in the area. Based on currently available information and steady state calibration, the following Mine related boundaries were represented using General Head Boundaries (GHBs) within the Model during the steady state, pre-ACP underground mining:

- Ravensworth No. 2 Pit and Ravensworth South Mine have been substantially backfilled with overburden. The GHB associated with the Ravensworth No.2 pit was set at the water level (+35mAHD) monitored in the spoil of that area in 2008. The final void of the Ravensworth South Mine is believed to act as an evaporative discharge for groundwater, so the general head boundary in the Model was set to 30mAHD in this area.
- The Narama Mine, south of the former Ravensworth pits, is still in operation and is being mined as a north-south strip advancing from the west towards the east. The GHBs in this area were set at the level of the Bayswater Seam.
- Towards the southwest, the Model extends as far as Hunter Valley Operations (HVO). The mining complex at HVO has grown through a process of expansion and acquisitions since 1979. The Lemington Pit marks the boundary of the groundwater model and GHB levels were set largely on the basis of iterations during the steady-state calibration.
- Other pits such as the Camberwell and Glennies Creek mines were included in the Model. These are situated on the eastern side of the Camberwell anticline so have less influence on groundwater levels in the ACP underground area.

1.8 Specific Model Simulation Approaches

A number of physical hydrogeological effects that are expected to occur as a result of the proposed longwall mining project have been represented using specific modelling approaches, including:

- Simulation of aquifer dewatering caused by both open cut and underground mining activities;
- Changes to the hydraulic properties of overburden strata caused by the caving and subsidence above longwall panels; and
- Further changes to strata previously affected by PG Seam extraction, due to the cumulative effects of two seams of longwall extraction.

1.9 Simulation of Underground Mine Voids

Underground mining and dewatering activity is represented in the Model using drain cells within the mined coal seams, with modelled drain elevations set to 0.1m above the base of the relevant coal seam layers. These drain cells were applied wherever workings occur and were progressed in accordance to the ACP and Ravensworth mine plans as detailed in **Table C3**. In addition to the drains, the hydraulic conductivity of the remnant roadways/cut-throughs and goaf material left within the coal seams was increased to a high value (50m/d).

In order to simulate the active dewatering that will occur in the Mine, all drain cells remained active in the Model until the scheduled completion of mining.

1.10 Simulation of Overburden Hydraulic Conductivity during Mining

The PG Seam overburden has been subdivided into six layers to allow subsidence caving and fracturing effects to be simulated to various heights above the Seam, so that the impact of progressive caving and fracturing associated with the mining of the four seams could be adequately represented.

The impact of multi-seam mining on the hydraulic conductivity of caved overburden has been based on the experience of monitoring and groundwater modelling gained at the ACP site to date. This is combined with the most recent research available for subsidence impacts on aquifer materials. The SCT 'Aquifer Inflow Prediction above Longwall Panels' report to the Australian Coal Association Research Programme (ACARP) (SCT, 2008) includes assessments of the impact of longwall caving on overlying rock mass hydraulic conductivity, based on the depth of overburden above the longwall seam and the degree of subsidence associated with the longwall panel. This includes more general assessments based on worldwide empirical experience; and some site specific computer modelling of hydraulic conductivity impacts at the ACP underground mine.

For the PG Seam extraction, the modelling in the ACARP report (SCT, 2008) and the transient calibration for this study, indicated that three 'zones' of subsidence hydraulic conductivity should develop above the PG coal seam:

- A high hydraulic conductivity, which is in a caved zone that extends 60 to 70m above the Seam (represented by Layers 6 and 7 in the Model). This is where there is direct connectivity with the mine goaf and vertical hydraulic conductivity has been increased to 5m/d. Because of the 'blocky' nature of the caving and the fact that a large degree of bed separation occurs, the horizontal hydraulic conductivity is assessed to be higher than this (50m/d).
- A zone of 'tortuous cracking' that extends for a further 60 to 80m above the cave zone. Within this zone the enhanced hydraulic conductivity occurs due to discrete

vertical fractures that connect with horizontal layer separation features, allowing water to travel between and along layer boundaries. The 'tortuous' flow paths that are created along bed layers and down fractures result in a zone where the overall hydraulic conductivity is lower than the caved zone below. The SCT modelling indicates that the degree of connective horizontal and vertical fracturing should be similar within this zone; therefore a value of 0.05m/d has been assigned to both the horizontal and vertical hydraulic conductivity. This has been set based on the SCT analysis, which suggests that the in-situ vertical hydraulic conductivity will increase by three orders of magnitude following subsidence.

- A 'barrier' zone above this, with no change to the in-situ hydraulic conductivity.

For the ULD Seam extraction, hydraulic conductivity values from the SCT report have been used as a guideline, although experience has shown that these tend to over-estimate impacts. For the mining of the ULD Seam with a maximum predicted surface subsidence of around 3m, the SCT approach suggests that a vertical conductivity between 100 and 1000m/d should be used assuming cumulative disturbance from the mining of both seams. However, this only considers fracturing in the rock mass and does not allow for any infilling due to slaking of clays, mobilisation of fines, or variable plasticity leading to localised closing of fractures. These factors are believed to result in an over-prediction of hydraulic conductivity within the subsidence fracture system. Results of monitoring, as described in the End of Longwall Panel Reports (Aquaterra, 2009b) have shown that a 'self healing' of fractures and a reduction in mine inflow rates certainly occurs after the initial longwall stresses, and is not accounted for in the SCT modelling. A vertical hydraulic conductivity of 5m/d has been assumed for the 'tortuous' and 'barrier' zones (i.e. two orders of magnitude increase), and 50m/d has been assumed for the caved zone above the PG and ULD seams.

It should be noted that the Model is not highly sensitive to the assumed value of vertical hydraulic conductivity within the caved overburden once the PG Seam has been mined.

Based on the above, a summary of the adopted horizontal and vertical hydraulic conductivity of the rock mass above the longwall panels following secondary extraction is shown in **Table C2**.

Table C2: Hydraulic Parameters for Caved Overburden during Mining

Layer	Aquifer	Initial hydraulic conductivity values		Hydraulic Conductivity following PG mining		Hydraulic Conductivity following ULD mining	
		Kh (m/d)	Kv (m/d)	Kh (m/d)	Kv (m/d)	Kh (m/d)	Kv (m/d)
2	Pikes Gully Seam Overburden	5.00E-03	5.00E-05	no change	no change	5.00E+00	5.00E+00
3	PG Seam Overburden	5.00E-03	5.00E-05	5.00E-02	5.00E-02	5.00E+00	5.00E+00
4	PG Seam Overburden	5.00E-03	5.00E-05	5.00E-02	5.00E-02	5.00E+00	5.00E+00
5	PG Seam Overburden	5.00E-03	5.00E-05	5.00E-02	5.00E-02	5.00E+00	5.00E+00
6	PG Seam Overburden	5.00E-03	5.00E-05	5.00E+01	5.00E+00	5.00E+01	5.00E+01
7	PG Seam Overburden	5.00E-03	5.00E-05	5.00E+01	5.00E+00	5.00E+01	5.00E+01
8	PG Seam	8.00E-02	8.00E-04	5.00E+01	5.00E+01	5.00E+01	5.00E+01
9	PG - ULD Interburden	1.00E-03	1.00E-05			5.00E+01	5.00E+01
10	ULD Seam	2.00E-02	2.00E-04			5.00E+01	5.00E+01

In addition to the modelling of the subsidence zone itself, it is necessary to include an adjustment to the horizontal hydraulic conductivity that results around the periphery of the subsidence zone. As subsidence of the horizontal strata causes a dislocation of the predominantly horizontal flow paths at the edges of longwall panels, horizontal hydraulic continuity is reduced around the perimeter of the longwall extraction areas. This has been accounted for in the Model by a reduction in horizontal hydraulic conductivity (K_h) in the strata above the chain pillars and of the longwall panels (by an order of magnitude).

1.11 Simulation of Mine Plan

The ULD LW1 to 8 mine plan is offset by 60m to the west of the overlying PG mine plan.

During simulated mining of the PG Seam, chain pillars were maintained, and the in-situ hydraulic conductivity parameters in the chain pillars modified to simulate added stresses predicted to occur in layers above the mined PG coal seam within active coal mining areas. That is, the in-situ vertical hydraulic conductivities were maintained, whereas horizontal hydraulic conductivities were reduced by an order of magnitude to reflect the influence of added effective stress considered to occur in the stacked chain pillars.

With the initiation of the ULD Seam panel extraction, chain pillars in the PG (Layer 8) and above will be destroyed, leaving effective chain pillars only in the PG-ULD interburden and ULD Seam (Model Layer 9 and 10). However, external barriers effectively remain, so reduced horizontal hydraulic conductivities are maintained around the Mine perimeter.

1.12 Simulation of Open Cut Mines

For open cut mines, including the NEOC and proposed SEOC, the active area of operation was represented using drain cells within all model layers representing the open pits. This effectively removes groundwater from the active parts of the open cut mines. Where appropriate, and in accordance with the mine plans, areas of backfill were then simulated by switching off the drain cells and adjusting the hydraulic properties to representative backfill properties, as follows:

- Horizontal hydraulic conductivity was set to 1m/d.
- Vertical hydraulic conductivity was set to 0.1m/d.
- Recharge was set to 6.125×10^{-5} m/d which amounts to 0.3% of average annual rainfall.

1.13 Time Scale Selection

The need to change aquifer parameters with time to simulate the progressive advance of mining required a series of consecutive 'time slice' models, with hydraulic properties changed from one time slice to the next. For the transient calibration period, time slices of varying duration were used in order to match the progress of the completion of longwall panels as far as was possible. For predictive modelling, time slices were progressed as annual increments. The output heads from each time-slice model were used as starting heads for the next successive time-slice. Hydraulic conductivities were changed to reflect subsided strata above the extraction area for that time slice. This process was repeated until the entire mine plan had been simulated.

Table C3 outlines the Model time slice and stress period set-up for the transient calibration and prediction model runs. A stress period is the timeframe in the Model when all hydrological stresses (e.g. recharge) remain constant. Multiple stress periods have been used within the calibration time slices to ensure a more refined progression of the mine headings and longwalls within the Mine in order to achieve better calibrations to observed data. This has been designed to be entirely consistent with the mine plan.

Table C3: Model Stress Period Setup

Period	Time Slice	Stress Period	Length (days)	From	To	ACP Underground Mine		Ravensworth UG Mine		SEOC	NEOC	Subsidence Impacts	
						Development Heading	Longwall Panels	Development Heading	Longwall Panels			Ground Level	Recharge
Transient Calibration (History Match)	Time Slice 1	1	91.25	1/01/2004	31/03/2004	n/a	n/a	n/a	n/a	n/a	n/a	n/a	n/a
		2	91.25	1/04/2004	30/06/2004								
		3	91.25	1/07/2004	30/09/2004								
		4	91.25	1/10/2004	31/12/2004								
		5	91.25	1/01/2005	31/03/2005								
		6	91.25	1/04/2005	30/06/2005								
		7	91.25	1/07/2005	30/09/2005								
		8	91.25	1/10/2005	31/12/2005								
		9	91.25	1/01/2006	31/03/2006								
		10	91.25	1/04/2006	30/06/2006								
	Time Slice 2	11	91.25	1/07/2006	30/09/2006	LW1	LW1	LW3-4	LW5	n/a	n/a	n/a	n/a (Pikes Gully not significant to modelling)
		12	91.25	1/10/2006	31/12/2006								
		13	91.25	1/01/2007	31/03/2007								
		14	91.25	1/04/2007	30/06/2007								
		15	91.25	1/07/2007	30/09/2007								
		16	91.25	1/10/2007	31/12/2007								
		17	91.25	1/01/2008	31/03/2008								
	Time Slice 3	18	60	1/04/2008	31/05/2008	LW2	LW2	LW5	LW3	n/a	n/a	n/a	n/a
		19	60	1/06/2008	31/07/2008								
	Time Slice 4	20	60	1/08/2008	30/09/2008	LW4	LW3	LW5	LW4	n/a	n/a	n/a	n/a
		21	60	1/10/2008	30/11/2008								

Period	Time Slice	Stress Period	Length (days)	From	To	ACP Underground Mine		Ravensworth UG Mine		SEOC	NEOC	Subsidence Impacts		
						Development Heading	Longwall Panels	Development Heading	Longwall Panels			Ground Level	Recharge	
Predictive Modelling	Time Slice 5	22	61	1/12/2008	31/01/2009			LW6	LW5					
		23	58	1/02/2009	31/03/2009				LW5					
	Time Slice 6	24	274	1/04/2009	31/12/2009	LW5 & LW6	LW4	LW7	LW5		Mine Yr 6			
	Time Slice 7	25	365	1/01/2010	31/12/2010	LW7 & LW8	LW5 & LW6	LW8	LW6 & 7	Mine Yr 1	Mine Yr 7			
	Time Slice 8	26	365	1/01/2011	31/12/2011	ULD LW1&2	LW7 & LW8	LW9 & 10	LW8	Mine Yr 2				
	Time Slice 9	27	91	1/01/2012	31/03/2012	ULD LW3	ULD LW1							
		28	91	1/04/2012	30/06/2012		ULD LW2	LW11 & 12*	LW9 & 10*	Mine Yr 3				
	Time Slice 10	29	92	1/07/2012	30/09/2012	ULD LW4								
		30	92	1/10/2012	31/12/2012			LW13 & 14		Mine Yr 4				
	Time Slice 11	31	90	1/01/2013	31/03/2013	ULD LW5	ULD LW3							
		32	91	1/04/2013	30/06/2013									
	Time Slice 12	33	92	1/07/2013	30/09/2013	ULD LW6a	ULD LW3&4a							
		34	92	1/10/2013	31/12/2013									
	Time Slice 13	35	90	1/01/2014	31/03/2014	ULD LW6b	ULD LW4b						3.8m LW 6a**	None
		36	91	1/04/2014	30/06/2014		ULD LW5	LW15		Mine Yr 5				
Time Slice 14	37	92	1/07/2014	30/09/2014	ULD LW7	ULD LW5&6a								
	38	92	1/10/2014	31/12/2014		ULD LW6a								
Time Slice 15	39	90	1/01/2015	31/03/2015	ULD LW8	ULD LW6b			Mine Yr 6			3.8m LW 6 & 7	2E-3 LW7b, 6E-4 LW7a & LW6b	

2. Model Calibration

Calibration is the process by which the independent variables (parameters and boundary conditions) of a model are adjusted, within realistic limits, to produce the best match between simulated and measured data. The realistic limits on parameter values are constrained by the range of measured values from pumping tests and other hydrogeological investigations.

Model calibration performance is demonstrated in both quantitative (head value matches) and qualitative (pattern-matching) terms, by:

- Contour plans of modelled head, with posted spot heights of measured head.
- Hydrographs of modelled versus observed bore water levels.
- Water balance comparisons.
- Scatter plots of modelled versus measured head, and the associated statistical measure of the scaled root mean square (SRMS) value. It is generally considered that a 10% SRMS value on aquifer water levels is an appropriate target for models of this type, as described in the Australian best practice modelling guidelines (MDBC, 2001).
- Baseflow impacts of modelled versus actual impacts.
- Mine inflow of modelled versus measured inflow.

Steady state calibration was followed by transient or 'history match' calibration to better determine (i.e. confirm) recharge, hydraulic conductivity, storativity and boundary conditions. The transient calibration period extended to the commencement of April 2009, which included both open cut mining and underground mining, up to completion of longwall extraction of LW3 and development headings for LW4.

The final calibrated hydraulic parameters that were used in the base model for this assessment have already been shown in summary in **Table C1**. Final values used for all layers, including specific zones that have been used to describe known, discrete hydrogeological features (such as the PG shear zone, enhanced hydraulic conductivity near Glennies Creek and the vertical hydraulic conductivity of the Permian subcrop area) are provided in **Figures C5 to C14**.

2.1 Steady State Calibration

Steady state calibration was carried out entirely against pre-underground mining records of potentiometric head. Calibration was achieved through changes in recharge, hydraulic conductivity and modifications to boundary conditions.

There are 112 targets contained within the steady-state calibration data set. Many of these (46) were in Layer 1 due to the intensive investigation programs that have been carried out in the alluvium with 66 targets screened within the Permian model layers. Steady state calibration against groundwater targets are shown in **Table C4** as is a summary of steady-state calibration statistics.

Table C4 Steady State Model Calibration Performance

Bore	Easting (MGA)	Northing (MGA)	Model Layer	Observed Head (mAHD)	Modelled Head (mAHD)	Head Difference (m)
Oxbow	318330	6405744	1	56.72	58.7	-2.0
PB1	317556	6405223	1	55.88	55.0	0.8
PB2	318231	6406288	1	60.55	60.2	0.3
RA02	317712	6405233	1	55.38	55.5	-0.1
RA10	317639.7	6404335	1	50.49	52.4	-2.0
RA14	317643.4	6404698	1	52.14	53.9	-1.8
RA15	317420.5	6404748	1	51.55	53.4	-1.9
RA17	317695.5	6404876	1	54.04	54.6	-0.6
RA18	317821.7	6405434	1	56.84	56.6	0.3
RA27	317952.1	6403738	1	50.05	48.7	1.4
RA30	317810.6	6406501	1	61.17	60.3	0.9
RA8	317887.2	6404193	1	50.46	53.1	-2.6
RM03	317668	6404845	1	53.58	54.4	-0.9
RM04	317403	6405316	1	55.73	55.1	0.6
RM06	317872	6405890	1	58.49	57.6	0.9
RM07	318092	6405763	1	58.48	57.8	0.7
RM09	318166	6406380	1	61	60.3	0.7
RM10	317590	6405294	1	55.89	55.3	0.6
T10	317683.6	6404450	1	50.86	53.2	-2.3
T1-A	318337.7	6406309	1	61.13	60.6	0.6
T2-A	317583.3	6405217	1	55.83	55.1	0.7
T3-A	317654.2	6404708	1	51.69	54.0	-2.3
T4-A	317685.8	6404323	1	51.11	52.6	-1.5
T4-P	317682.2	6404319	1	51.68	52.5	-0.9
T5	317946.1	6406549	1	61.71	60.3	1.4
T6	317975.1	6406675	1	62.07	60.8	1.3
T7	317717.4	6406336	1	61.21	59.7	1.5
T8	317707.8	6404630	1	51.51	53.9	-2.3
WML112C	317563.7	6404450	1	51.75	52.7	-0.9
WML113C	317376.8	6404526	1	51.08	51.8	-0.7
WML115C	317888.3	6406710	1	61.82	61.0	0.8
WML120B	319293.6	6404588	1	52.42	51.9	0.5
WML129	319468.4	6403528	1	50.99	50.2	0.8

Bore	Easting (MGA)	Northing (MGA)	Model Layer	Observed Head (mAHD)	Modelled Head (mAHD)	Head Difference (m)
WML145	319459.3	6404180	1	52.76	51.2	1.6
WML146	319420.7	6404178	1	54.36	51.2	3.2
WML154	319532.5	6404580	1	53.99	52.0	1.9
WML166	319469.9	6403825	1	54.01	50.7	3.3
WML175	317179	6404030	1	50.09	49.0	1.1
WML240	319499.9	6404000	1	52.756	51.1	1.7
WML243	319643.3	6403226	1	51.345	50.1	1.3
WML247	319734.4	6404472	1	54.241	52.5	1.8
WML248	319706.1	6403936	1	52.152	51.9	0.3
WML249	319577.4	6404300	1	52.831	51.6	1.2
WML250	319454.6	6404302	1	52.804	51.2	1.6
WML252	319621.5	6403684	1	52.395	50.9	1.5
RM02	317943	6404508	2	51.32	53.8	-2.5
RM05	317487	6406003	2	53.63	56.2	-2.6
T1-P	318356.9	6406304	2	61.41	60.4	1.0
T2-P	317587.1	6405222	2	55.45	53.3	2.1
T3-P	317650.1	6404701	2	51.03	52.5	-1.5
T9	317764.5	6404530	2	51.59	52.9	-1.3
WML110A	318005.3	6404244	2	50.36	53.5	-3.2
WML110B	318006.9	6404247	2	51.31	53.5	-2.2
WML111B	317774.6	6404363	2	51.17	52.4	-1.3
WML112B	317567.4	6404450	2	50.49	51.3	-0.8
WML113-40m	317368.8	6404529	2	49.48	50.5	-1.0
WML113B	317373	6404528	2	50.48	50.5	0.0
WML114B	318148.4	6405238	2	58.76	57.9	0.8
WML115B	317880.7	6406704	2	61.65	61.1	0.6
WML213-48m	317210.2	6404154	2	49.09	49.1	0.0
WML109B	318210.9	6404081	3	57.23	54.0	3.3
WML110-38m	318005.3	6404244	3	52.08	53.4	-1.3
WML110-65m	318005.3	6404244	3	56.14	53.4	2.7
WML111A-24m	317775.7	6404367	3	49.88	52.3	-2.4
WML111A-54m	317775.7	6404367	3	53.87	52.3	1.6
WML112A-101m	317563.7	6404450	3	54.18	51.5	2.6
WML112A-43m	317563.7	6404450	3	55	51.5	3.5
WML112A-72m	317563.7	6404450	3	51.03	51.5	-0.5

Bore	Easting (MGA)	Northing (MGA)	Model Layer	Observed Head (mAHD)	Modelled Head (mAHD)	Head Difference (m)
WML113-65m	317368.8	6404529	3	49.93	50.9	-1.0
WML113-95m	317368.8	6404529	3	54.9	50.9	4.0
WML115A-72m	317873.6	6406708	3	58.91	61.1	-2.2
WML108A	318446.5	6403975	4	60.92	57.5	3.4
WML108A-53m	318446.5	6403975	4	59	57.5	1.5
WML110-90m	318005.3	6404244	4	57.6	53.2	4.4
WML114-63m	318151.6	6405239	4	60.11	57.3	2.8
WML107A-69m	318674.3	6403828	6	52.92	52.6	0.3
WML108A-80m	318446.5	6403975	6	57	52.9	4.1
WML110-110m	318005.3	6404244	6	56.41	53.0	3.5
WML112A-130m	317563.7	6404450	6	57.49	52.4	5.1
WML114-88m	318151.6	6405239	6	60.82	56.9	4.0
WML115A-93m	317873.6	6406708	6	60.15	61.0	-0.9
WML189-49m	318657.2	6404569	6	57.48	55.8	1.7
WML191-52m	318623.9	6404335	6	56.8	54.7	2.1
WML106-68m	318860.9	6403493	7	52	51.2	0.8
WML114-108m	318151.6	6405239	7	60.77	56.5	4.2
WML213-185.5m	317210.2	6404154	7	52.3	51.0	1.3
WML106-84m	318860.9	6403493	8	52	51.1	0.9
WML115A-144m	317873.6	6406708	8	61	61.3	-0.3
WML119	319255.3	6403930	8	52	51.0	1.0
WML120A	319292	6404580	8	52.32	51.7	0.7
WML181	319214	6403957	8	48.692	51.0	-2.3
WML182	319156	6404133	8	46.6	51.1	-4.5
WML183	319188	6404325	8	50.202	51.2	-1.0
WML184	319179	6404530	8	51.896	51.5	0.4
WML185	319200	6404642	8	53	52.5	0.5
WML186	319219	6404746	8	47.772	53.8	-6.0
WML21	318245	6406340	8	64.66	60.5	4.2
WML191-100m	318623.9	6404335	9	55.89	53.5	2.4
WML144A-26m	319500	6404170	10	51.74	53.2	-1.4
WML189-101m	318657.2	6404569	10	54	54.3	-0.3
WML191-132m	318623.9	6404335	10	56.71	53.6	3.1
WML213-247m	317210.2	6404154	10	53.82	51.7	2.1
WML144A-32m	319500	6404170	11	51.96	53.6	-1.6

Bore	Easting (MGA)	Northing (MGA)	Model Layer	Observed Head (mAHD)	Modelled Head (mAHD)	Head Difference (m)
WML144A-45m	319500	6404170	11	51.92	53.6	-1.6
WML144A-50m	319500	6404170	12	52.34	53.9	-1.5
WML191-155m	318623.9	6404335	12	56	53.9	2.1
WML144A-58m	319500	6404170	13	55	54.3	0.7
WML144A-81m	319500	6404170	13	53.42	54.3	-0.9
WML19a	319949.6	6406544	13	61.96	62.4	-0.4
WML144A-98m	319500	6404170	14	53.5	54.6	-1.1
WML191-200m	318623.9	6404335	14	55.59	54.3	1.3

It should be noted that a 'true' steady state calibration is not possible for this area, as groundwater level records are not available before the Ravensworth or Narama open cut mines were started. A steady state model effectively runs over an infinite timescale, which means that the Ravensworth/Narama boundary condition will have reached equilibrium with the hydrogeological regime within the steady state model. Although the Narama pit is relatively shallow, affecting the upper coal seams, the effective timescales involved in a steady state model will have resulted in depressurisation of lower levels as well.

The few early monitoring records that are contained within the EIS (HLA Envirosiences, 2001) were taken only ten years after the start of the Narama open cut mining, so they will tend to show higher potentiometric heads within the Permian than the steady state model.

Conversely, although monitoring records are available from the ACP monitoring network prior to the start of underground mining, some of the potentiometric heads down to the Lower Barrett seam will have been slightly affected by the early NEOC mining prior to installation of the monitoring bores. Some of these records will therefore tend to under-estimate 'steady state' groundwater levels.

Although this complicates the steady state calibration, a large number of bores were available as potential calibration target levels. Suitable calibration targets were selected by screening all of the available monitoring data and selecting records that had not been too heavily influenced by perched aquifer conditions, the effect of NEOC mining, or any effects from early underground mining at the ACP. Other calibration target levels have been inferred by back-projection of hydrograph trends or hydrostatic head profiles. A scatter plot of the steady-state calibration performance is shown in **Figure C15**.

Steady state calibration achieved an SRMS of 11.65%. This was considered acceptable given the large number of adopted calibration targets, the wide spatial and depth range involved, and the fact that target levels had been obtained at differing times in a non-static system. The steady-state water balance yielded an acceptable balance discrepancy of 0.01%.

2.2 Transient Model Calibration

Modelled Mine Plan/Schedule

The transient calibration model includes five time slice models, covering the period from 1 January 2004 to 31 March 2009.

Match to Measured Groundwater Heads

Transient calibration hydrographs were produced for around 150 piezometers, which measured groundwater levels in multiple seams from the alluvium through to the Lower Barrett Seam. Calibration hydrographs are presented in **Figures C16 to C40**. In general, results were extremely good, particularly given the stresses placed on the Model by the mining activities and the head differential that occurred within the different model layers at the start of the modelling period.

A few observed effects were not well represented by the Model, but these are not considered to be significant to the impact assessment. The hydrographs listed below, and displayed in **Figures C16 to C40**, showed levels or responses that were not well reproduced in the Model:

- For Layer 1, the Model consistently predicted lower heads than observed for boreholes WML110C and RA16. However, both bores are located in areas where there are believed to be perched water tables in the weathered regolith/colluvium.
- Bores WML114 and WML109, in the mid Lemington seams (Layer 4) to the west of LW3, showed unexpectedly large (and non-predicted) responses to the mining of LW2. These are too distant to be caused by actual dewatering and are believed to be pressure-storage responses to transient increases in storage above the ribs of LW2, caused by stress relaxation, as described in **Section 4.2.3** ('Impact of Mining Operations to Date'). WML108 shows a similar, large response during the mining of LW3. It is noticeable that two of these bores show a 'bounce-back' in water levels, caused by re-compression of strata during the mining of subsequent longwall panels, or by the settling of strata over time. The observed 'bounce-back' supports the conclusion that the potentiometric response is being caused by changes in storage within these highly confined layers above the longwall panel, rather than by dewatering.
- Observed water level recession (not predicted) in Layer 2 (upper Lemington Seams and overburden) within boreholes WML111, 112 and 113 in the south eastern part of the proposed mining area is believed to be associated with either regional impacts, or a distance response to the pressure-storage effect referred to above. In this case, any pressure-storage response is likely to have been caused by increases in storage caused by unconnected surface fracturing in the tensile zone above the longwall.
- Bores WML107 and WML110 in the PG overburden (Layers 6 and 7) initially match well with modelled data as they start to be affected by longwall mining, but then appear to recover. Neither of these bores was undermined in the monitoring period, and it appears that the enhanced hydraulic conductivity initially caused by the longwall mining has 'self-healed' to a certain extent by the movement of fines and swelling of clay within mudstone. This effect is not simulated in the operational modelling, but does support the approach adopted during the recovery phase whereby the vertical hydraulic conductivity of the caved material is reduced in order to represent this effect. It also shows that the operational model tends to be conservative in its assessment of impacts in layers that are affected by mine depressurisation.

- There is an unpredicted drawdown effect within the PG (Layer 8) in borehole WML213, next to the Hunter River. This is too distant from the Ravensworth or ACP underground mining activities within the modelled period to have been caused by either of those mines.
- Bore WML191 is located within the chain pillar between LW2 and LW3, and has a vibrating wire piezometer within the PG Seam (Layer 8). This piezometer shows a continuing drawdown (not predicted) through the period which is not clearly related to mining of either LW2 or LW3. These may be stress effects penetrating from the PG Seam through to the ULD Seam (Layer 10) and even the Upper Lower Liddell Seam (Layer 12), but are more likely to be responses to mining in the NEOC. Borehole WML189, which is located in the same chain pillar to the north of WML191 shows a clearer stress response in Arties Seam, some 8m below the floor of the PG Seam.
- Modelled predictions for WML144 are reasonable in Layers 11-14, but there is a slight, unknown, regional dewatering impact that is not reflected in either the Model or in the overlying ULD Seam (Layer 10) most likely due to regional stresses.

In summary, the majority of the hydrograph effects that are not well predicted by the Model are inferred to be either associated with changes in storage caused by stress re-distribution in the rock mass, or are due to some unknown regional effect unrelated to mine inflows and mine dewatering.

The pressure-storage effects are transient impacts that only affect pressure heads in highly confined strata. They have little or no influence on flow patterns within the general hydrogeological environment and they have not been included in the modelling process as they have no effect on the overall impact assessment. International research (Booth, 2006) confirms that these transient pressure-storage effects can typically be seen up to 500m from the workings.

The source of the regional effects described in boreholes WML144 and WML213 is not known, but will not materially affect the degree of impact on the groundwater environment caused by the ACP underground mine.

Transient Water Balance

The water balance error for the transient model at the end of each stress period was generally less than 1%. This was achieved for most stress periods except in stress periods 7 and 8 within time slice 1. These water balance outcomes were found to be due to a mass balance error in a small area of drain cells in Layer 8 within the NEOC. As this area is not within the main impact region from the ULD Seam underground mining, the cumulative volume balance was deemed acceptable and is not expected impact on predicted groundwater levels.

Match to Underground Mine Inflows

Throughout the model calibration runs, the failure zones invoked in the Model above the extracted longwall panels were progressed in accordance with the mine plan. A summary of the Model predicted inflows compared with measured inflows is shown in **Figure C41**.

The rate and salinity of inflows to the PG Tailgate 1 (TG1) have been measured separately to other mine inflows, as they are thought to be a fair basis for calculating the amount of water that the Glennies Creek alluvium is losing to the underground mine. The Model was also calibrated

against the measured inflow rate by comparing the model-predicted baseflow losses in Glennies Creek against the alluvium losses calculated from the measured inflows. A comparison of the model-predicted baseflow losses versus measured TG1 inflow rates is shown in **Figure C42**. This indicates that there is generally a very good match against the initial inflow rate; however measured inflow rates have been declining steadily since then. It is clear from **Figure 42** that Model does not predict the decrease in inflows. This could have been simulated in the Model by a progressive reduction in the hydraulic conductivity of the PG between the Mine and the Creek. This was not been done in order to ensure that the Model provides a conservative estimate of the impact of mining upon Glennies Creek and its associated alluvium.

3. Sensitivity Analysis

An automatic sensitivity analysis using the auto-sensitivity function within the Groundwater Vistas modelling software was conducted on the steady state model to determine sensitivity to the calibrated model parameters.

Overall the steady state model was insensitive to most parameters and the SRMS values for the calibrated model values were better than the sensitivity runs (indicating that the adopted hydraulic parameters in the calibrated model were appropriate) (**Figure C43**). However, given the potential uncertainty of the effect on enhancement of vertical hydraulic conductivity in the fracture zone, attention was given to the sensitivity of the Model to vertical hydraulic conductivities. The Model was found to be most sensitive to the following parameters:

- Recharge to the exposed Lemington Seam subcrops in the hillside above the underground mine area (recharge Zone 8);
- Horizontal hydraulic conductivity in the main rock mass in the Permian overburden and interburden layers (hydraulic conductivity Zone 7); and
- Vertical hydraulic conductivity in the main rock mass in the Permian overburden and interburden layers (hydraulic conductivity Zone 7).

4. Uncertainty Analysis

Uncertainty analysis is the process by which the impacts on model predictions and model reliability of variations in critical parameters to which the model has been found to be “sensitive” (during calibration) are assessed.

For the operational phase, the sensitivity analysis for the steady state calibration showed that results would be most significantly affected by variations in the assumed recharge rate over the Permian subcrop areas, and the assumed hydraulic conductivity of the in-situ rock mass within the Permian overburden and interburden layers.

Three uncertainty models were run to simulate the impacts of variations in key sensitivity parameters:

- Uncertainty model 1, in which recharge to the Lemington Seam sub-crop area above the underground mine (Zone 8) was increased by a factor of two.
- Uncertainty model 2, in which horizontal hydraulic conductivity of the in-situ Permian overburden layers (Zone 7) was increased by a factor of two and the vertical hydraulic conductivity increased by an order of magnitude.
- Uncertainty model 3, in which vertical hydraulic conductivity of the in-situ Permian

overburden layers (Zone 7) was increased by a factor of two and the horizontal hydraulic conductivity increased by an order of magnitude.

4.1 Baseflows

The results of the uncertainty analysis runs for baseflows are shown in **Figure C44**. This shows that changing recharge rates above the mine does not affect river/creek baseflows. The effects of changing the hydraulic parameters are as follows:

- When horizontal hydraulic conductivity (K_h) is increased by a factor of two and vertical conductivity (K_v) (Uncertainty Model 2) increased by a factor of ten, the Hunter River baseflow increases by $20\text{m}^3/\text{d}$. This trend remains relatively consistent throughout the uncertainty model simulations to the end of the ULD Seam LW8 (2016) (refer to **Figure C44a**).
- When horizontal hydraulic conductivity (K_h) is increased by a factor of two and vertical conductivity (K_v) (Uncertainty Model 2) increased by a factor of ten, the pre-mining Bowmans Creek baseflow is predicted to increase by 20 and $50\text{m}^3/\text{d}$ respectively (refer to **Figure C44b**).
- Predicted baseflows to Glennies Creek for the three uncertainty models are similar in trend to the predicted base case model with differences remaining stable following the initial impact from start of the PG Tailgate 1 (refer to **Figure C44c**).

It is important to recognise that the uncertainty analysis assesses the theoretical impact sensitivity of the model results to the assumed hydraulic conductivity distributions. Predicted increases in baseflow losses from Glennies Creek in the uncertainty runs are inconsistent with the observed impact (i.e. TG1 inflows gradually decreasing over time). Therefore the observed inflows support the adopted base case parameters.

4.2 Mine Inflows

The inflow rates predicted by the uncertainty analysis modelling are illustrated graphically in **Figure C45**. The predicted base case inflow rate is shown on this figure for comparison. Increasing recharge by a factor of two to the coal seam sub-crop area above the underground mine has only a minor influence on predicted inflows. However, increasing horizontal hydraulic conductivity for the in-situ rock mass within the Permian overburden and interburden layers (from Layer 2 to Layer 7) has a more significant influence. In this case, peak inflow could increase to $1,600\text{m}^3/\text{d}$ prior to the start of mining LW1 panel in ULD Seam. As with the baseflows, the higher inflow rates predicted by the uncertainty analysis prior to ULD mining are inconsistent with the observed inflow rates to date. Again, this analysis supports the base case parameters.

References

- HLA Envirosiences, 2001. 'Ashton Coal Project: Groundwater Hydrology and Impact Assessment'. Appendix H Report submitted in support of the 2002 Ashton Coal Project EIS.
- Aquaterra, 2008. 'Ashton Underground Mine: Bowmans Creek Alluvium Investigation'. Report submitted to ACOL.
- Aquaterra, 2009b. 'Ashton Coal: End of Panel 3 Groundwater Report' Monitoring Report submitted to ACOL.
- Aquaterra, 2009c. 'Bowmans Creek Diversion: Groundwater Impact Assessment Report'. Report submitted to ACOL in support of the Bowmans Creek Diversion EA.
- Booth, C.J. 2006. 'Groundwater as an Environmental Constraint of Longwall Mining'. *Environmental Geology* 2006; No. 49, pp 796 – 803.
- McDonald and Harbaugh, 1988. A modular three-dimensional finite-difference ground-water flow model. *Techniques of Water-Resources Investigations*, Book 6. U.S. Geological Survey.
- Murray Darling Basin Commission (MDBC), 2001. *Groundwater Flow Modelling Guideline*.
- SCT Operations Pty Ltd (SCT), 2008. 'ACARP Project C13013: Aquifer Inflow Prediction above Longwall Panels'. Report to the Australian Coal Association Program September 2008.

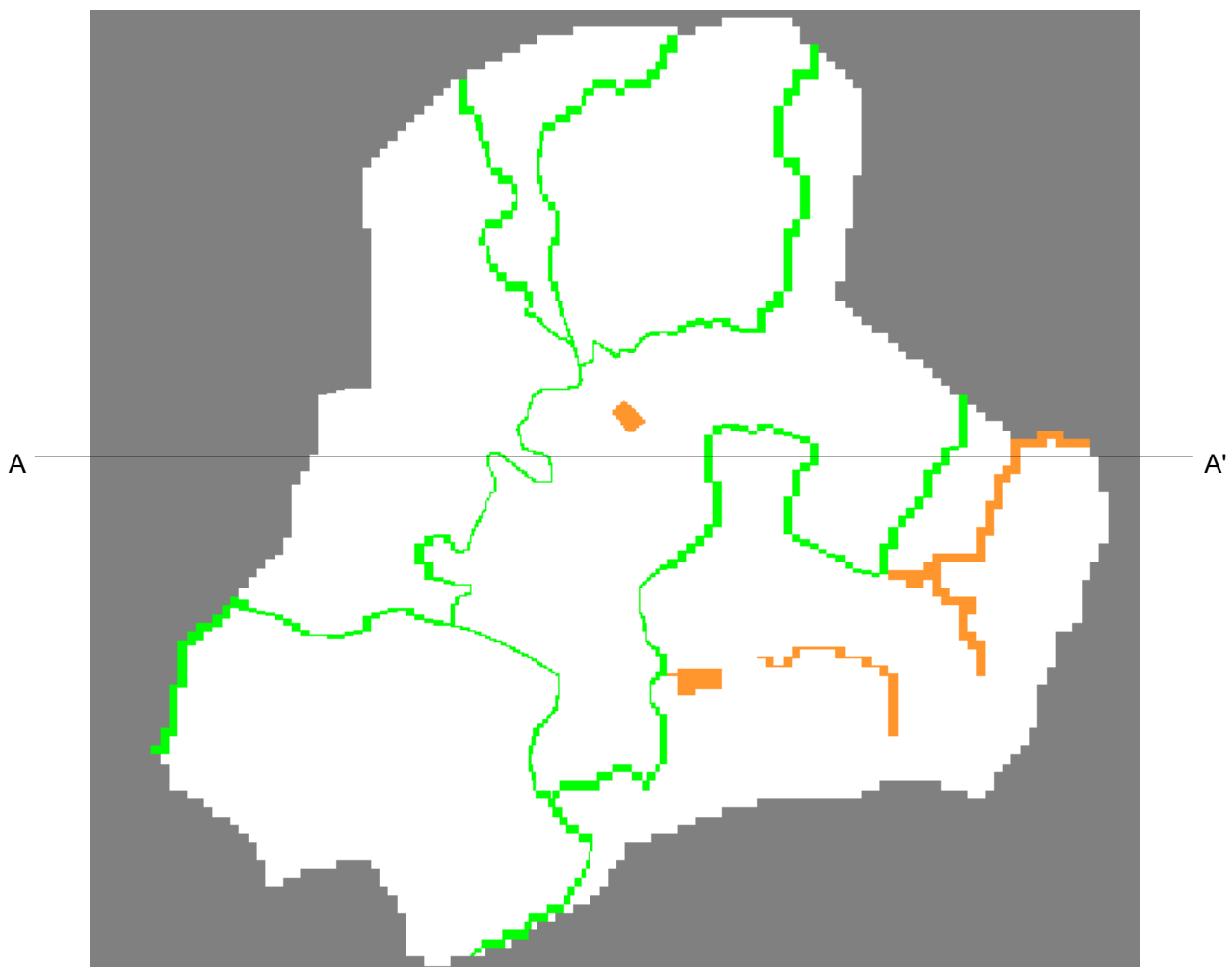


Figure C1

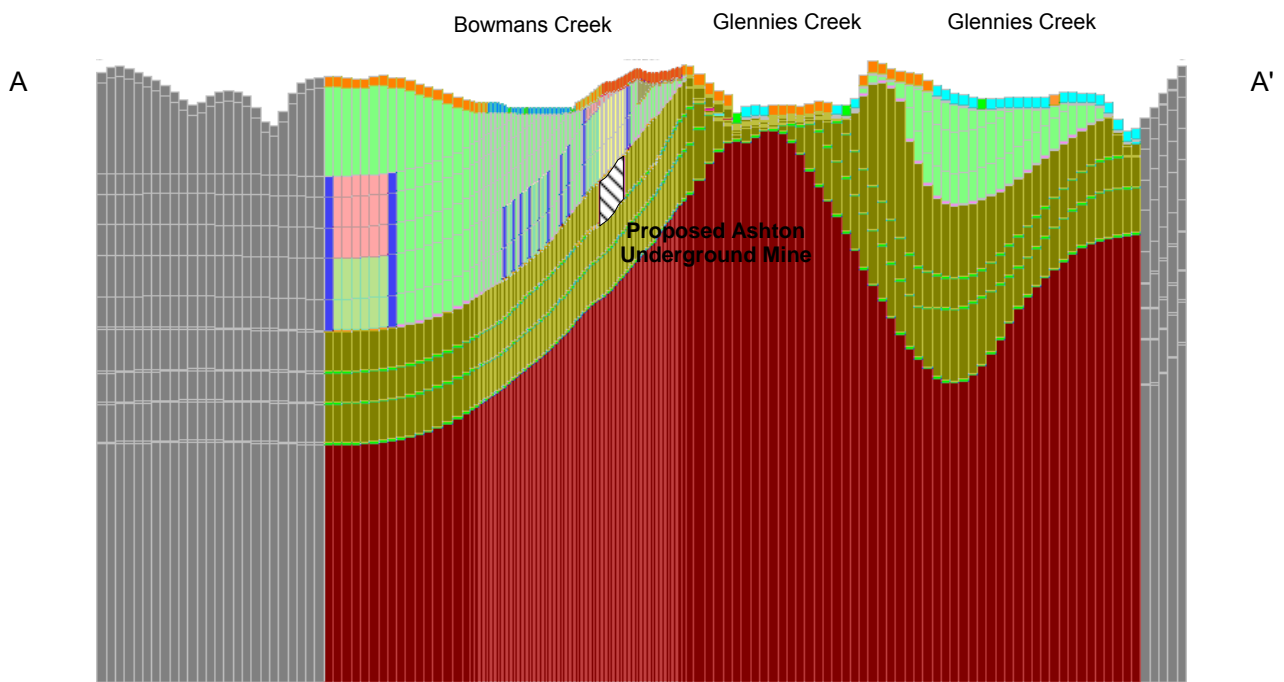
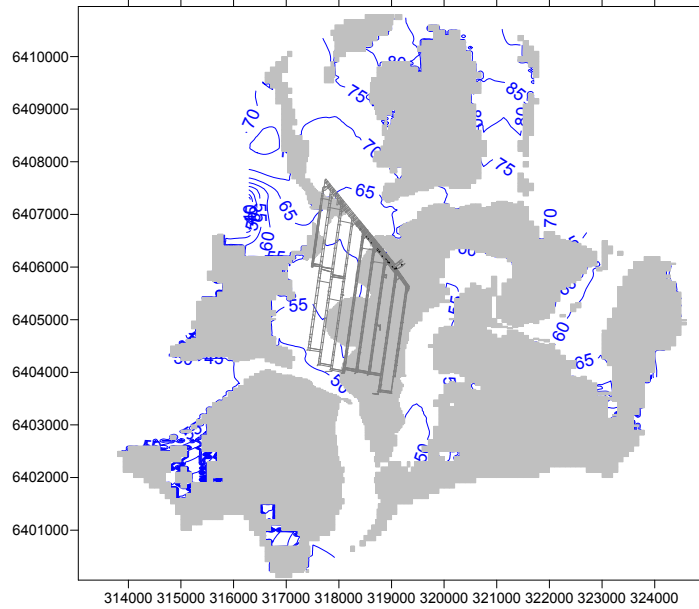


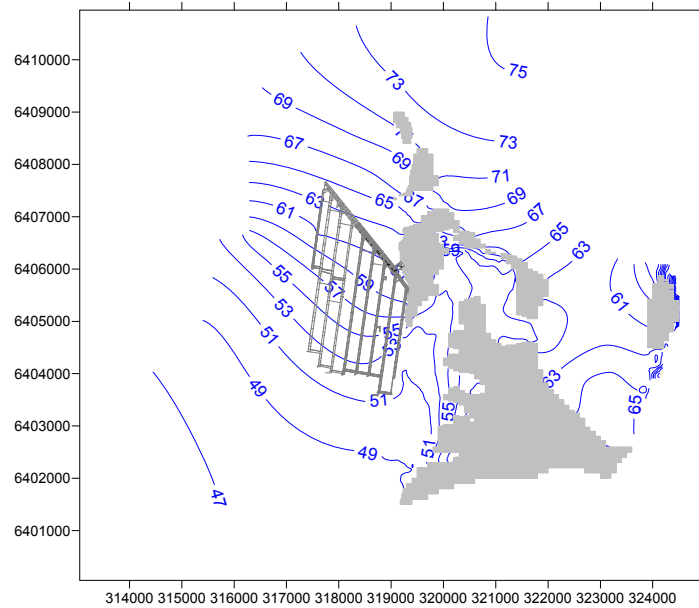
Figure C2

Date	1 September 2009	Scale	As Shown	Ashton Coal Operations Ltd Groundwater Model Domain Layer 1 and Cross Section
Initials	HZ	Project	S55F	
Drawing Number	S55F-301a	Revision	0	

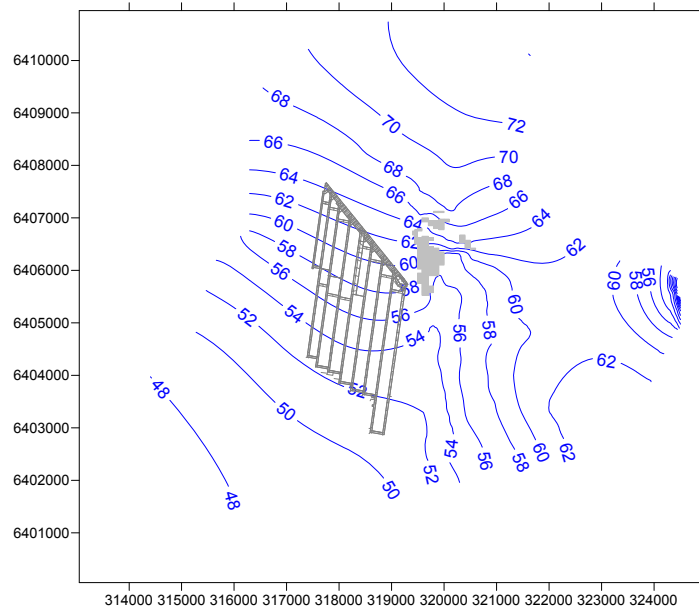
Alluvium and Regolith





Pikes Gully Seam



Upper Liddell Seam



 50 Predicted Groundwater Levels (mAHd)
 Dry Cells


Date	17 May 2011	Scale	As Shown	Ashton Coal Operations Ltd Modelled Groundwater Heads in the Steady State (Pre-Underground Mine) Model in the Alluvium, Pikes Gully Seam and Upper Liddell Seam
Initials	HZ	Project	S55J	
Drawing Number	S55J-201	Revision	A	
				Figure C3

Figure C4: Calibrated recharge zone (applied to the highest active layer)

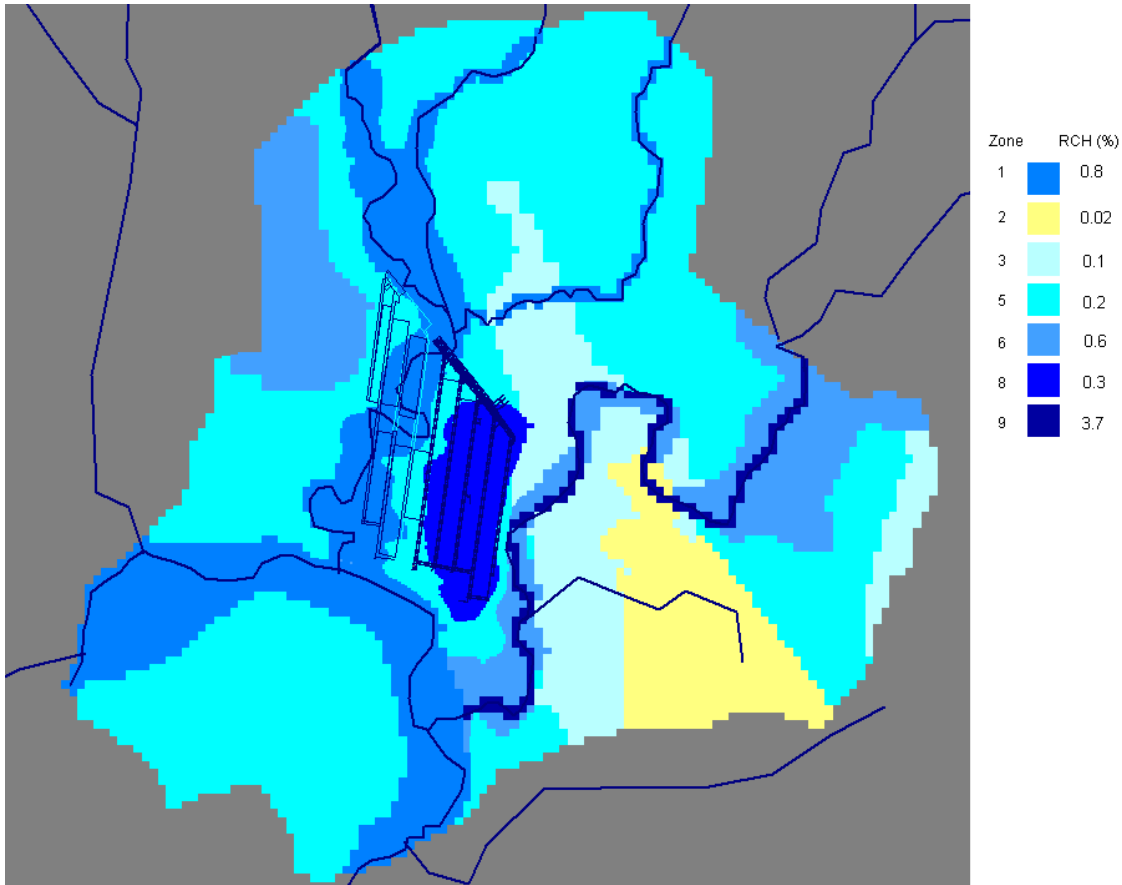


Figure C5: Hydraulic conductivity for Layer 1 (m/d)

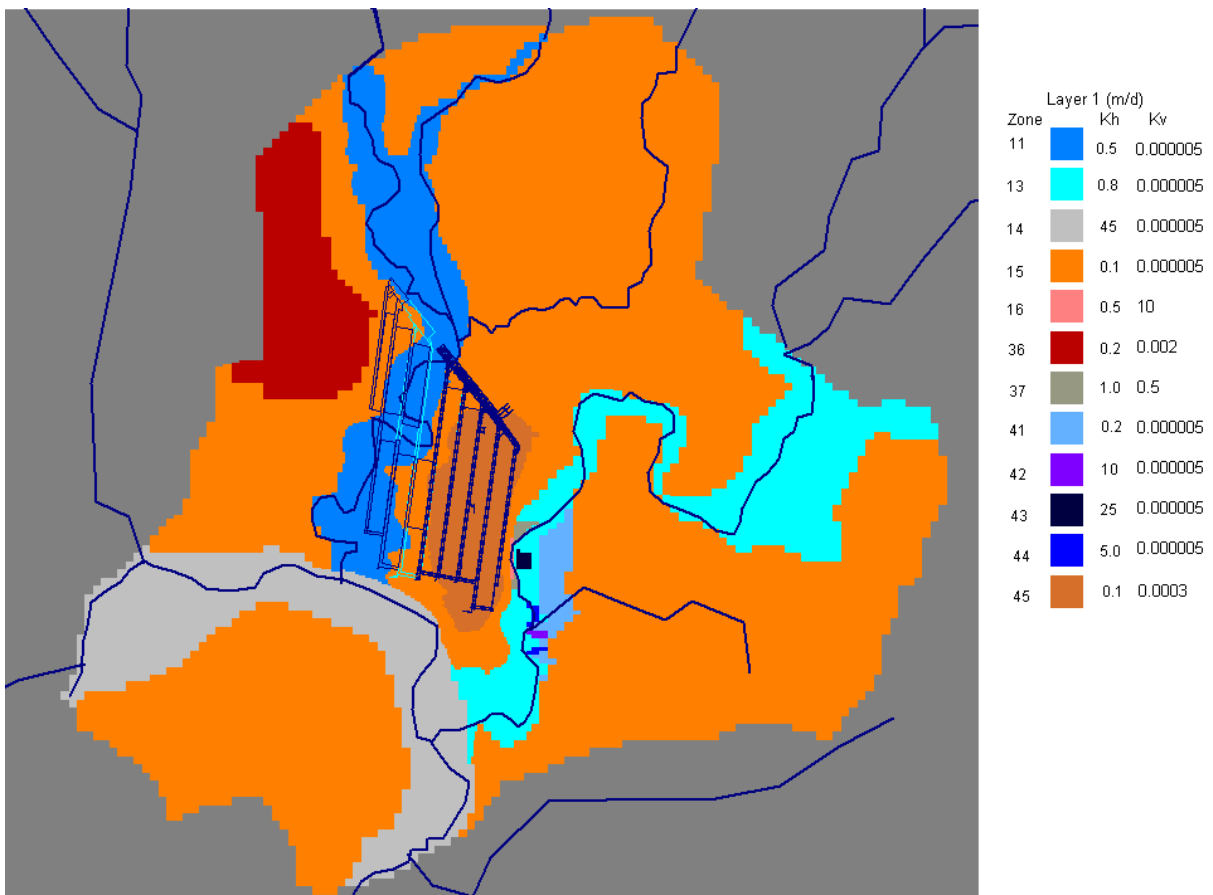


Figure C6: Hydraulic conductivity for Layer 2 (m/d)

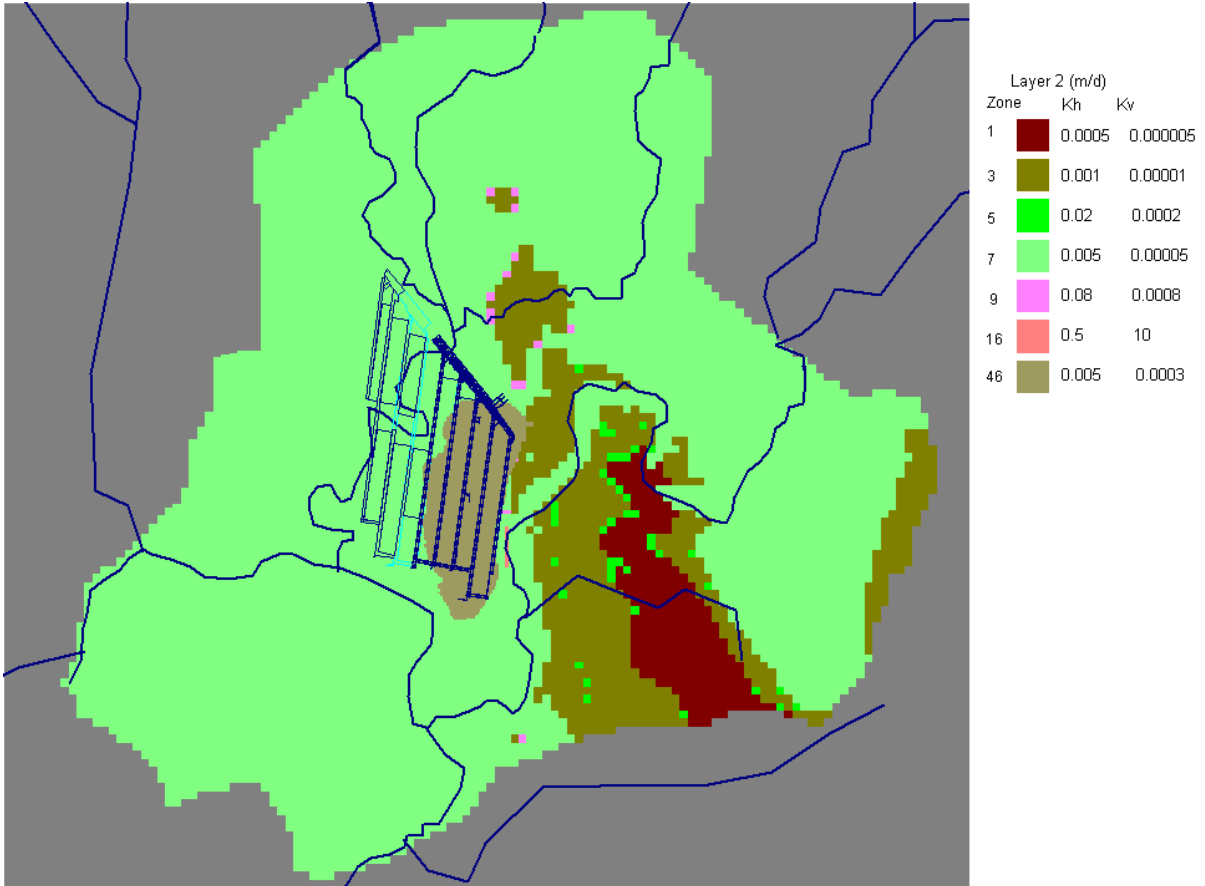


Figure C7: Hydraulic conductivity for Layer 3 (m/d)

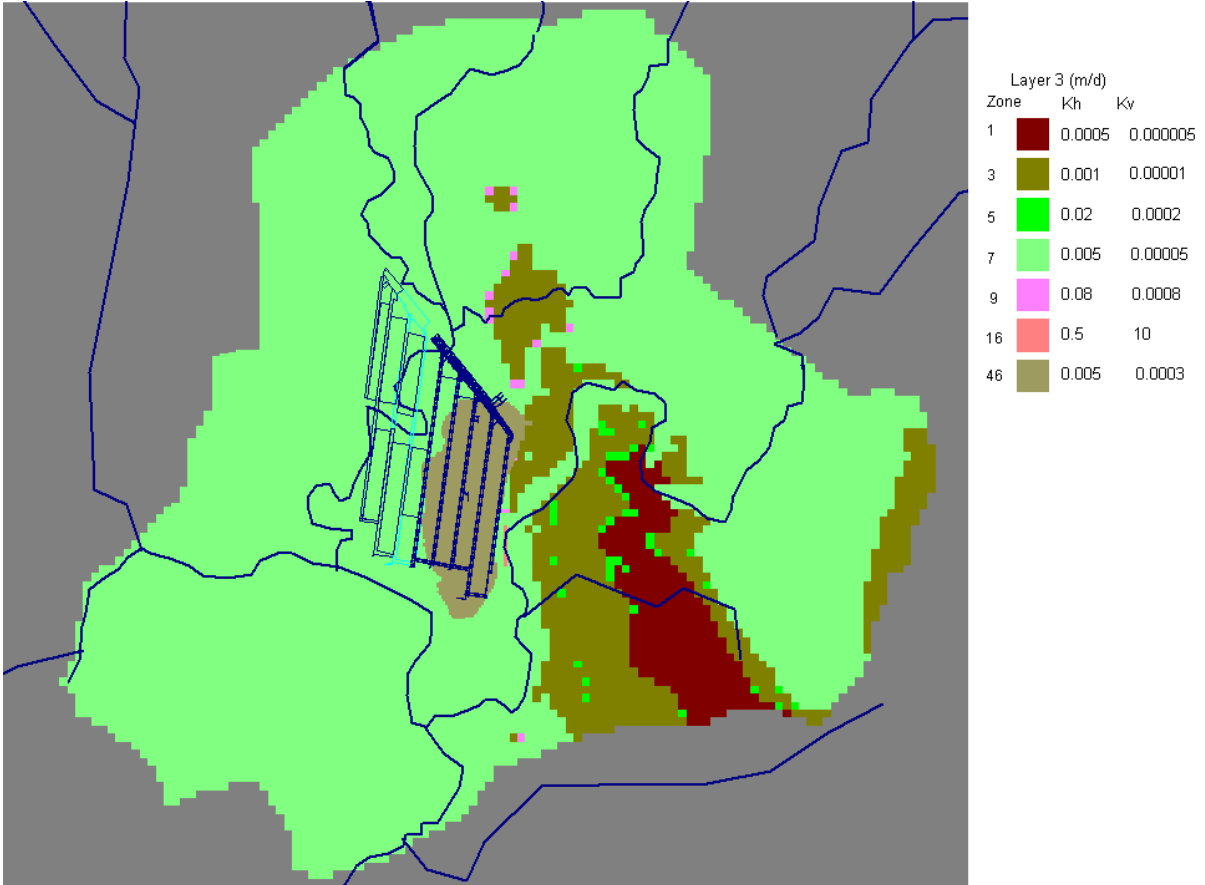


Figure C8: Hydraulic conductivity for Layer 4 (m/d)

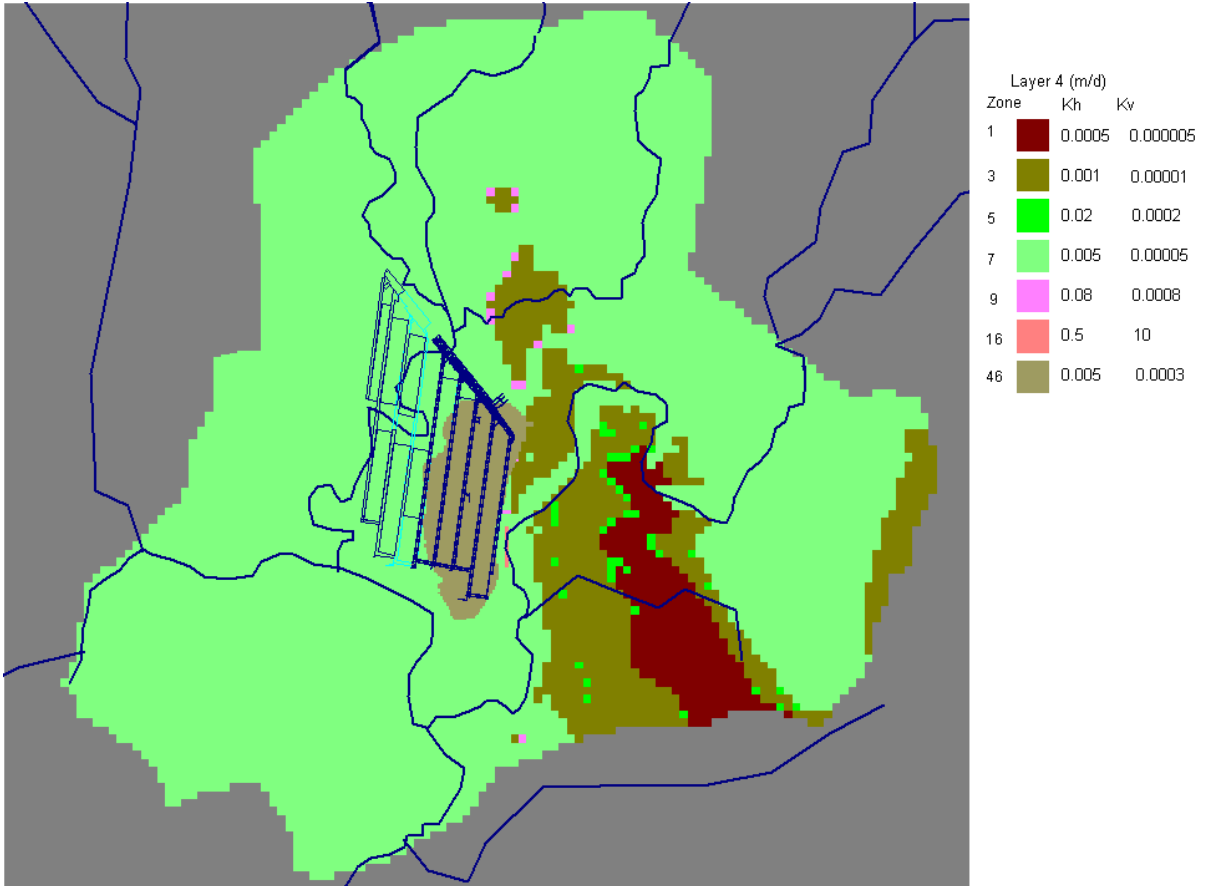


Figure C9: Hydraulic conductivity for Layer 5 (m/d)

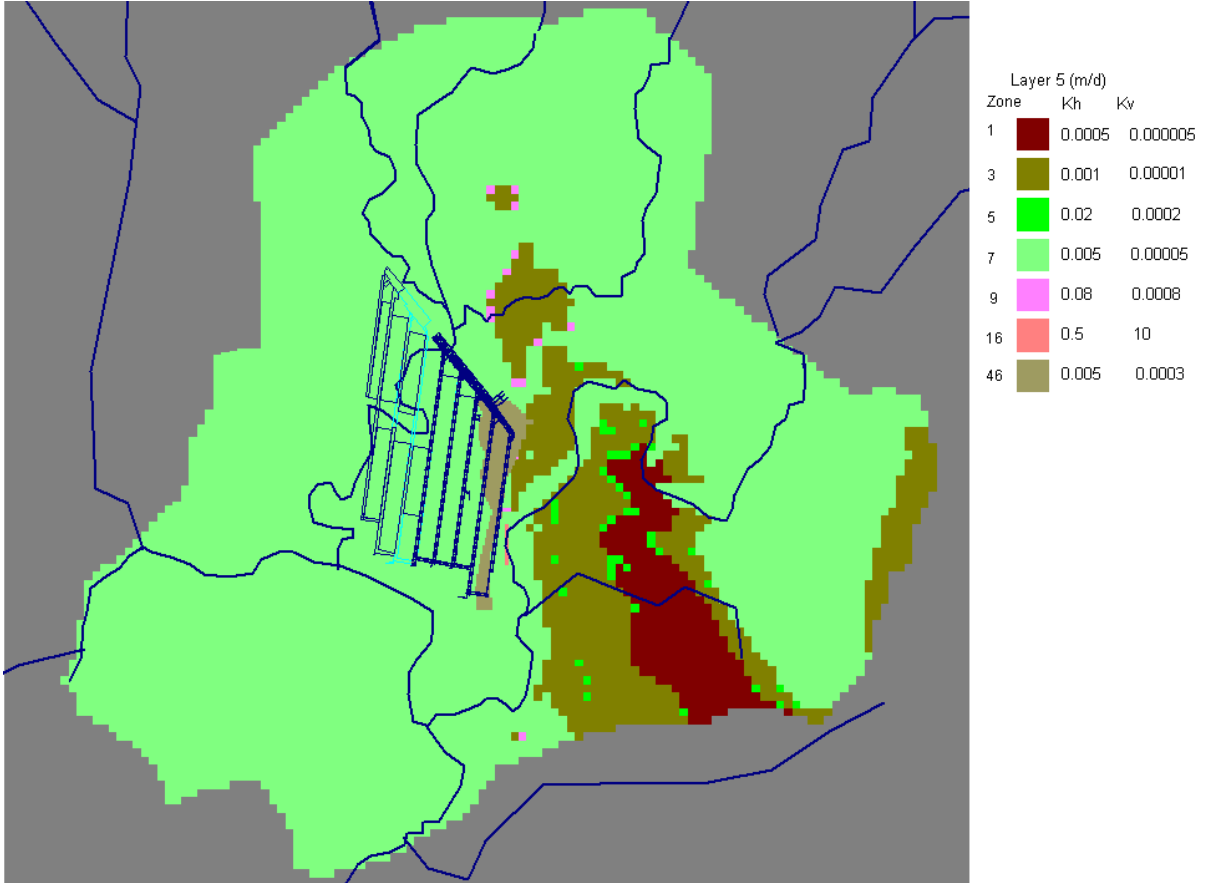


Figure C10: Hydraulic conductivity for Layer 6 (m/d)

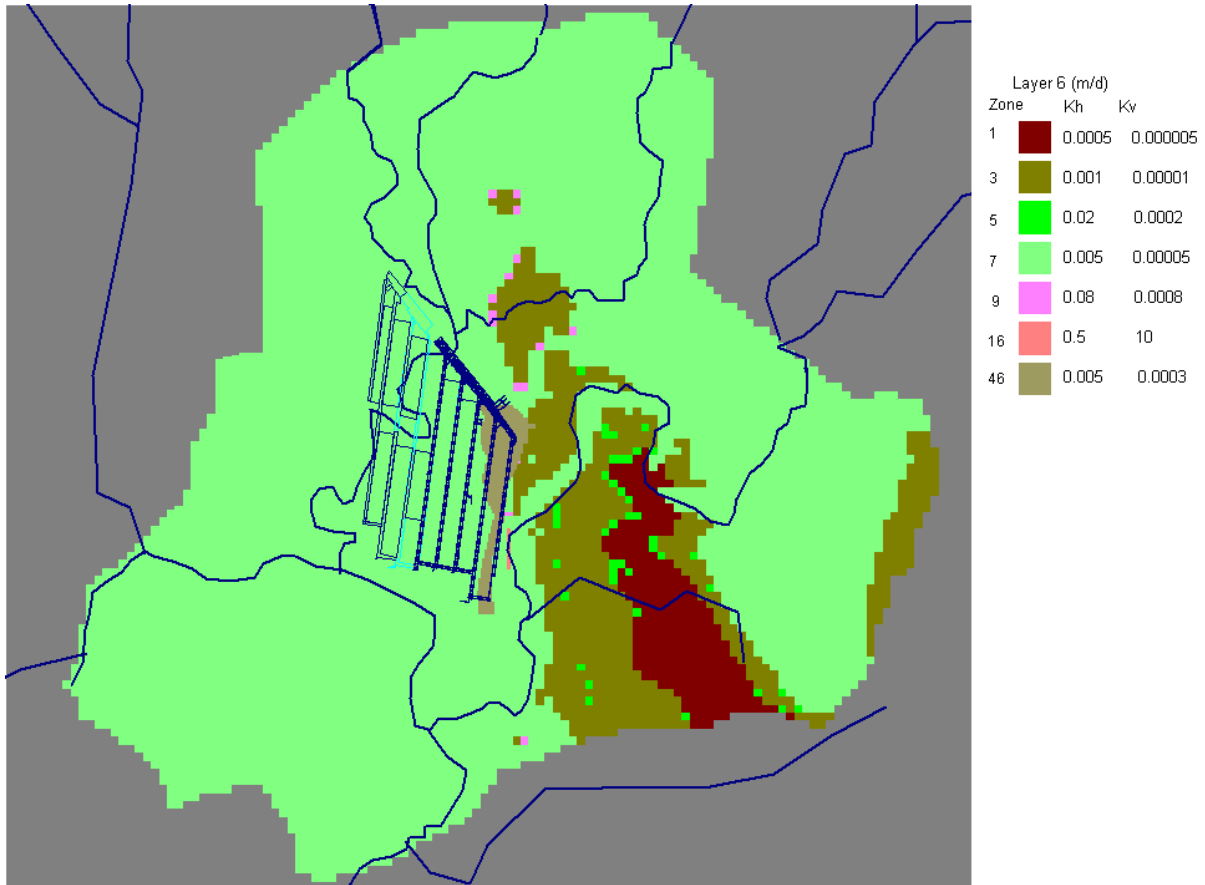


Figure C11: Hydraulic conductivity for Layer 7 (m/d)

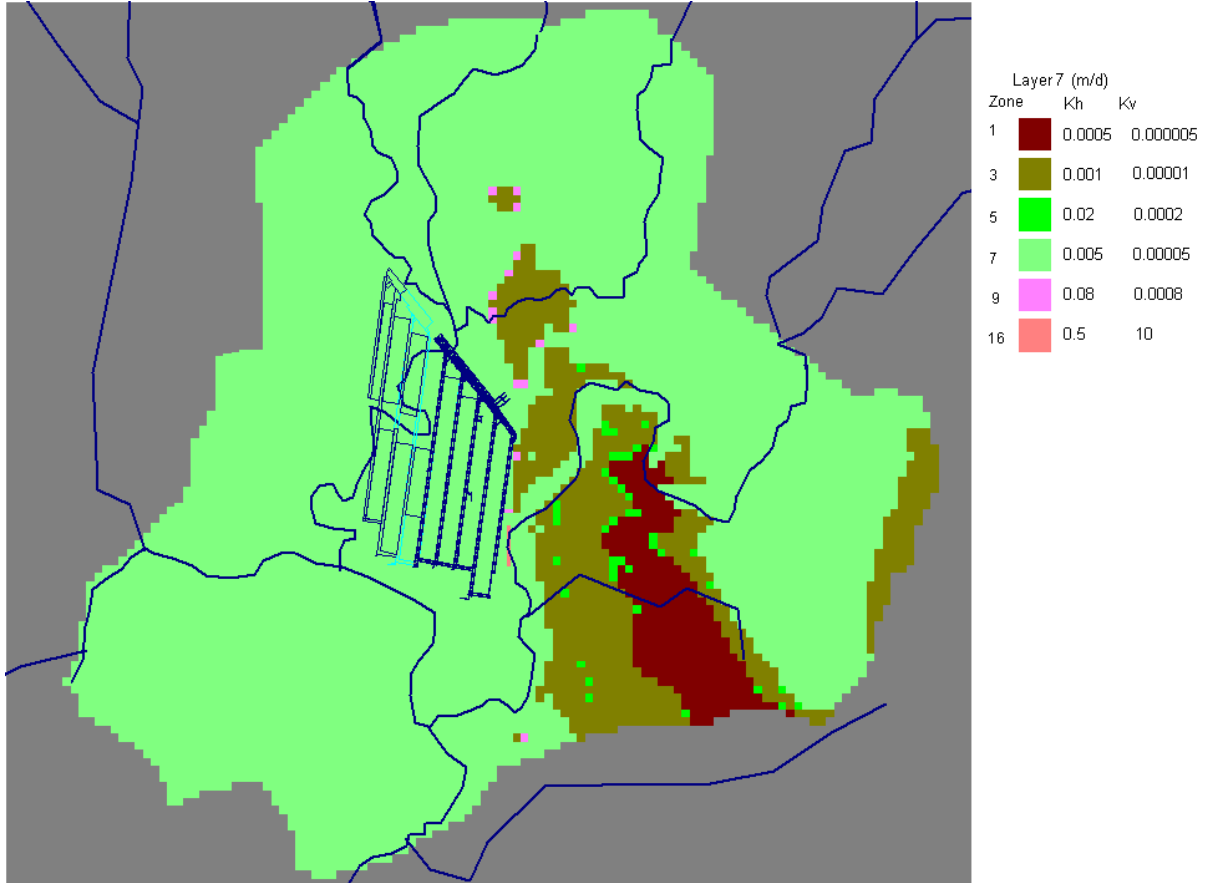


Figure C12: Hydraulic conductivity for Layer 8 (m/d)

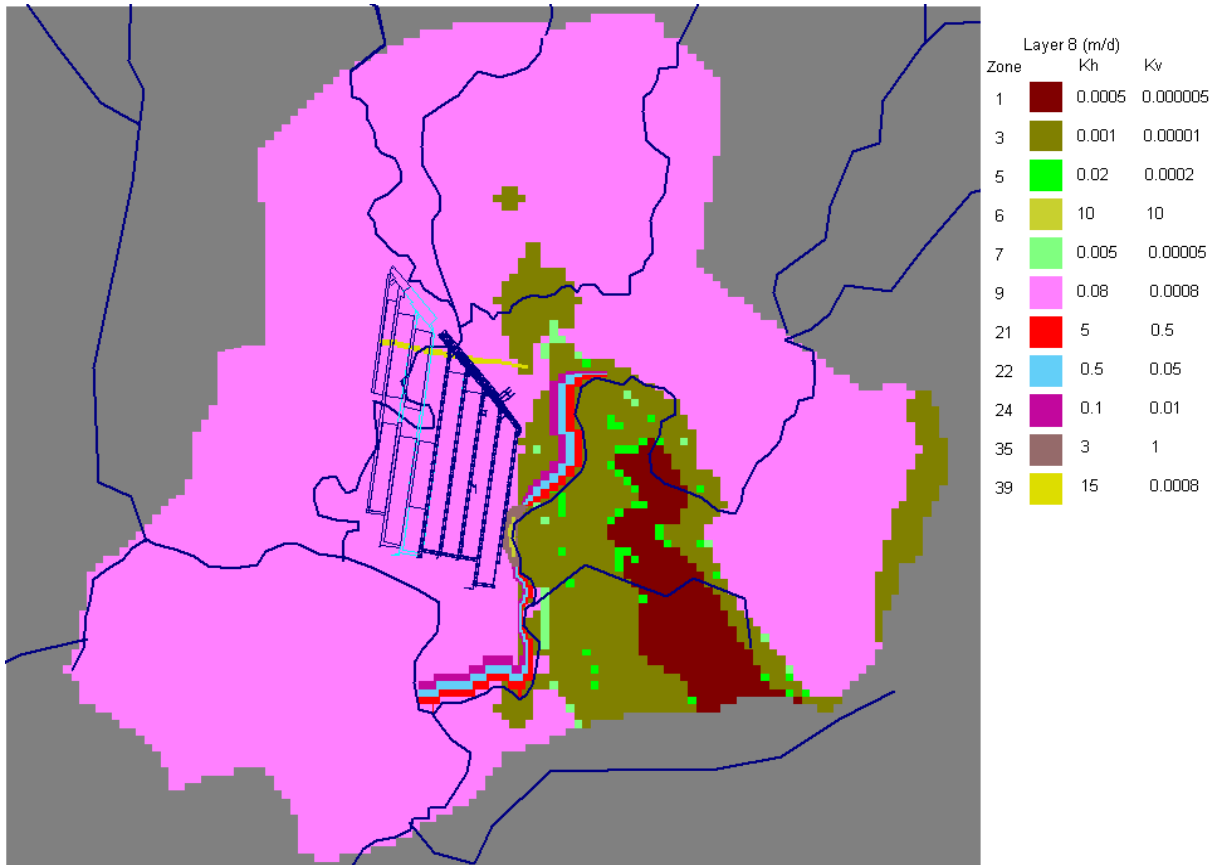


Figure C13: Hydraulic conductivity for Layer 9 (m/d)

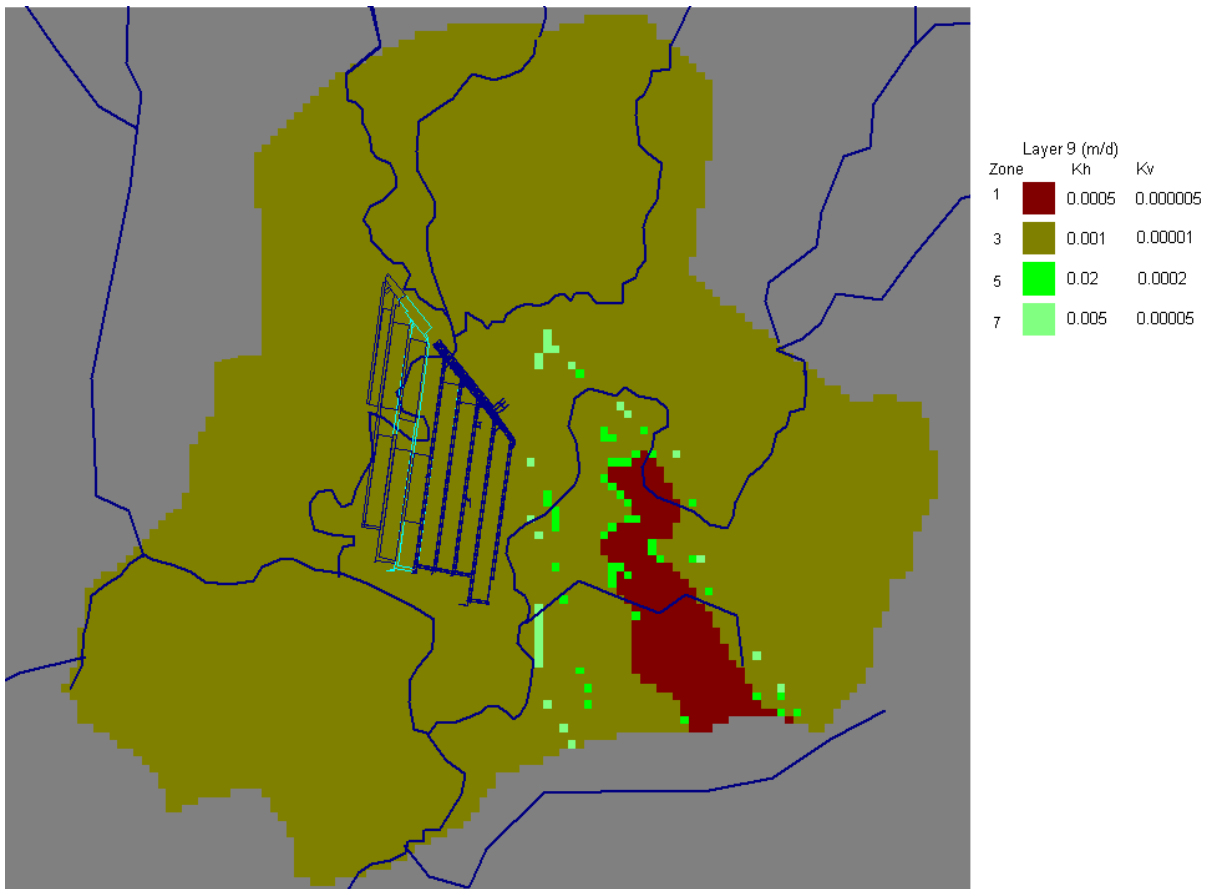


Figure C14: General Head Boundary (GHB) for all layers

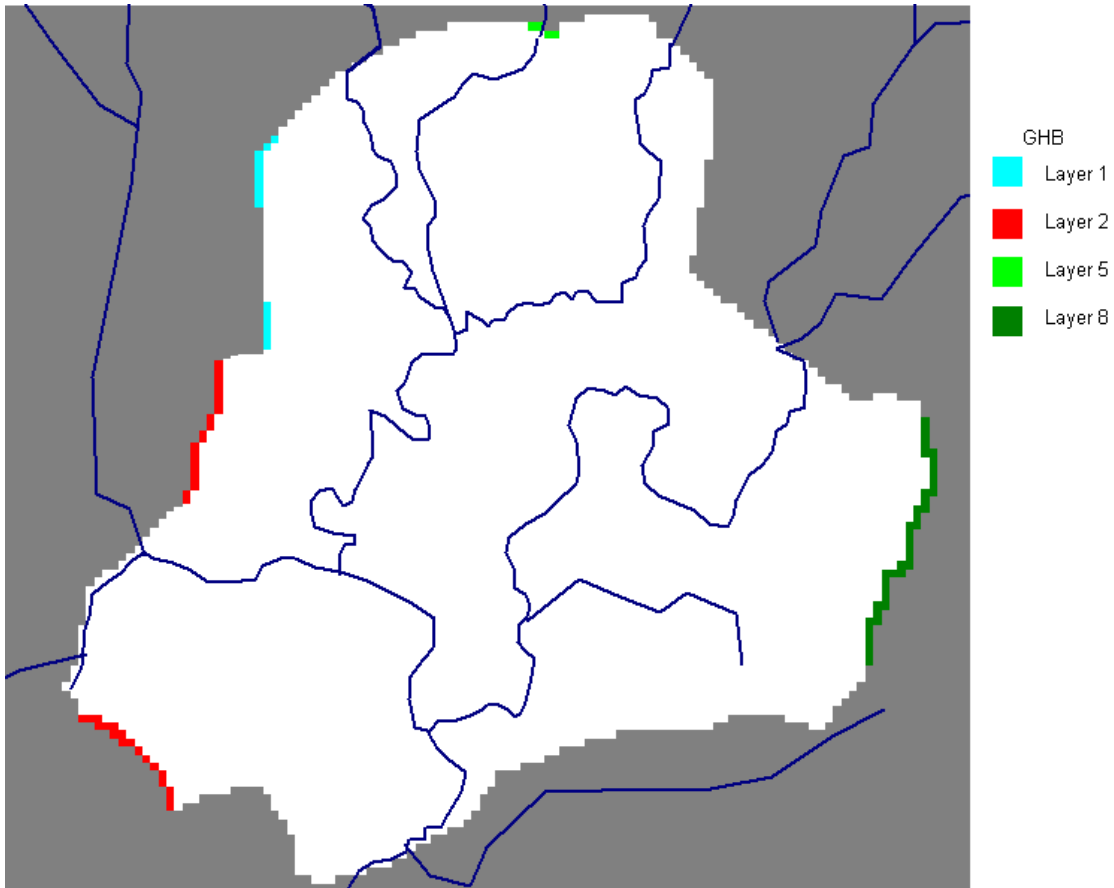
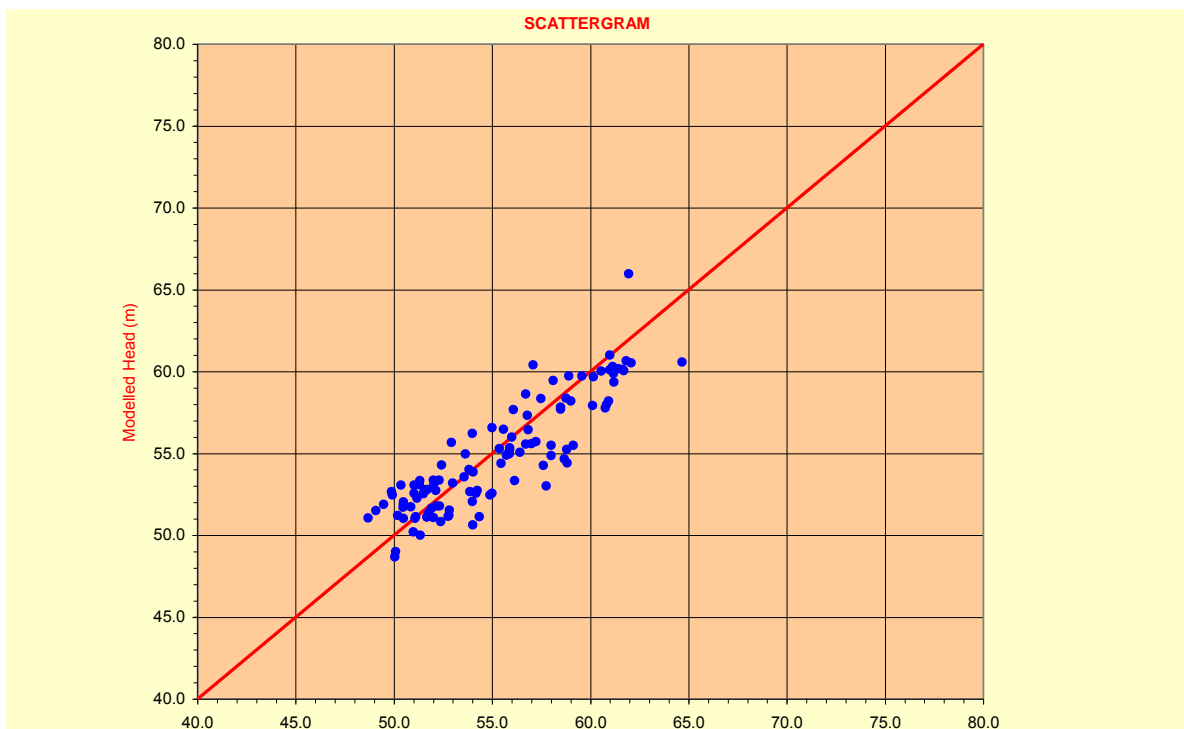
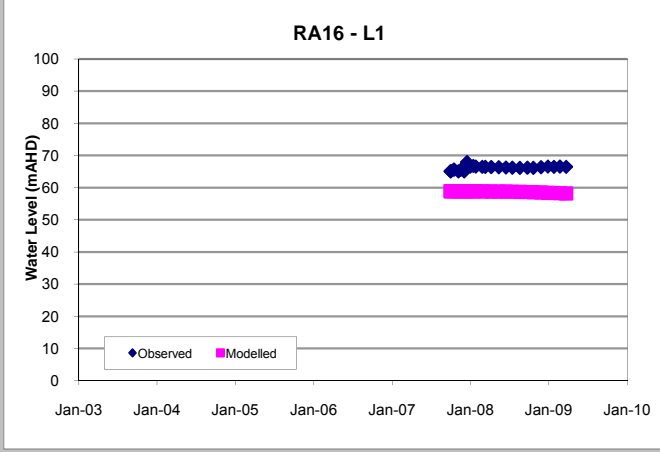
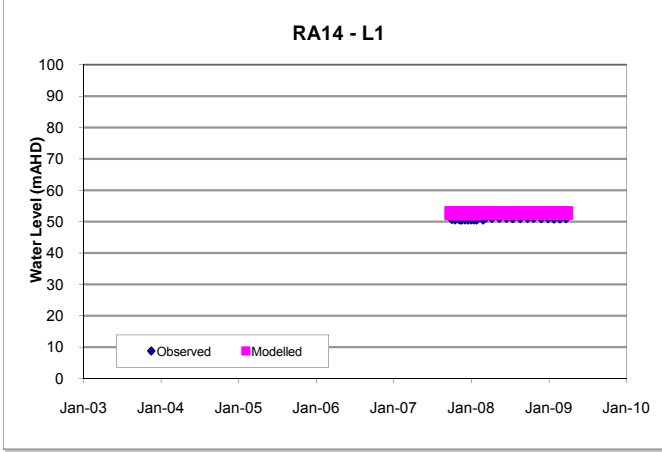
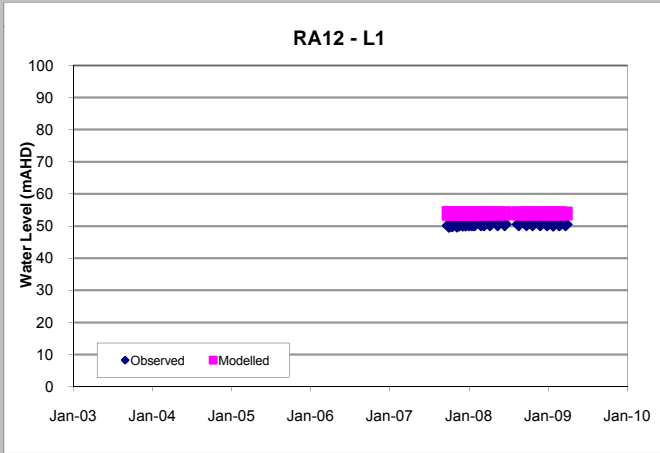
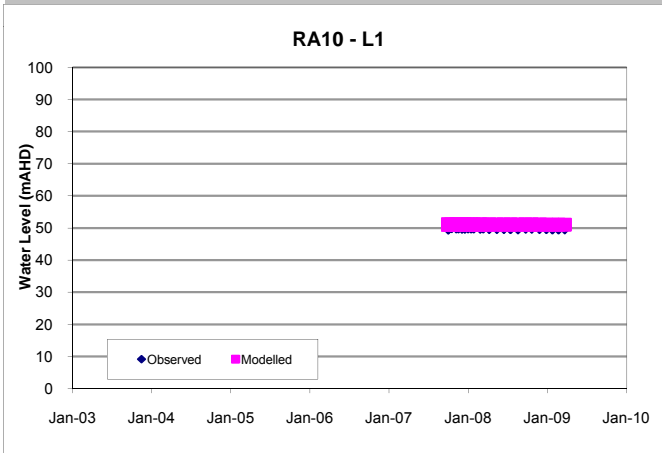
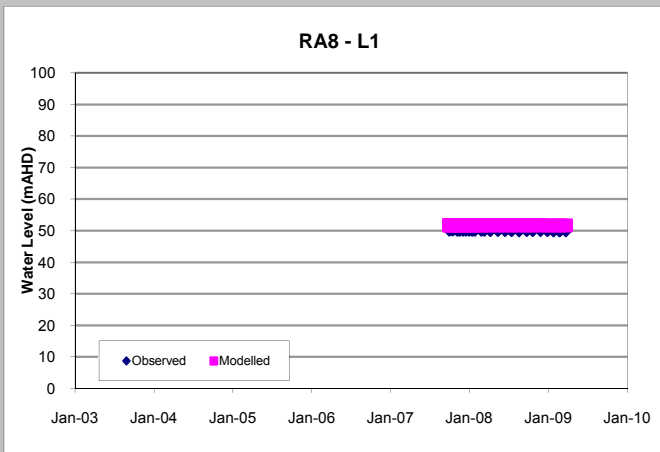
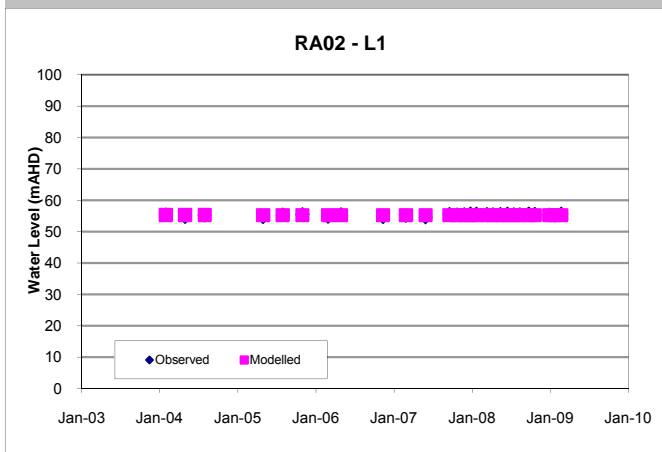
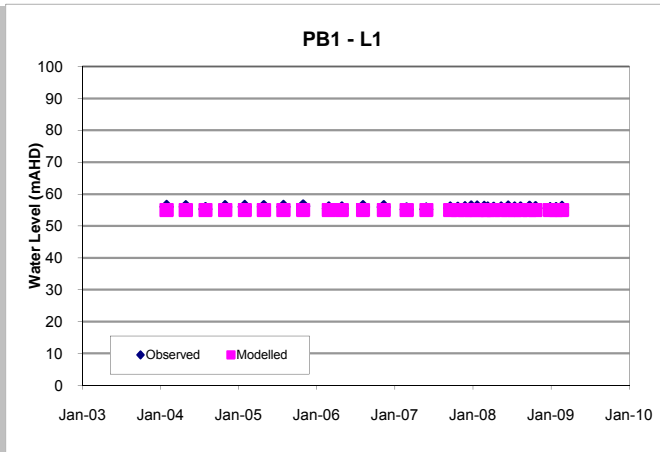
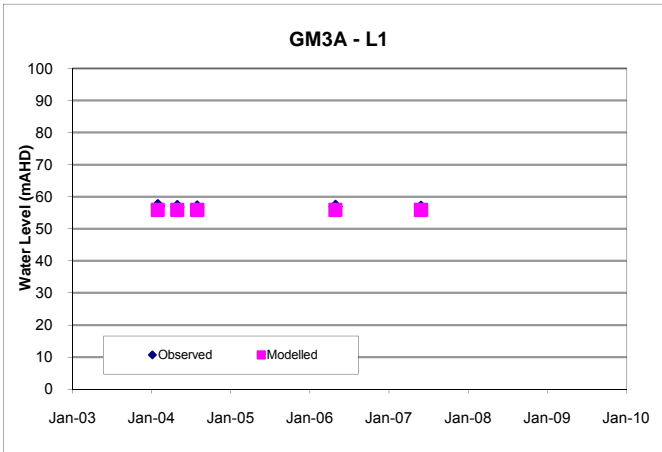
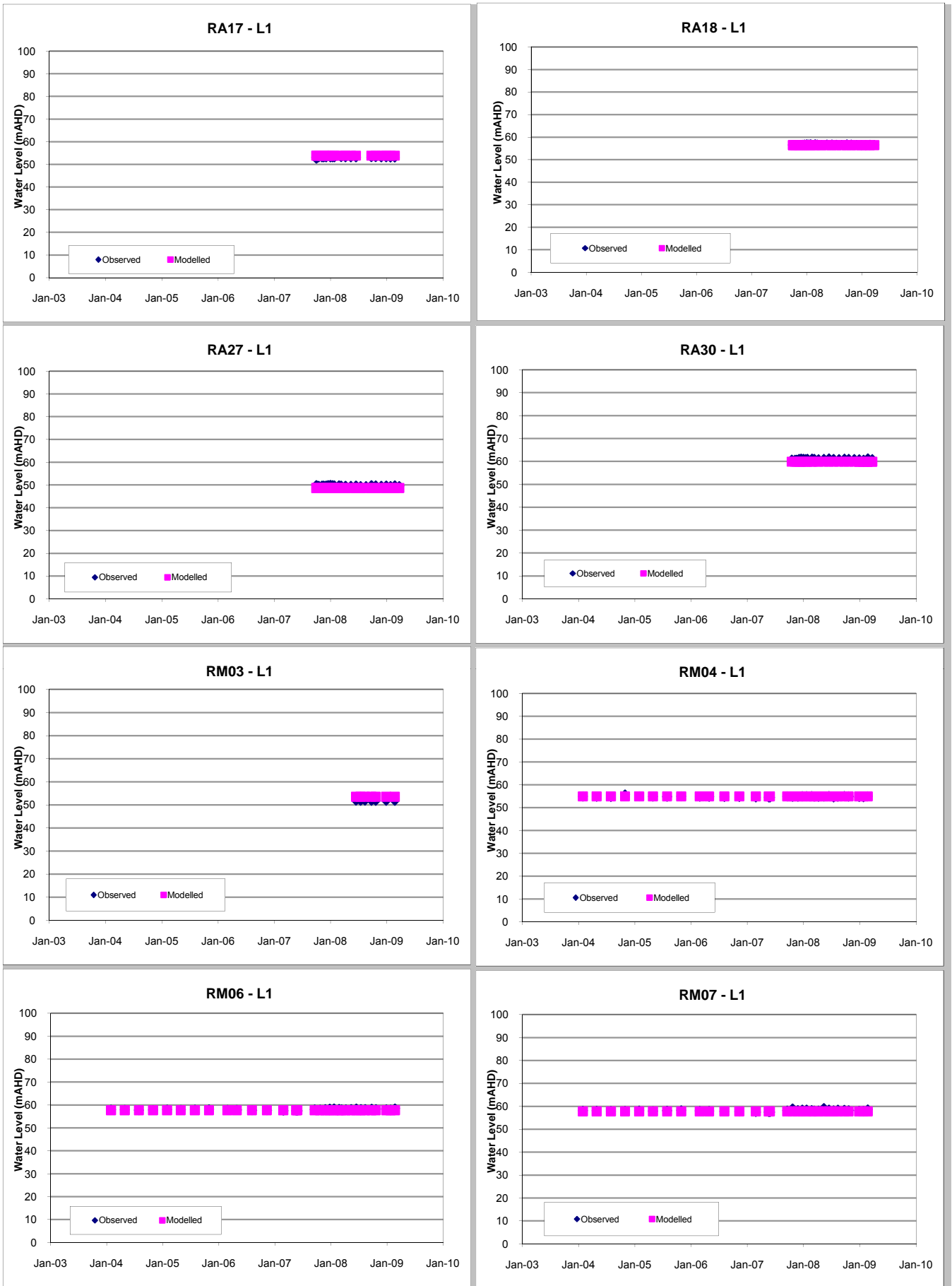
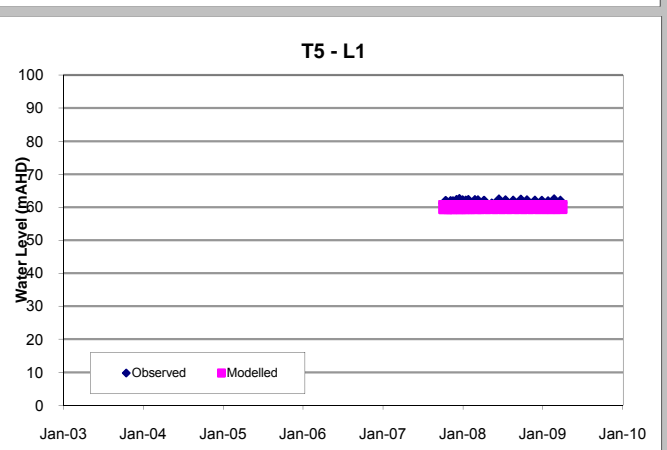
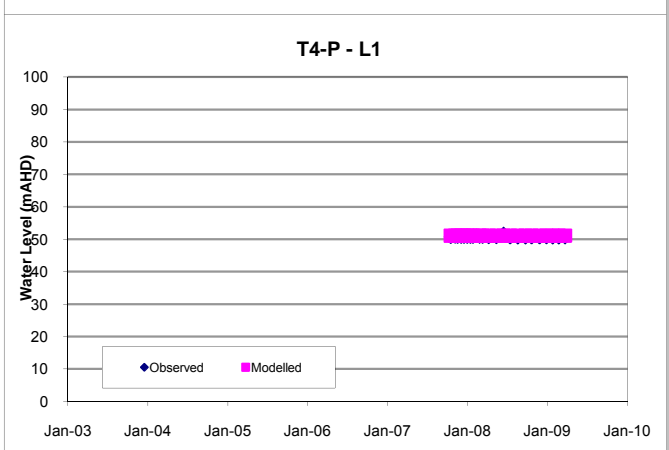
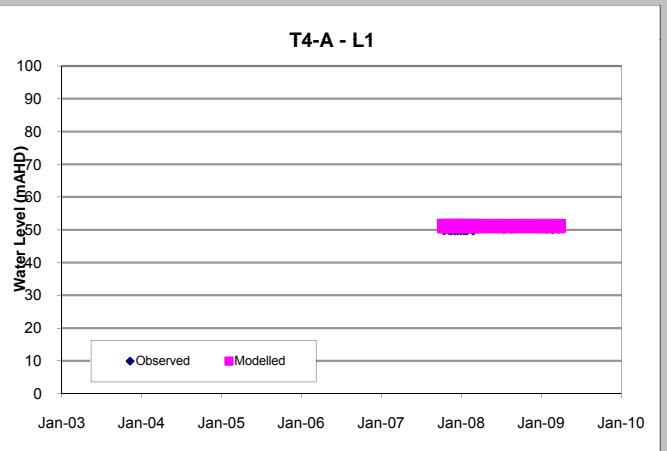
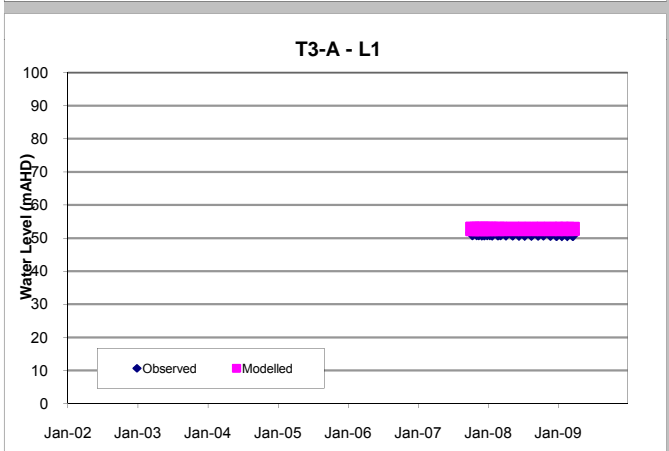
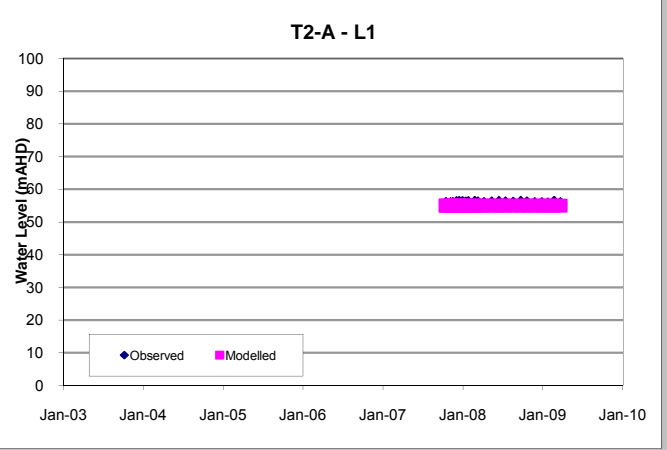
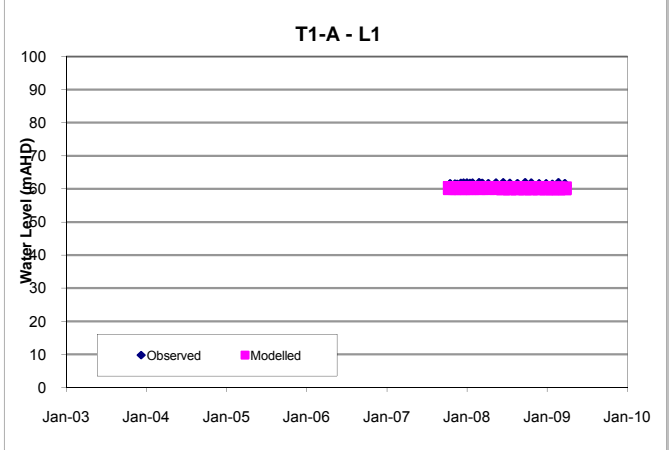
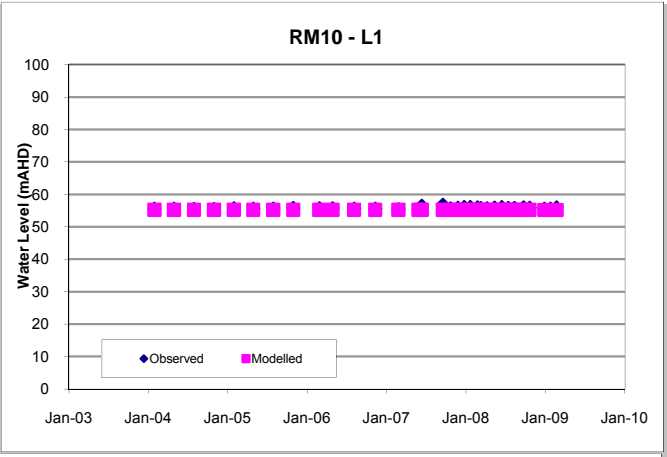
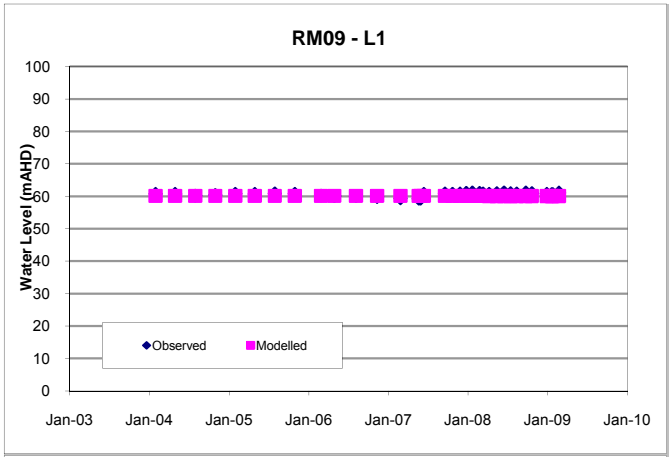


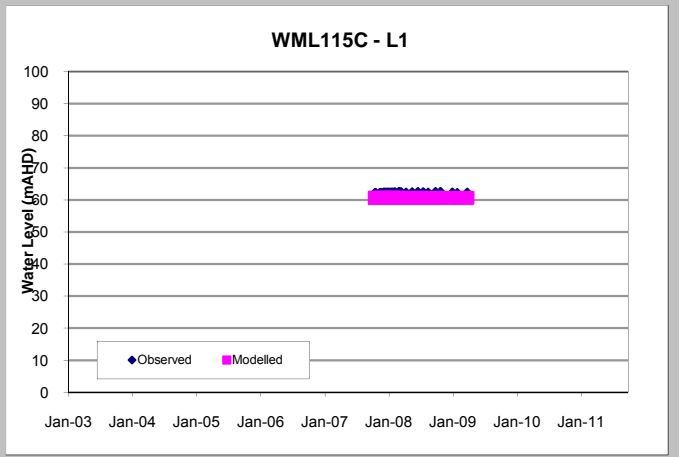
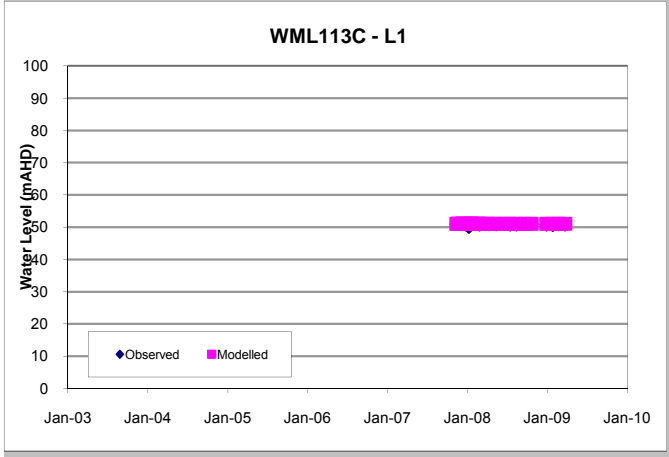
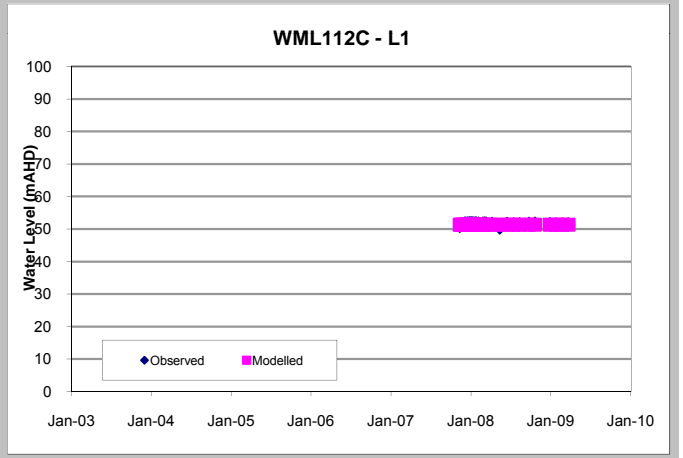
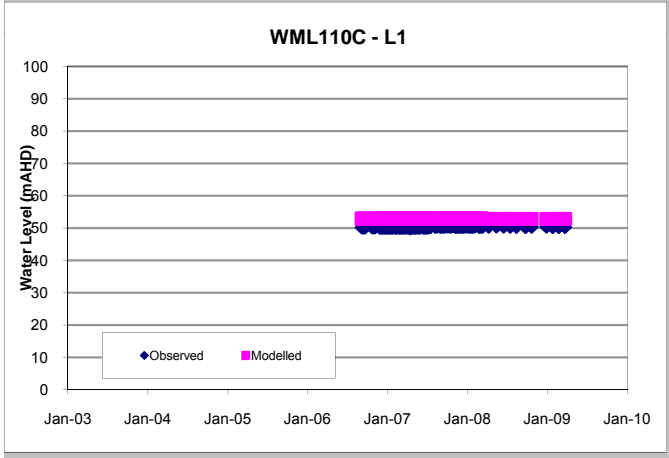
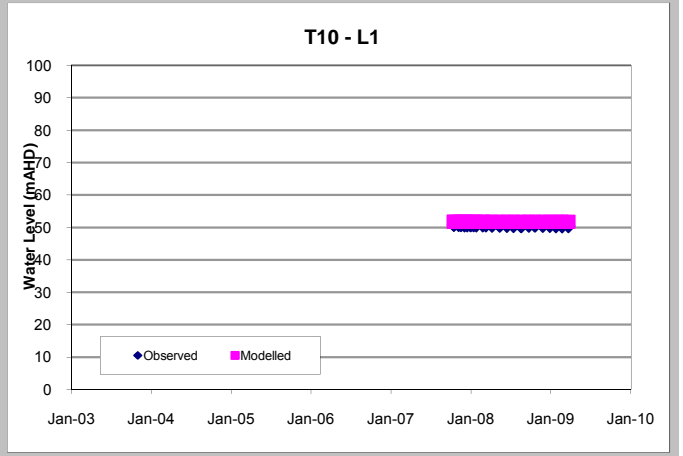
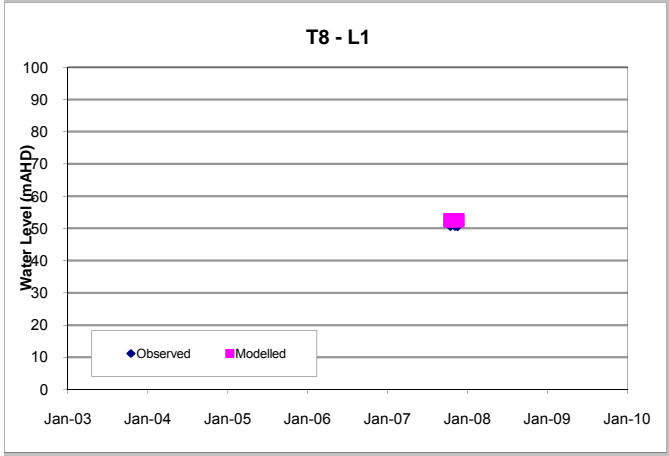
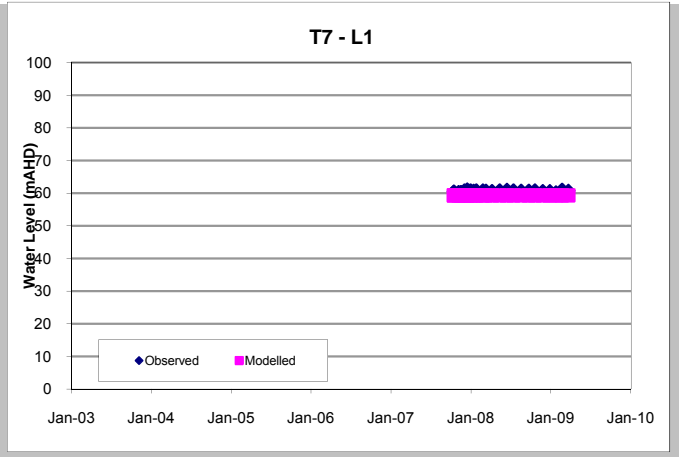
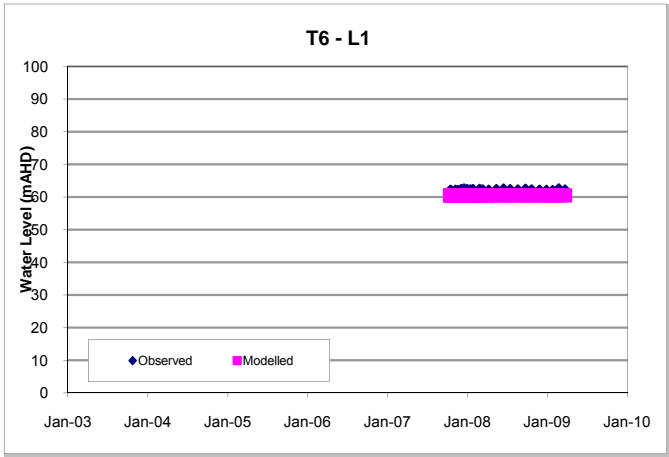
Figure C15: Scatter Plot of Steady State Calibration

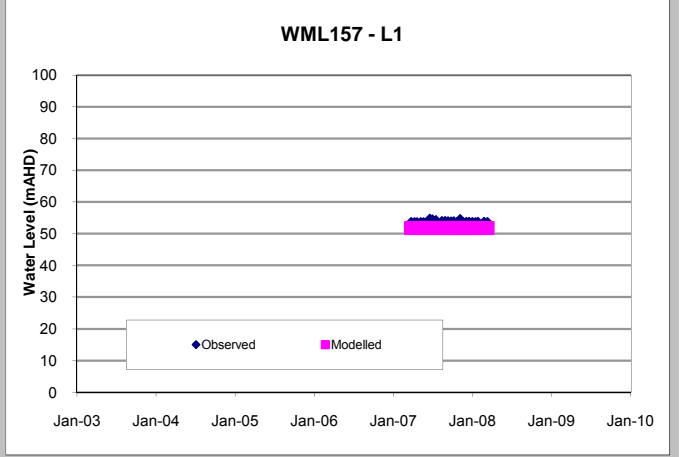
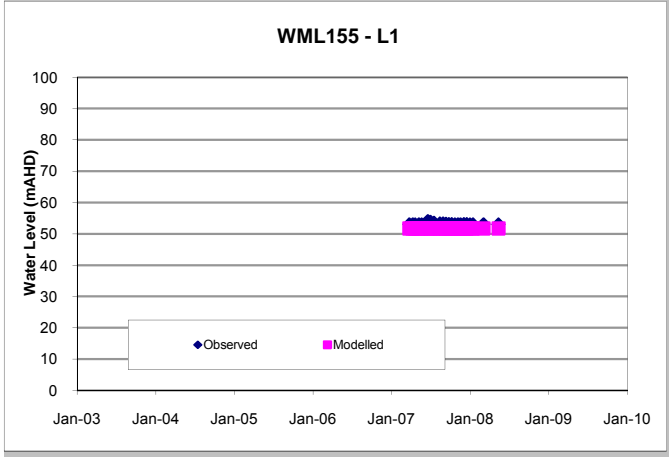
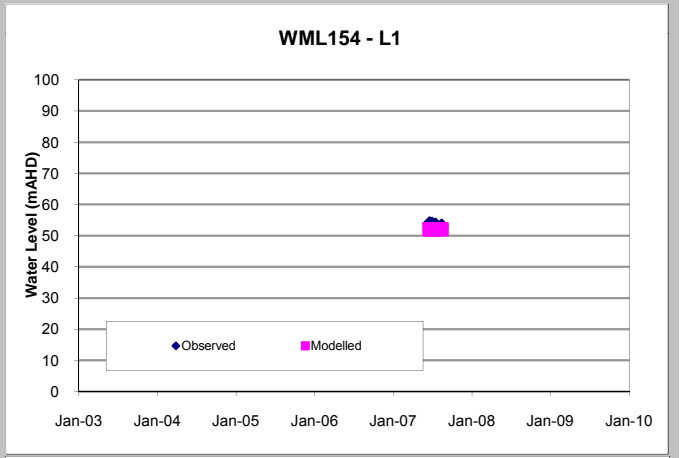
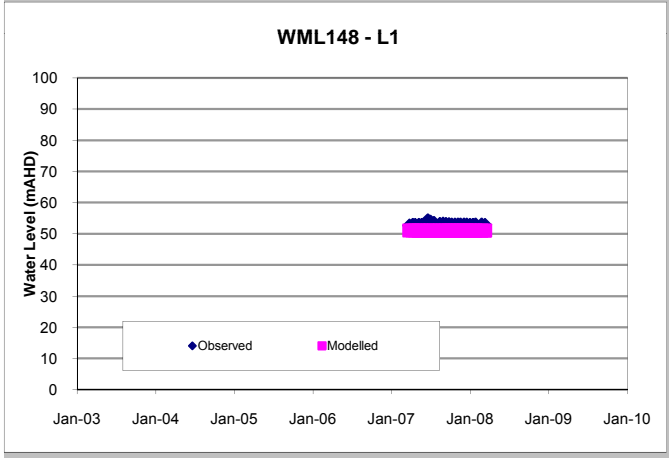
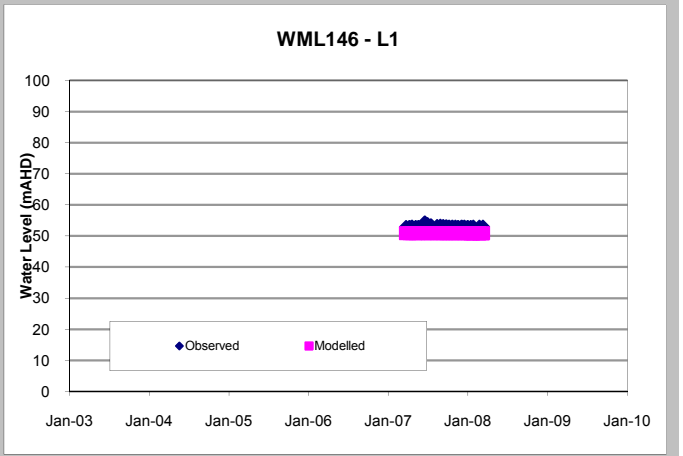
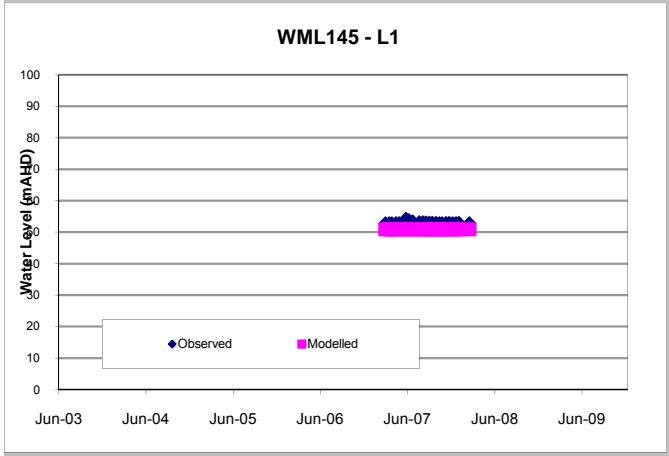
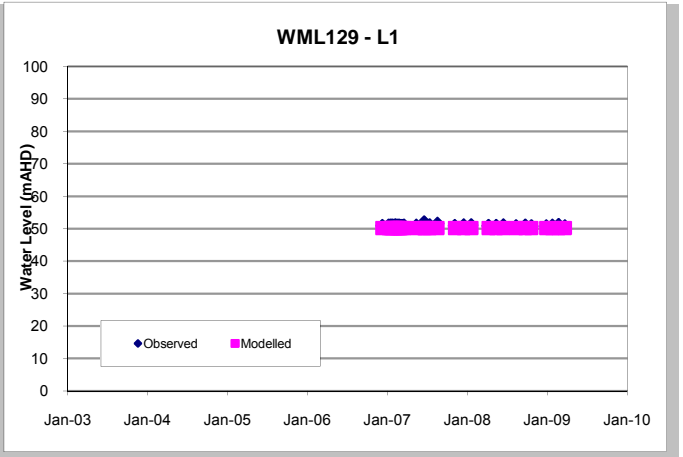
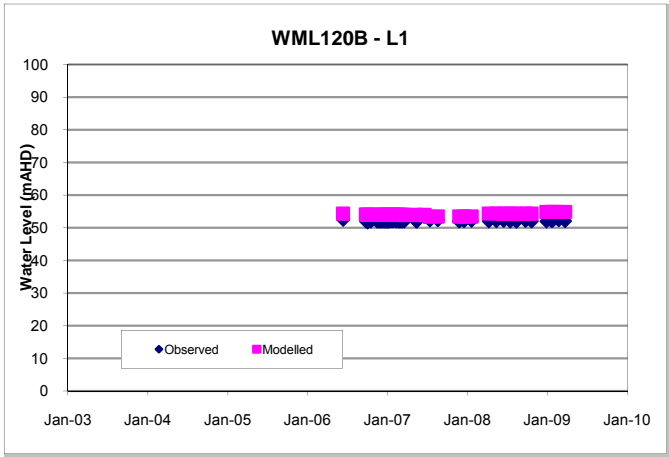


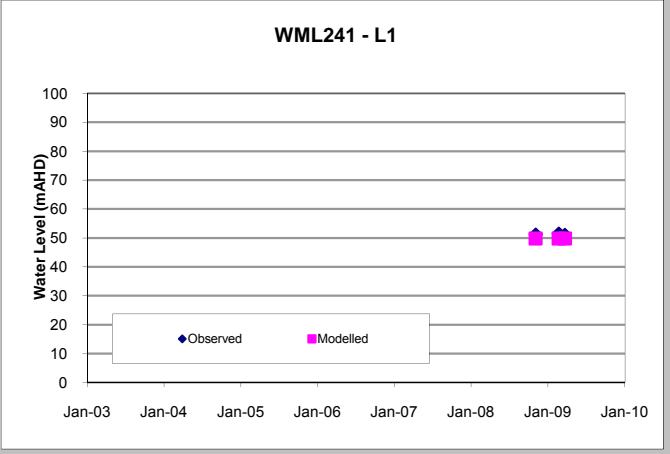
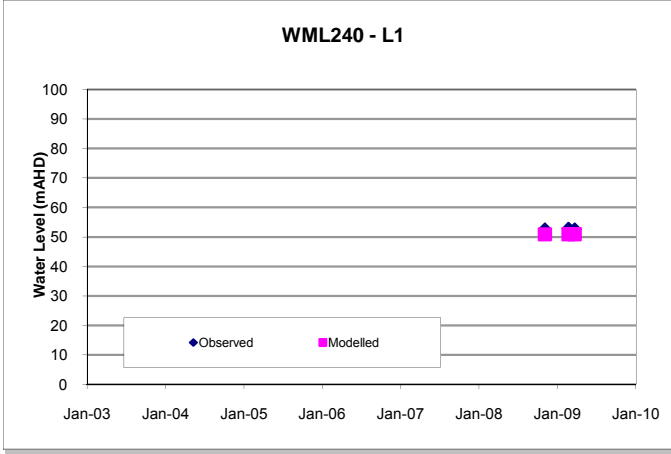
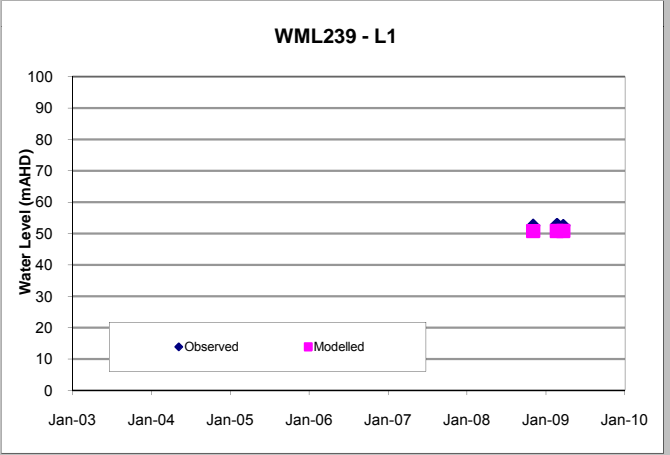
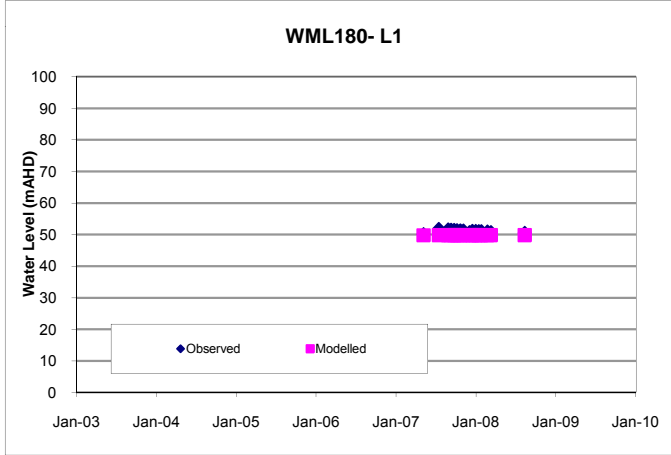
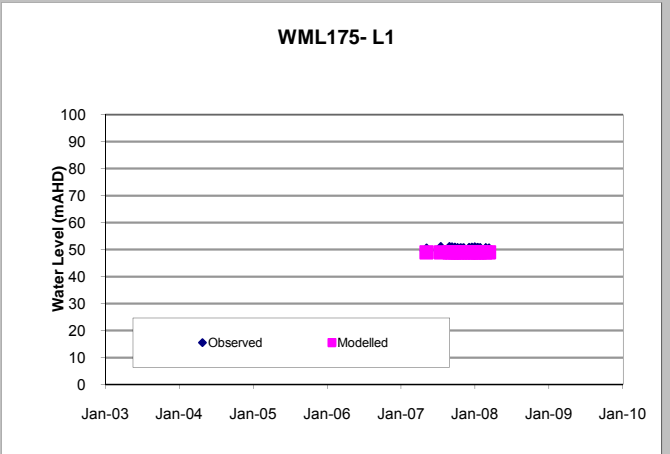
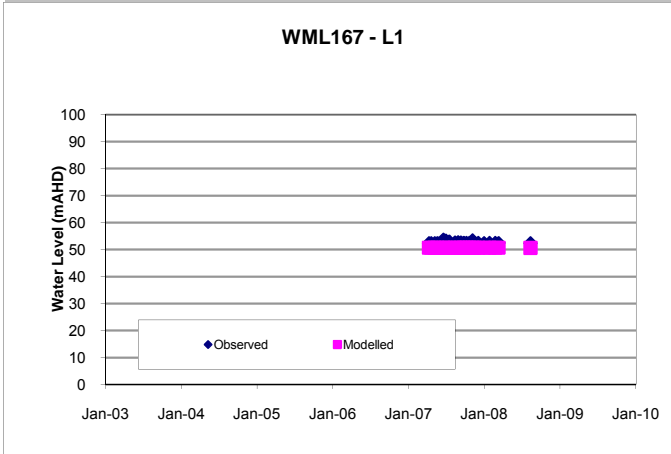
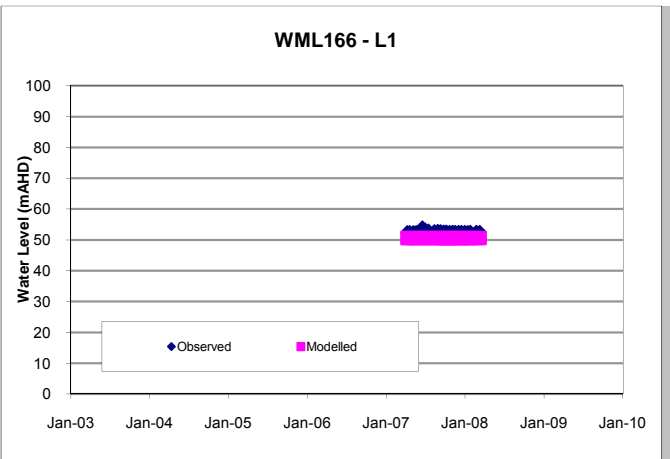
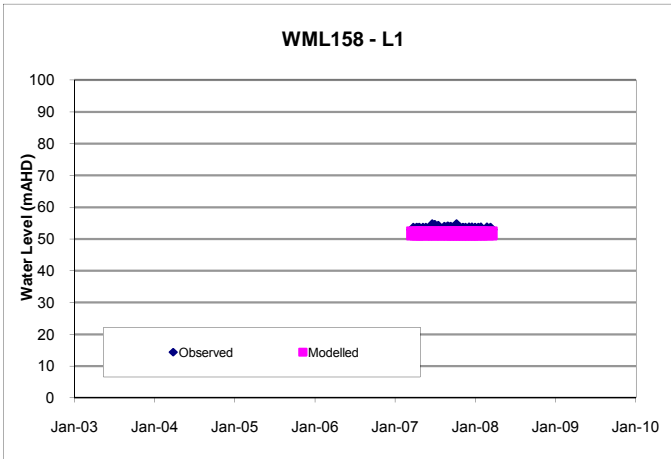




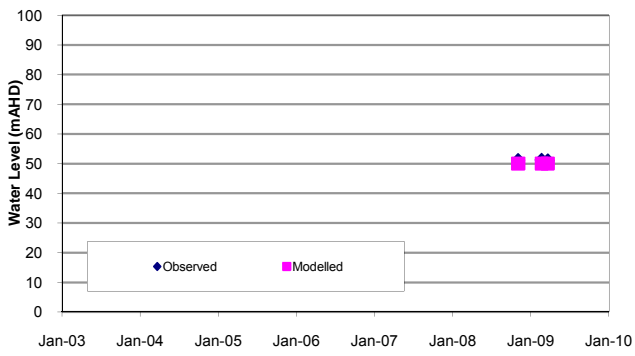




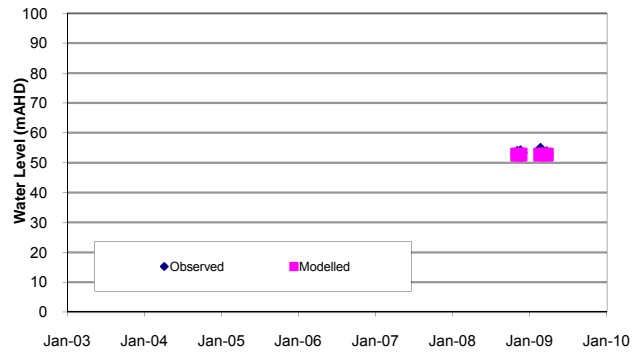




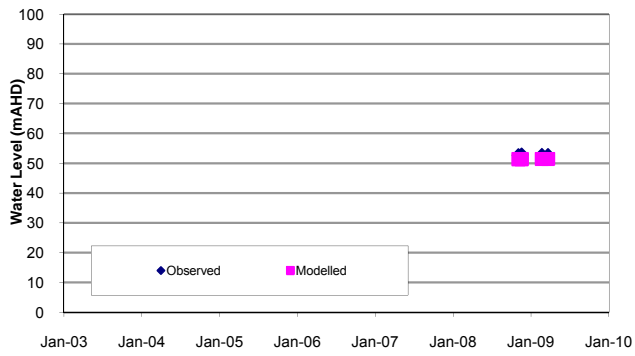
WML243 - L1



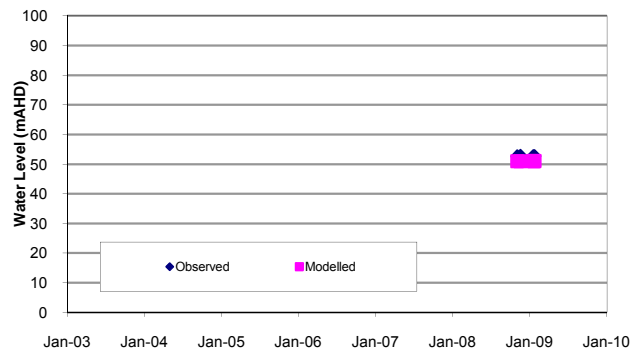
WML247 - L1



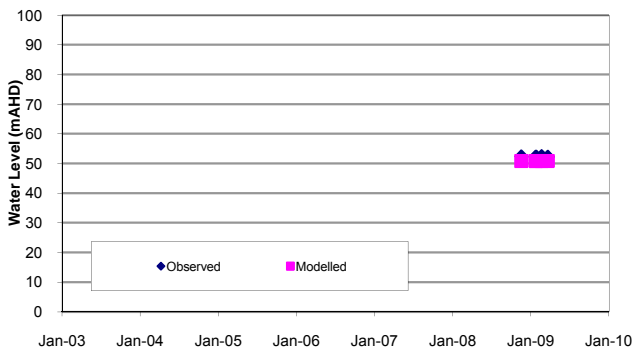
WML249 - L1



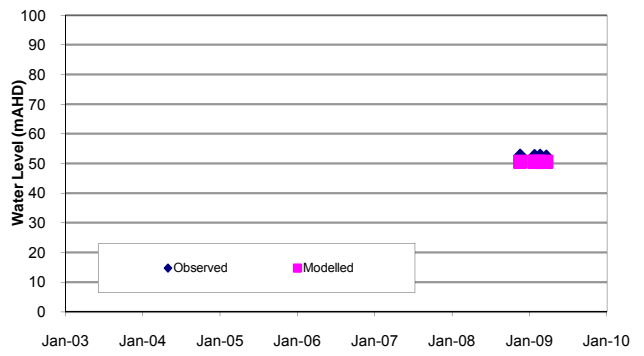
WML250 - L1



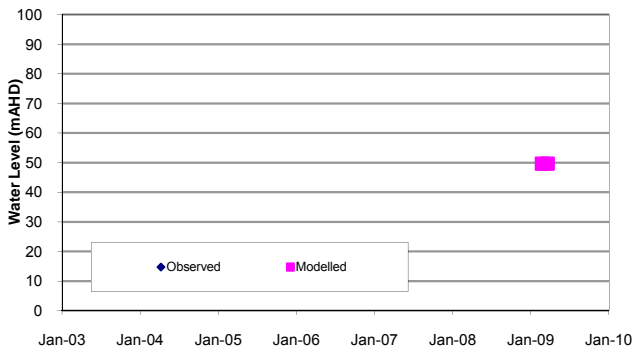
WML251 - L1

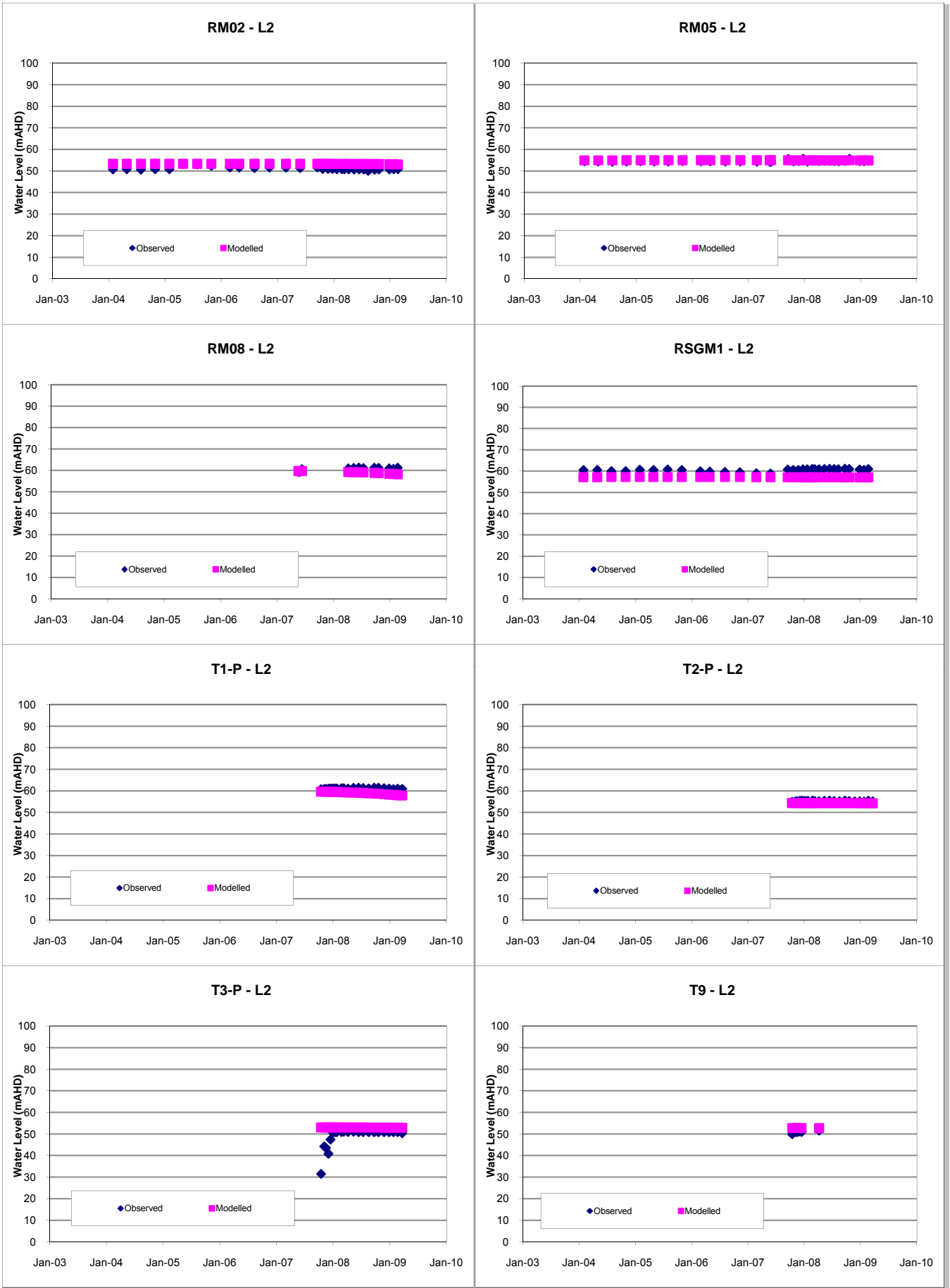


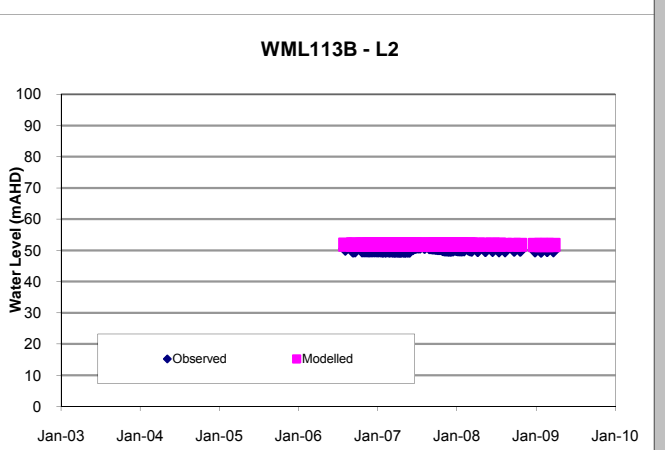
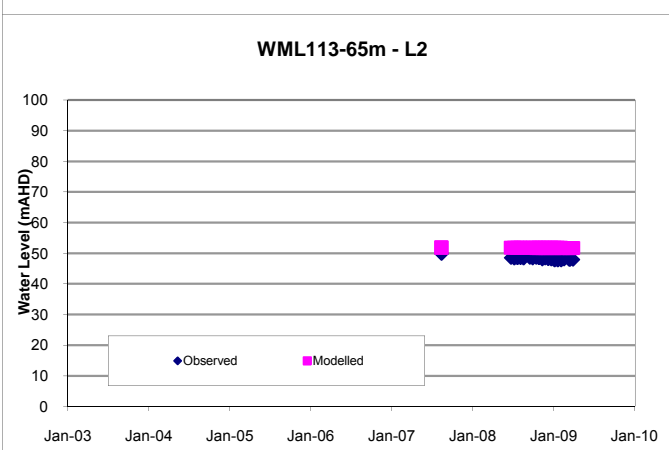
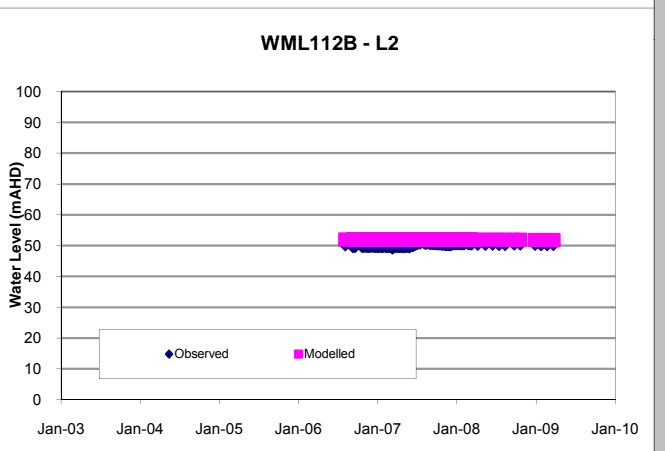
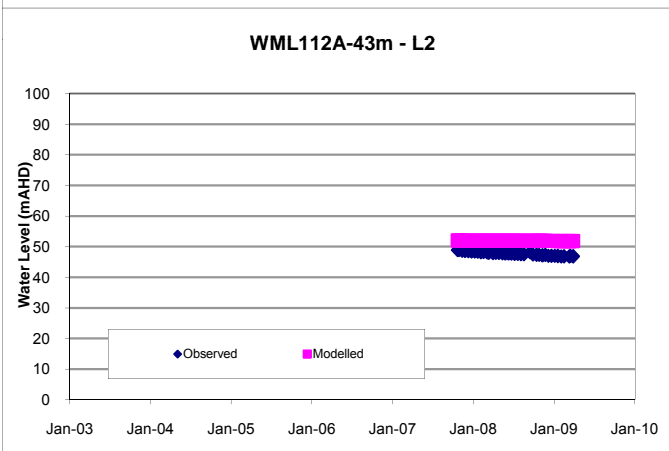
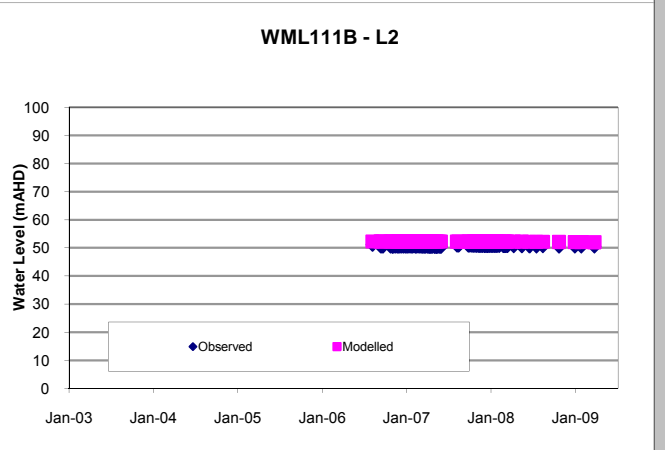
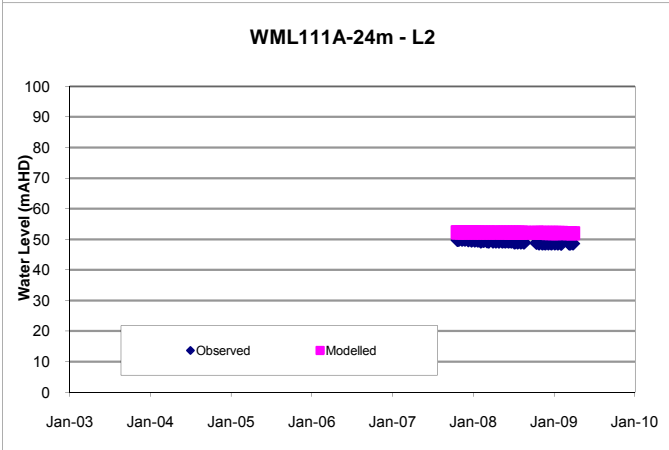
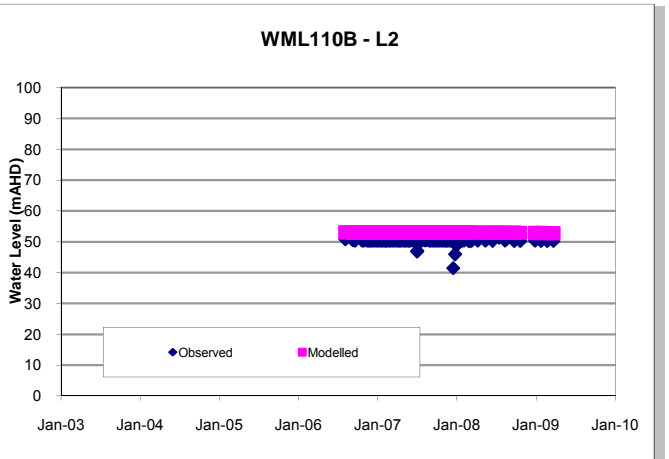
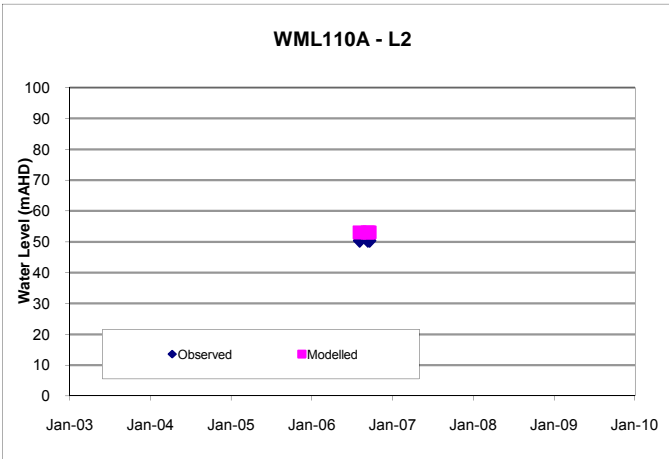
WML253 - L1



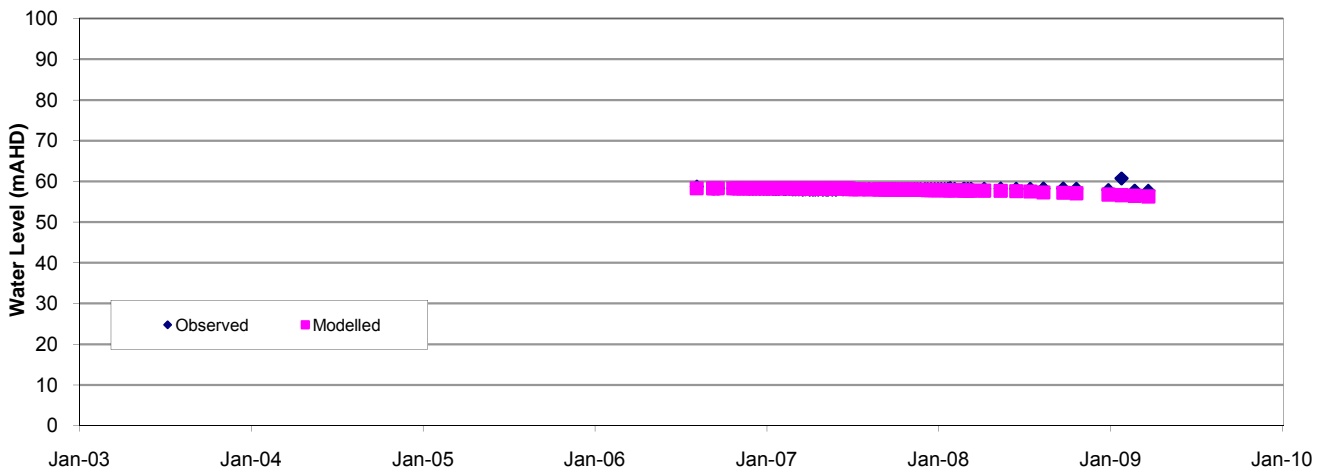
WML256 - L1



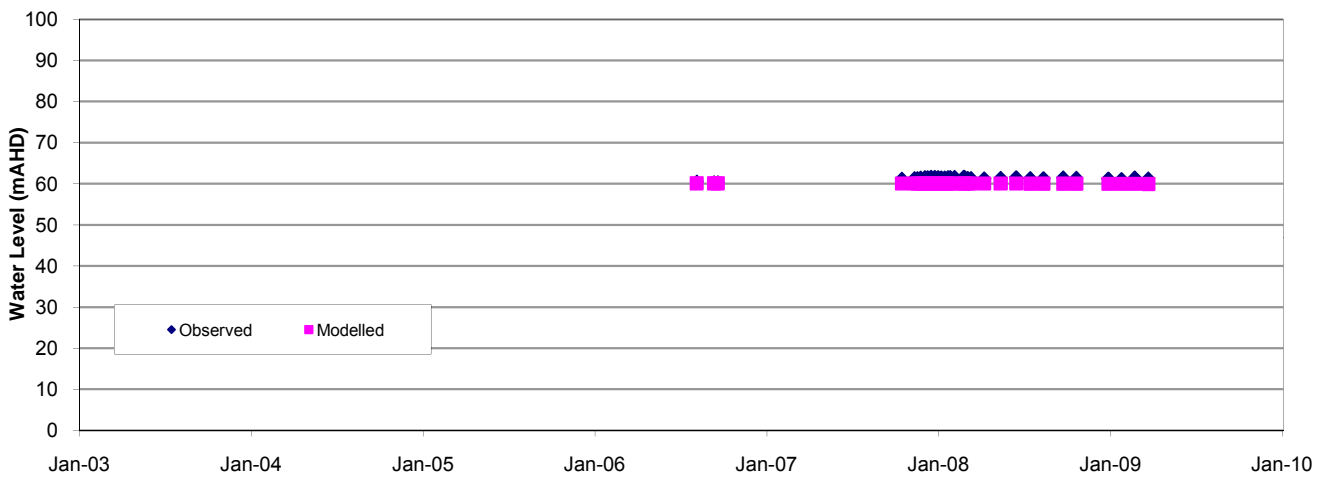




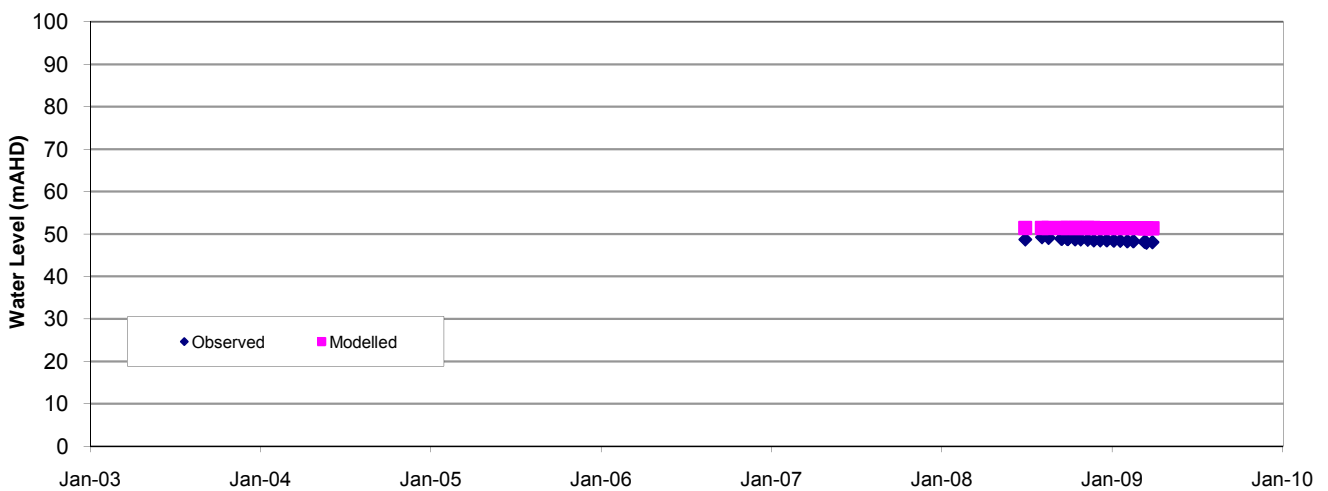
WML114B - L2

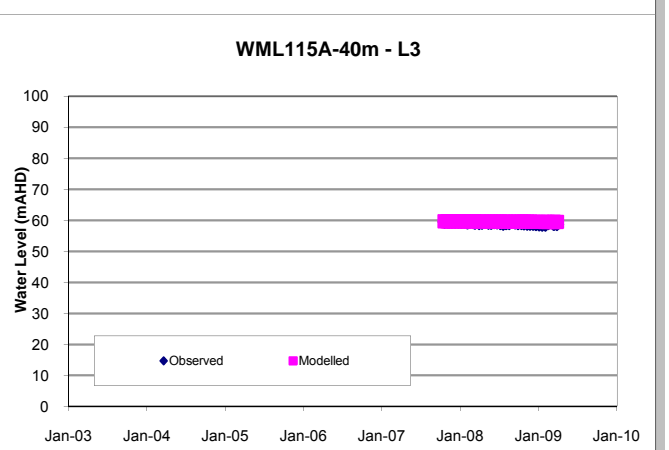
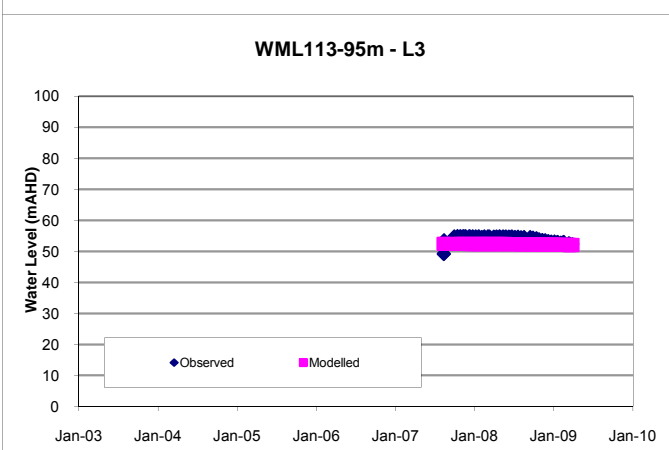
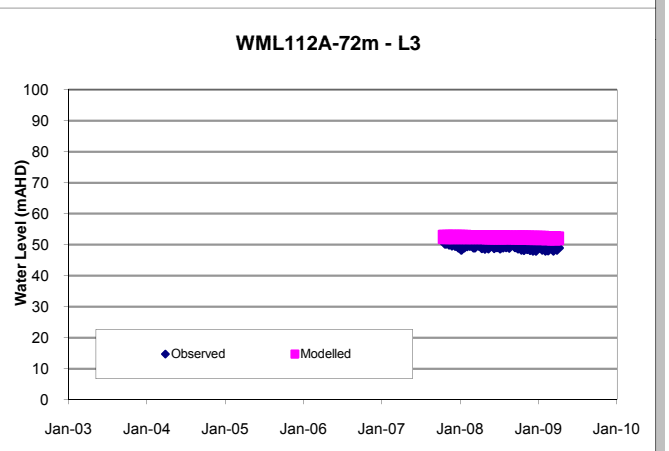
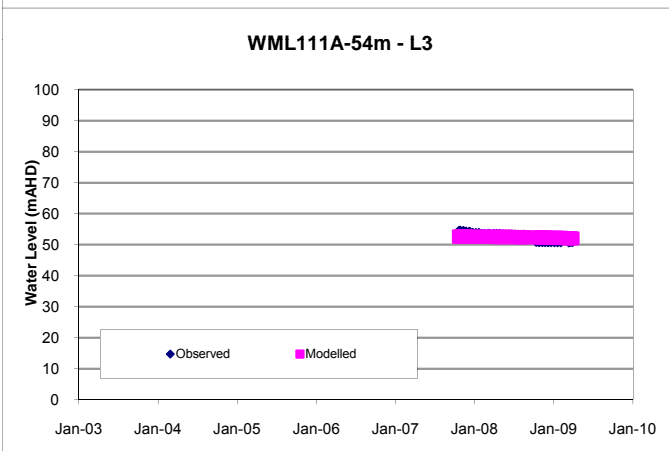
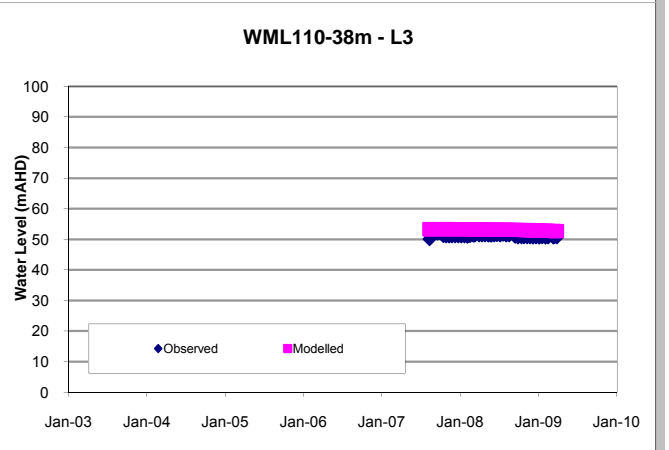
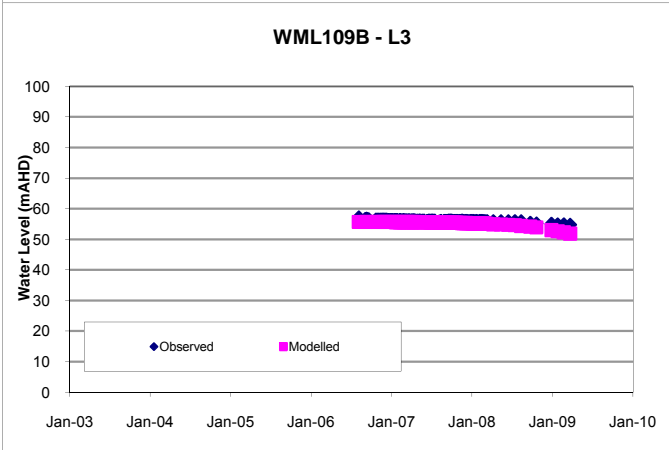
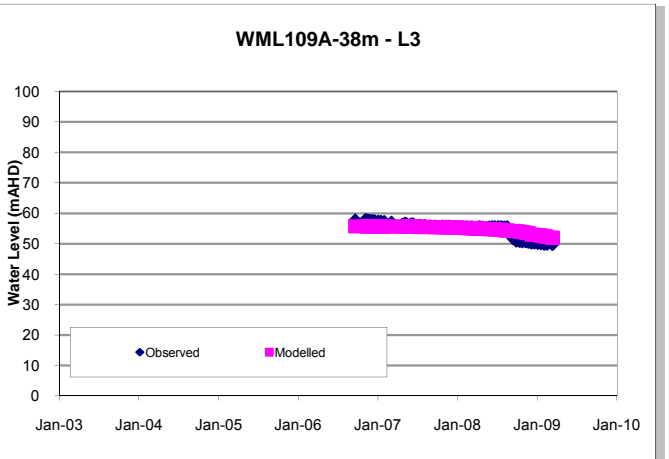
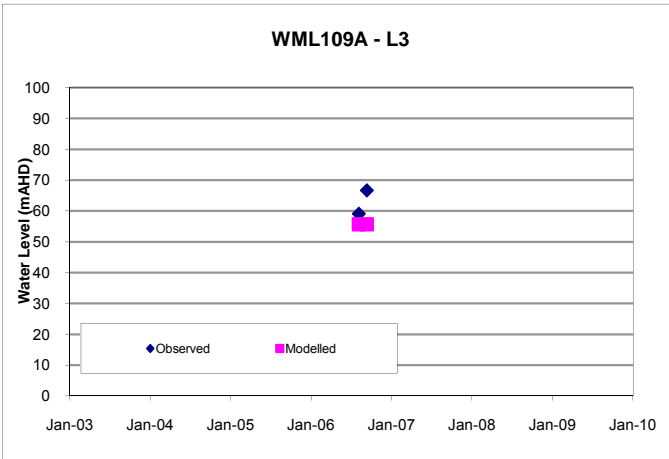


WML115B - L2

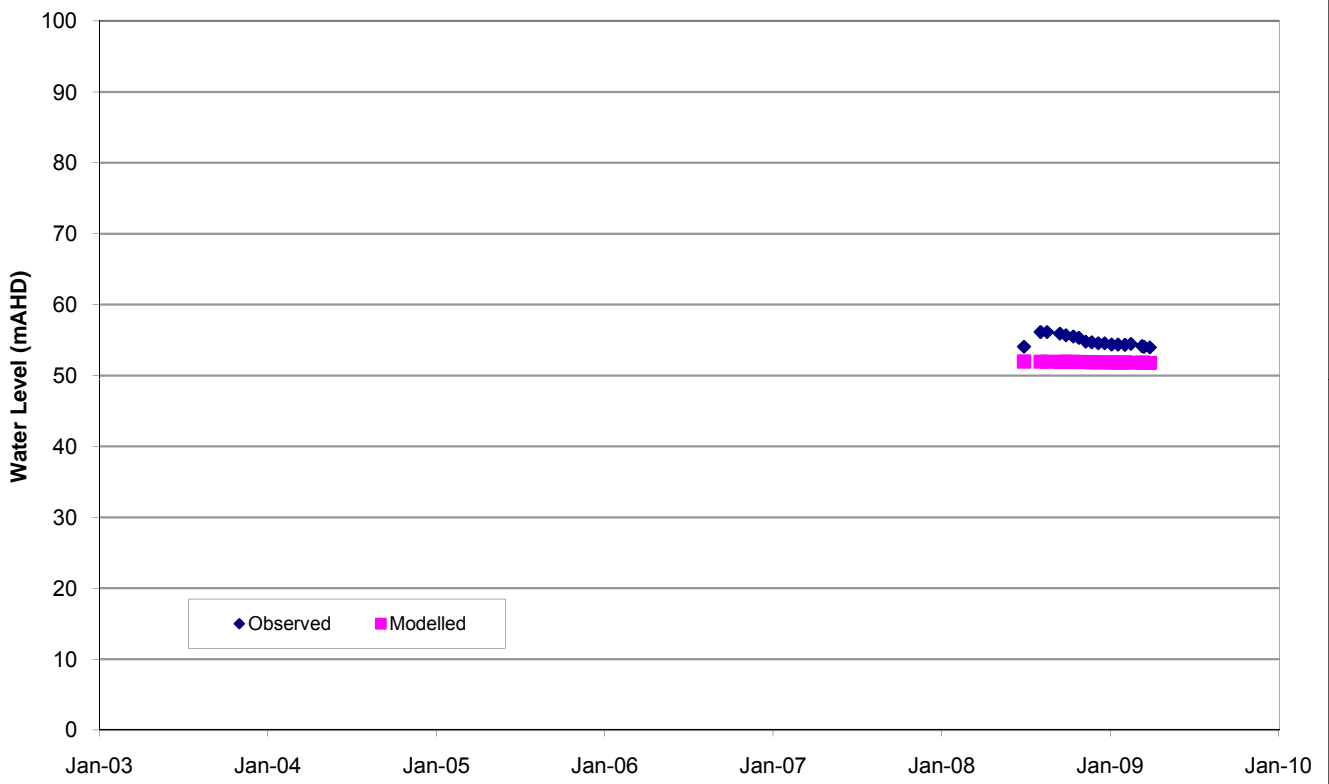


WML213-48m - L2

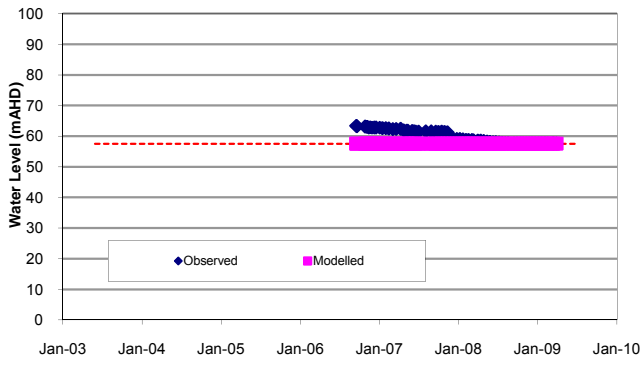




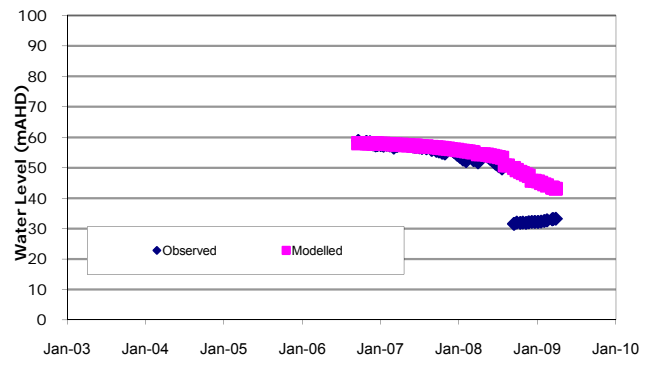
WML213-110.5m - L3



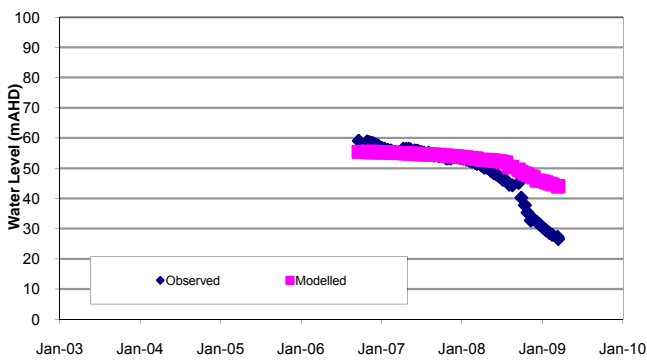
WML107A-38m - L4



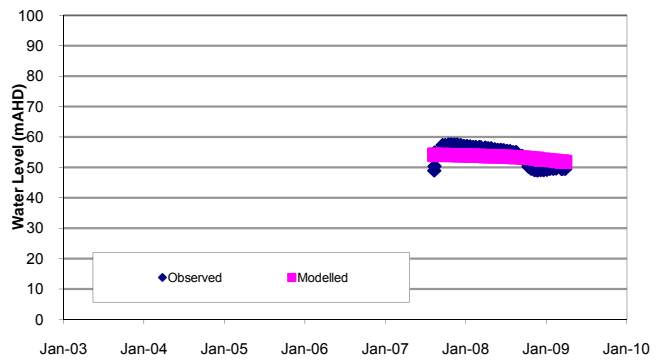
WML108A-53m - L4



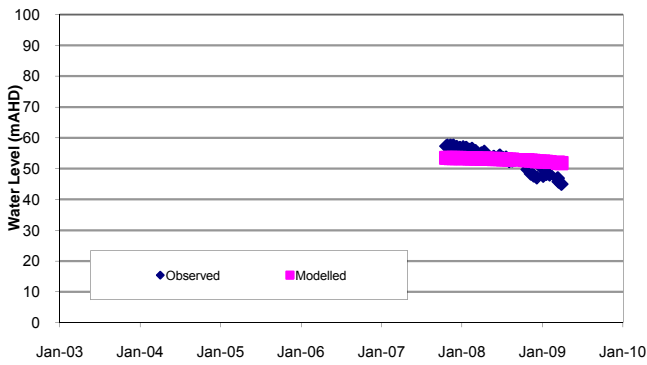
WML109A-65m - L4



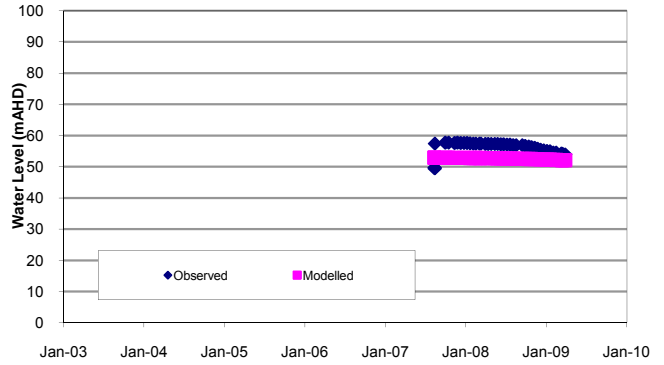
WML110-90m - L4



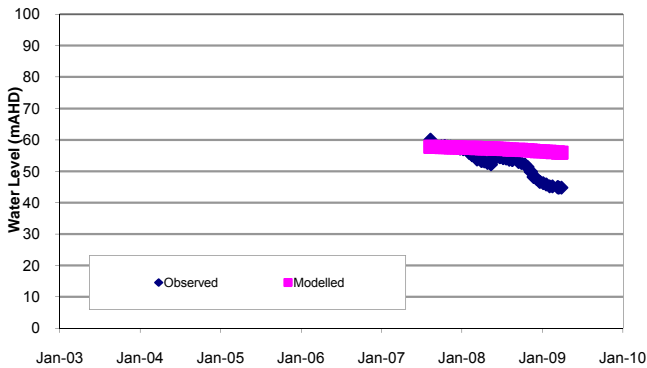
WML111A-90m - L4



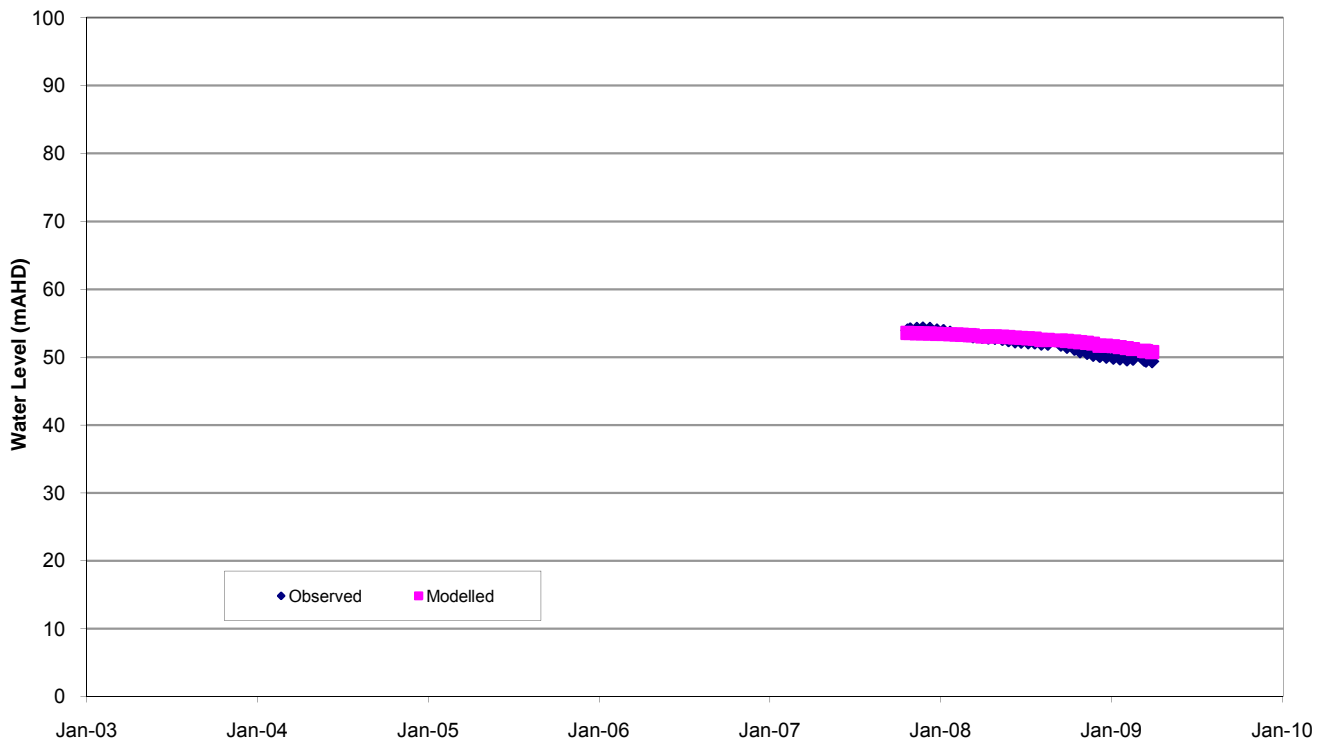
WML113-124m - L4



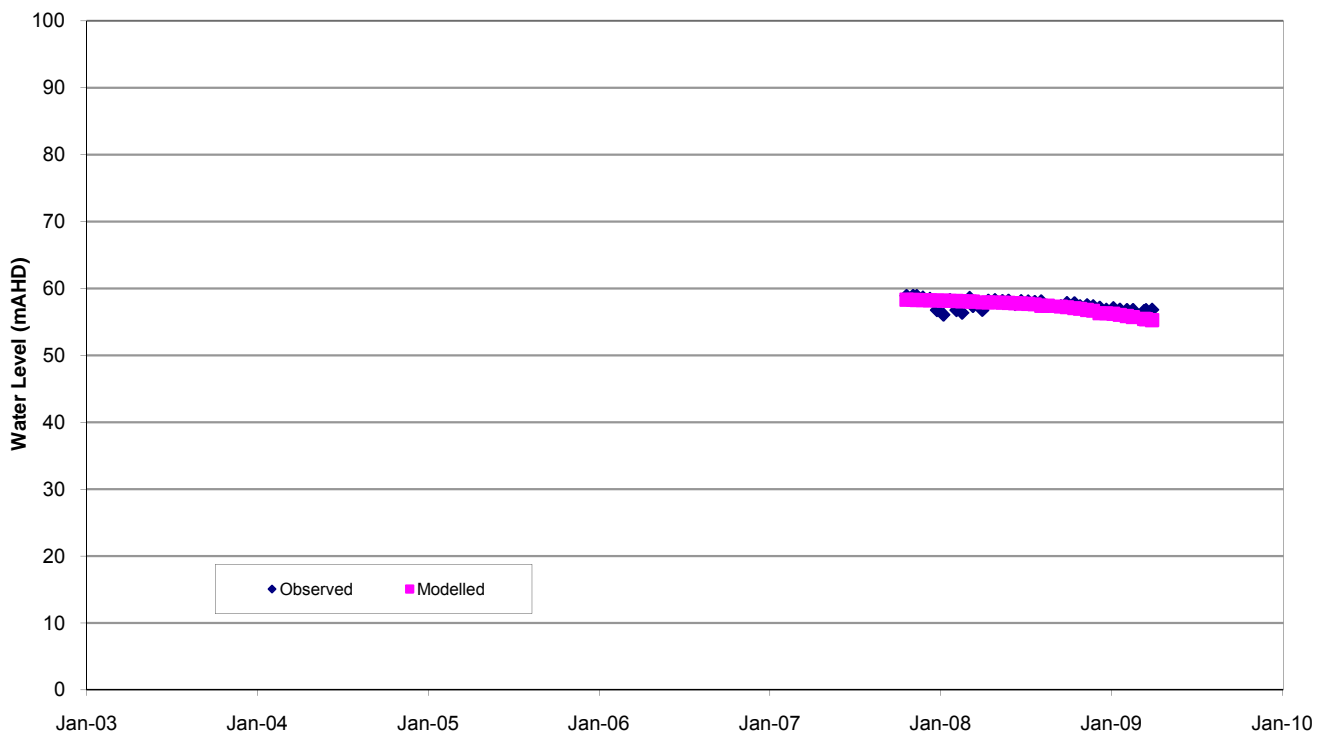
WML114-63m - L4

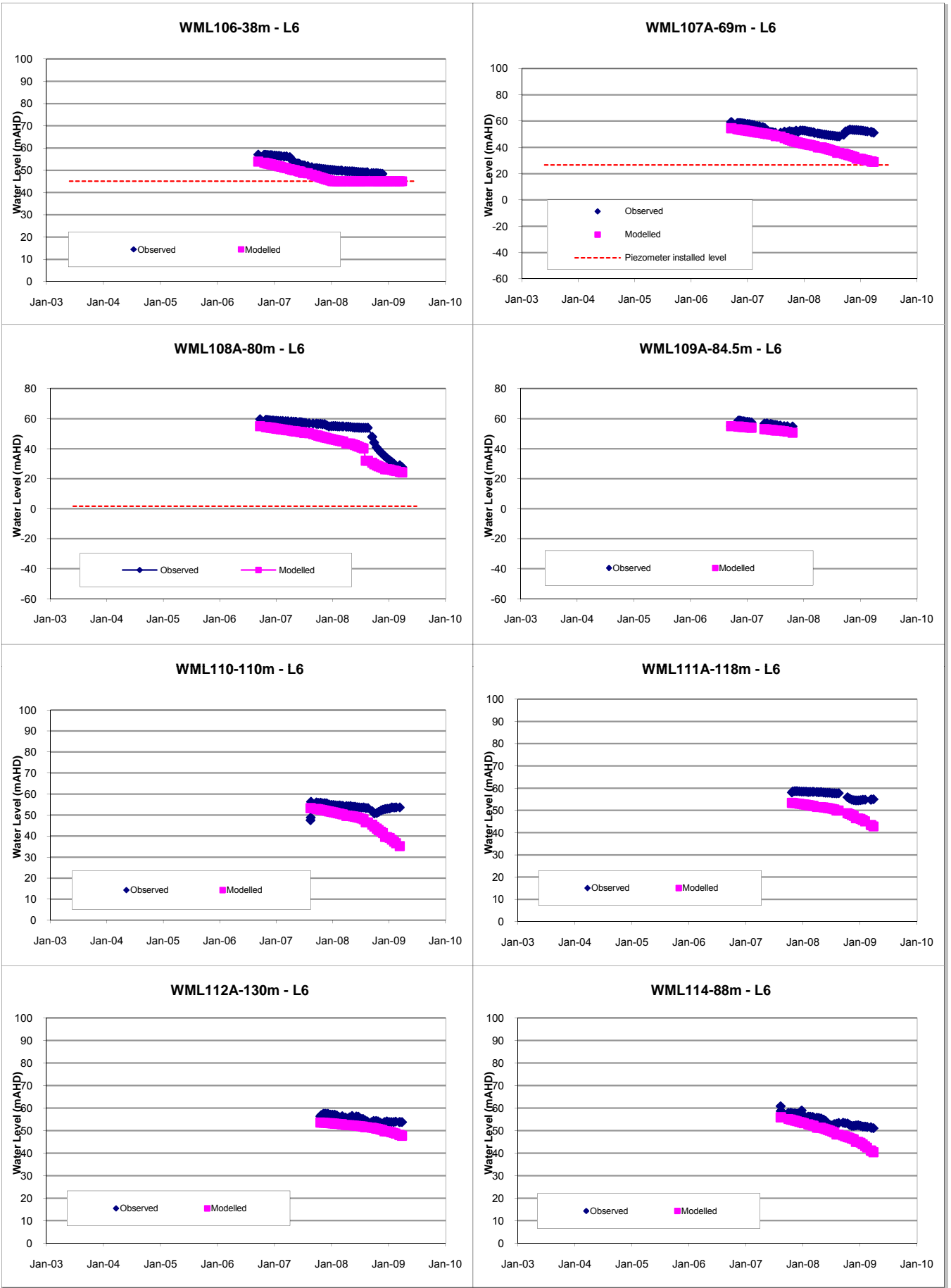


WML112A-101m - L5

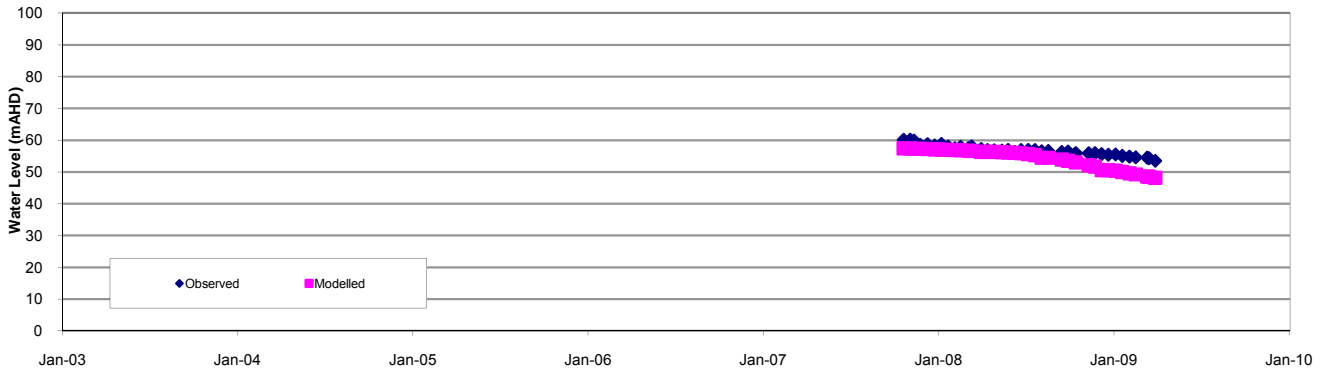


WML115A-72m - L5

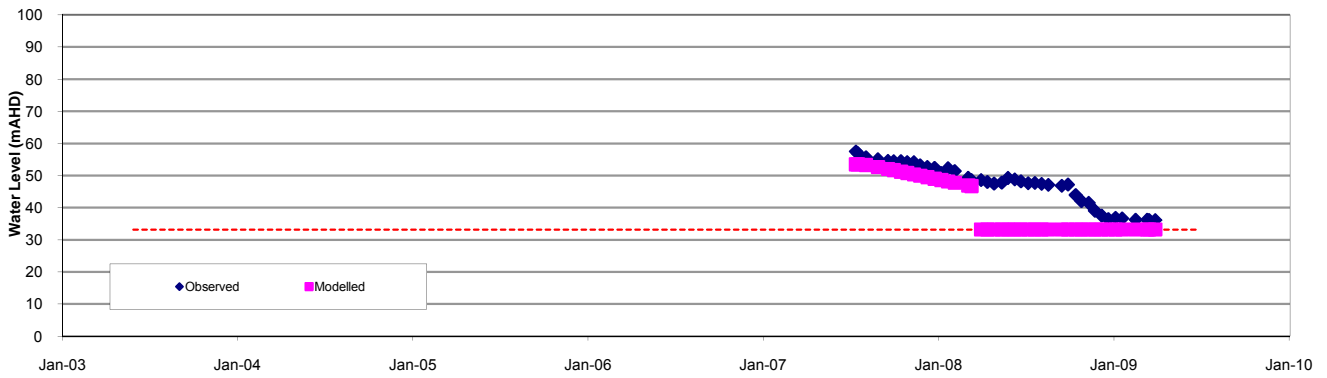




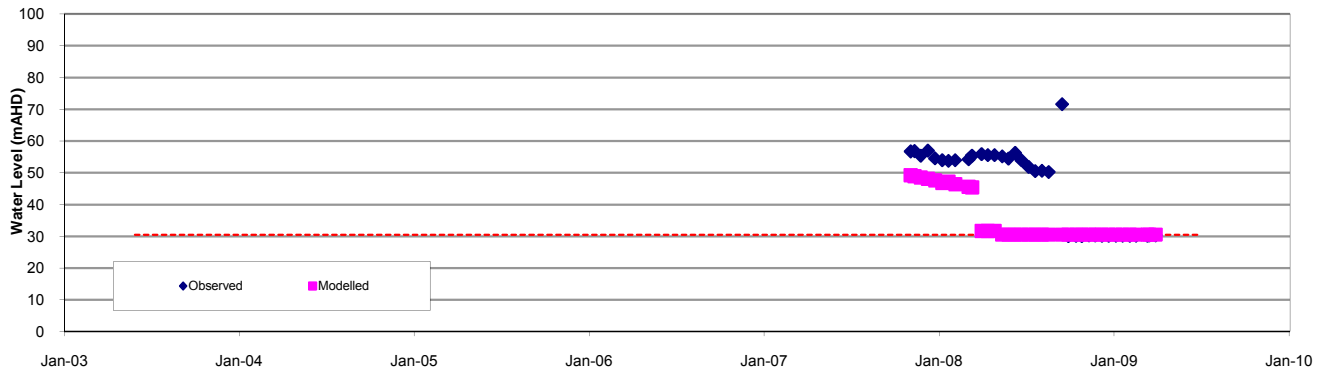
WML115A-93m - L6



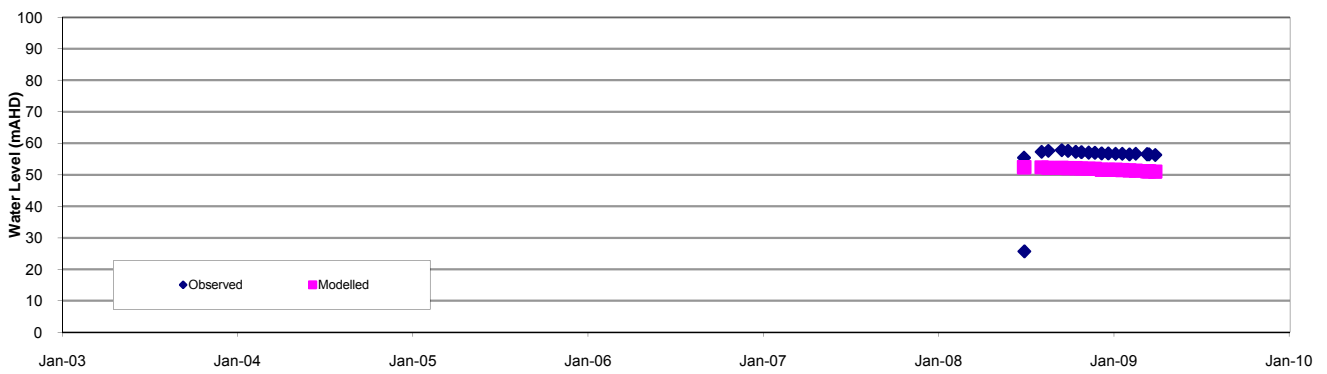
WML189-49m- L6



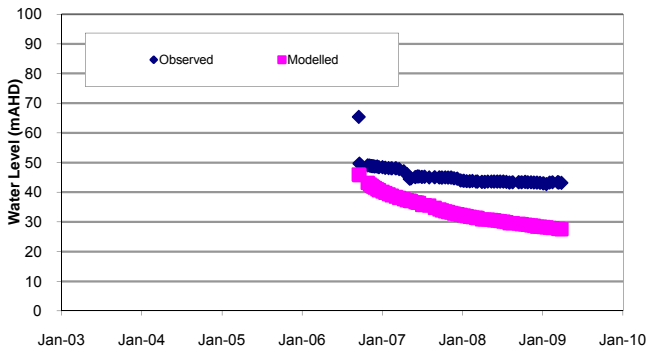
WML191-52m- L6



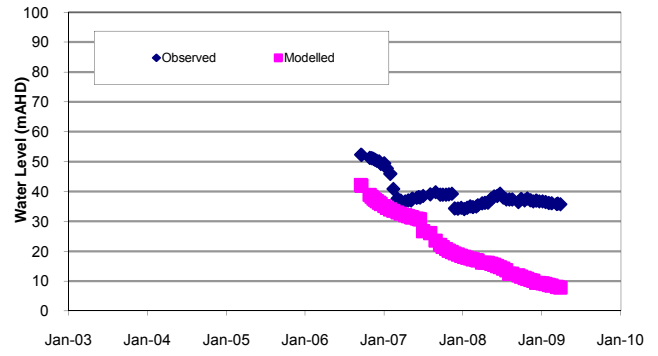
WML213-169.5m - L6



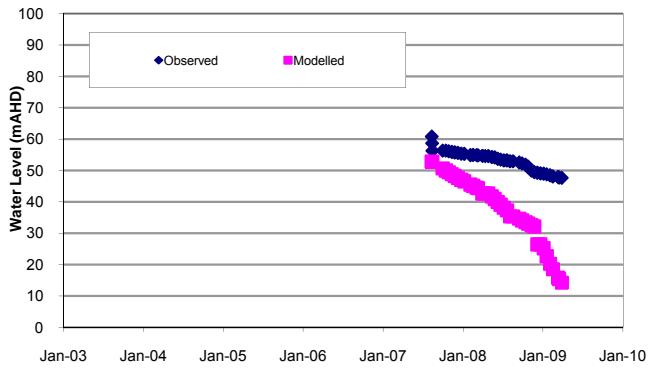
WML106-68m - L7



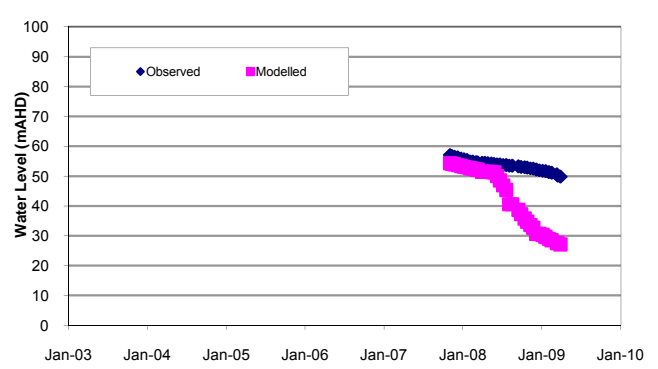
WML107A-98m - L7



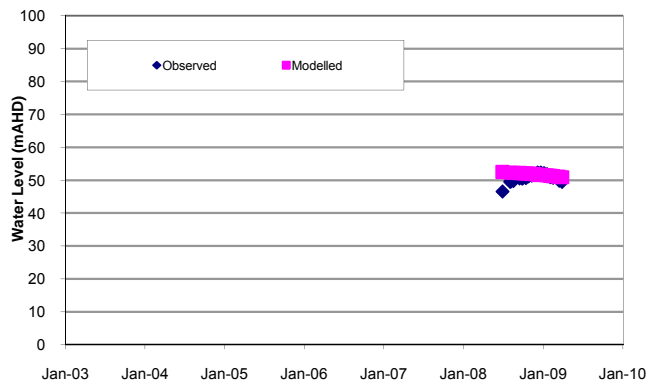
WML114-108m - L7

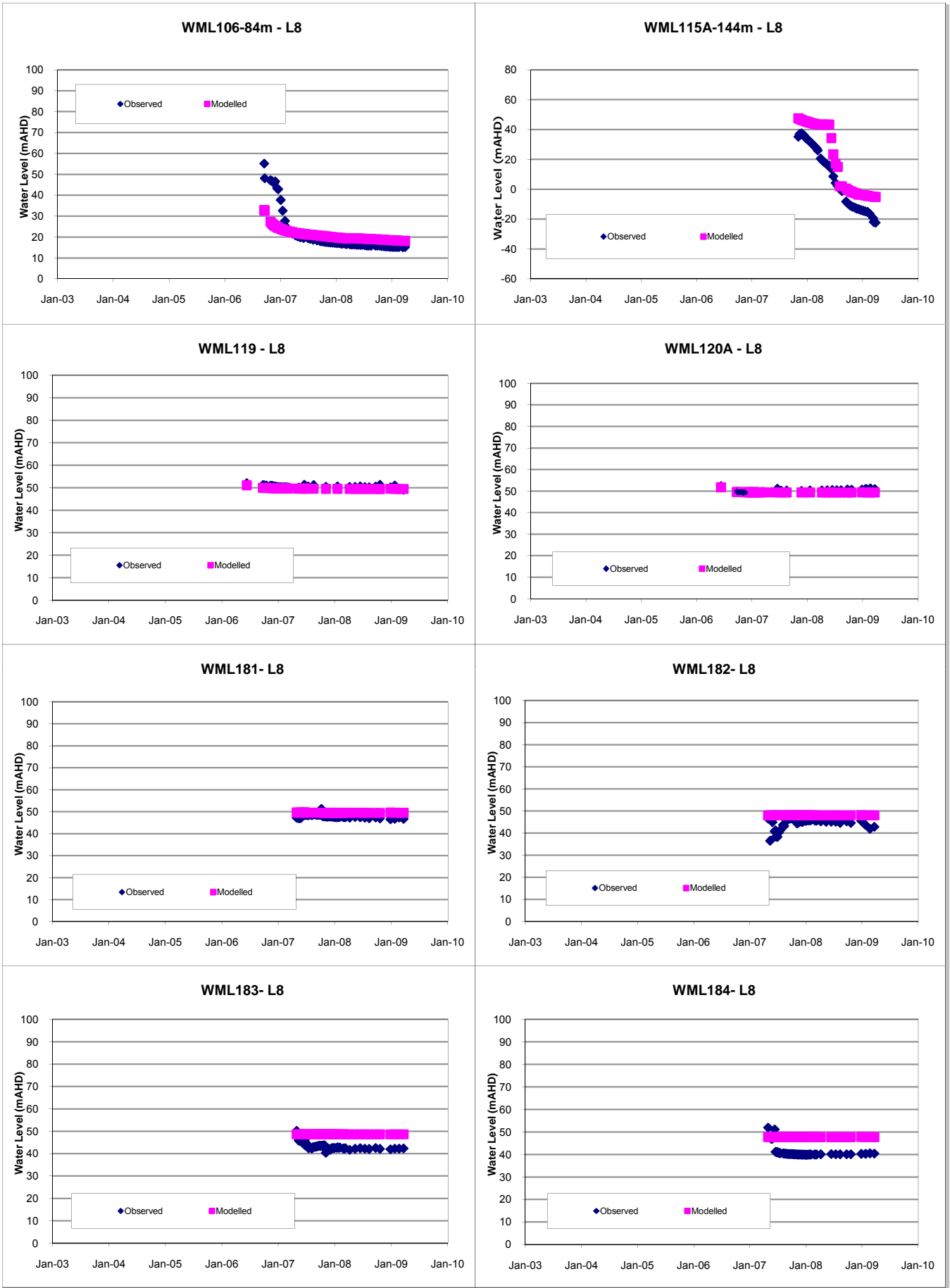


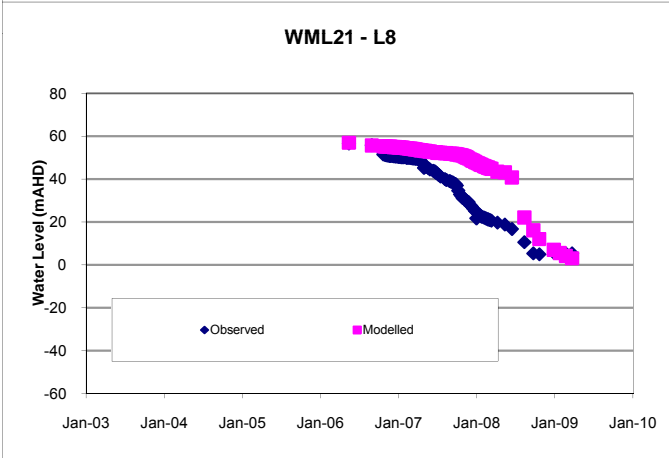
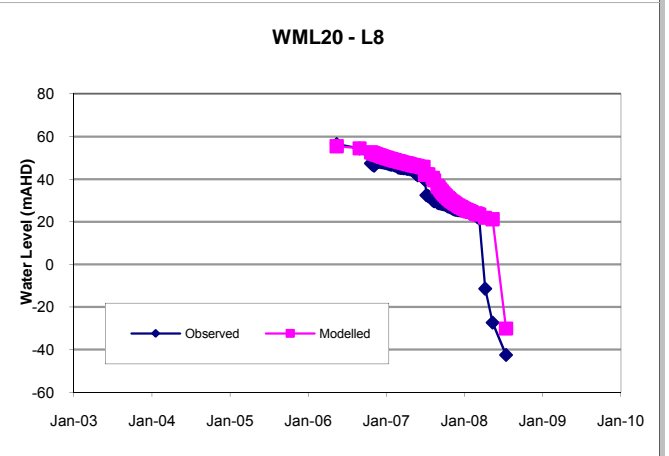
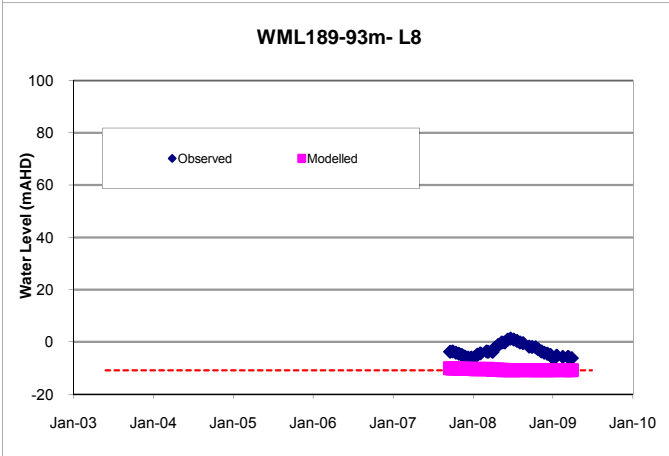
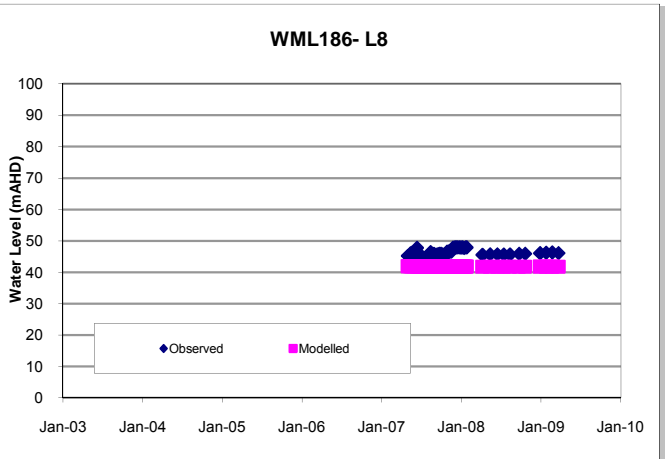
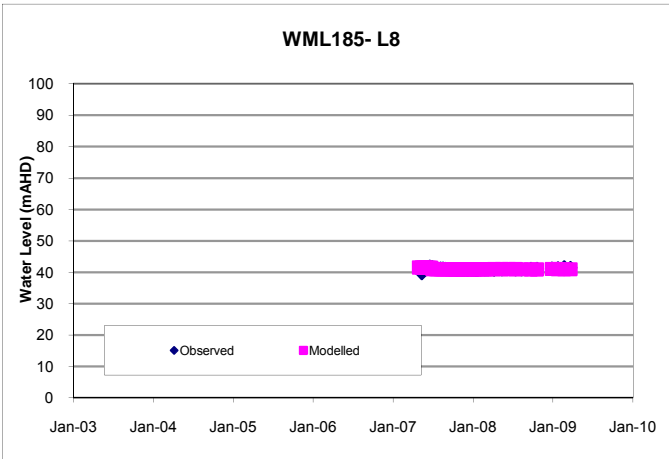
WML115A-120m - L7

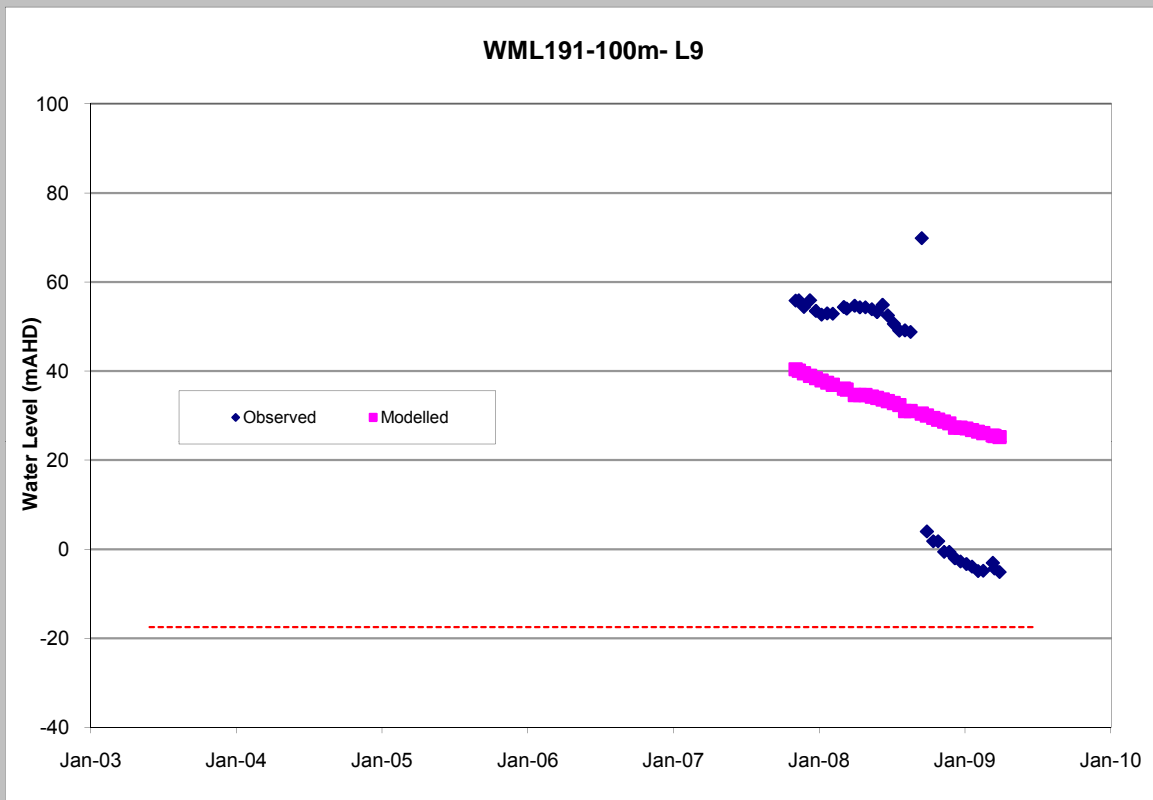


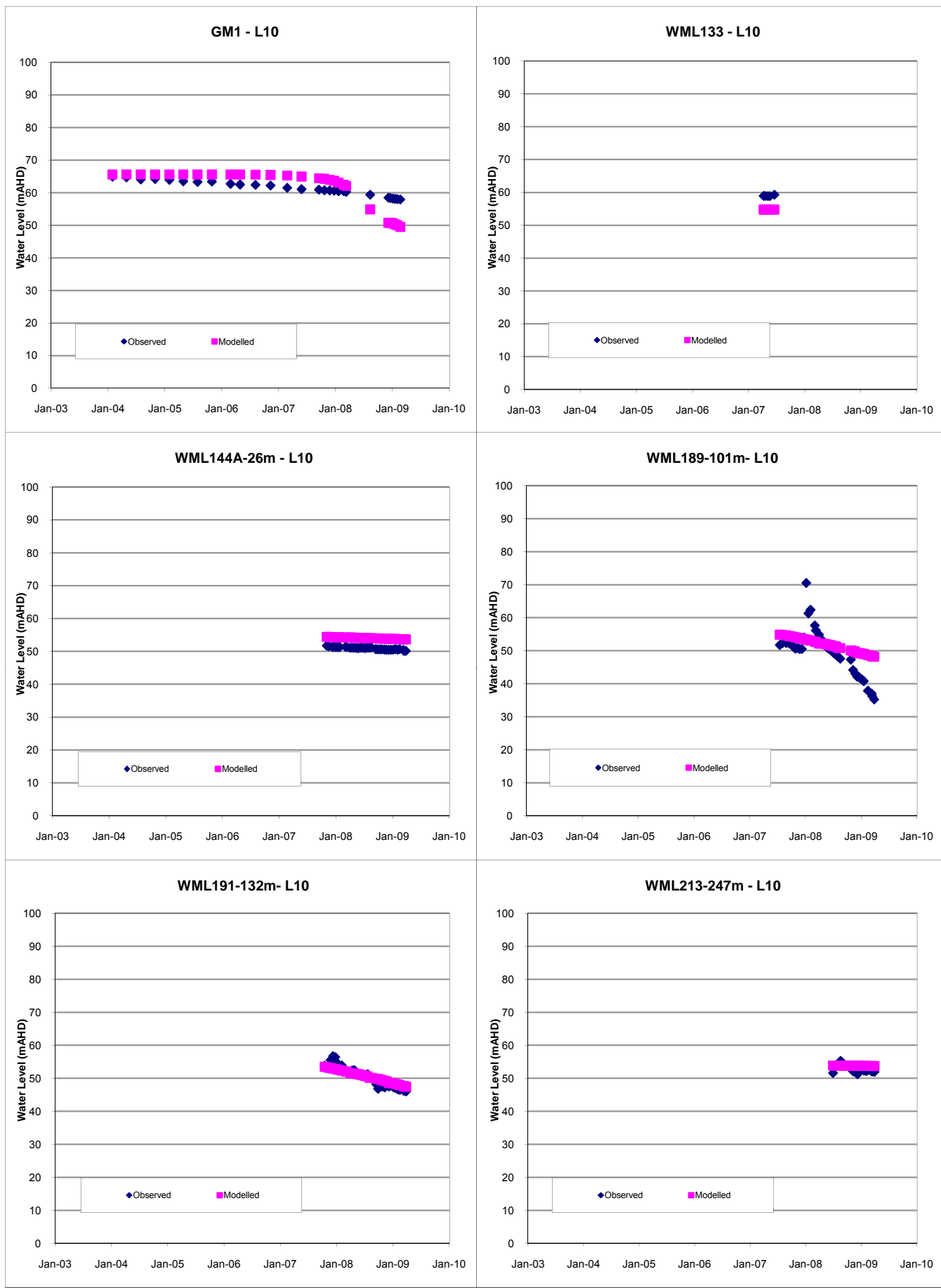
WML213-185.5m - L7



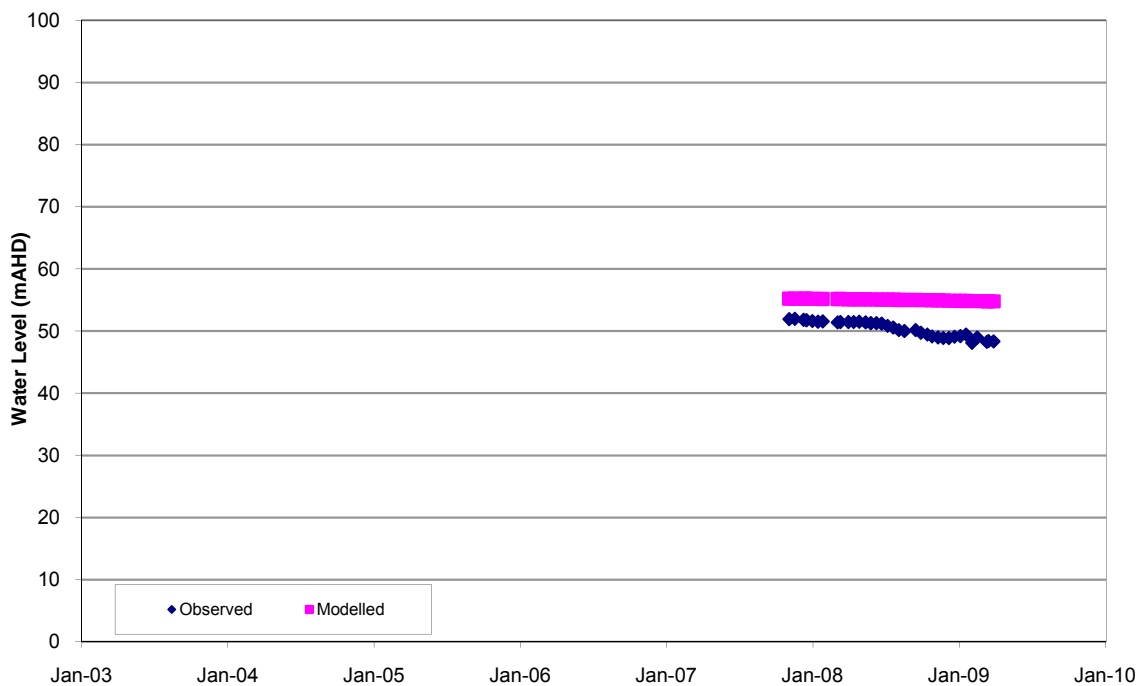




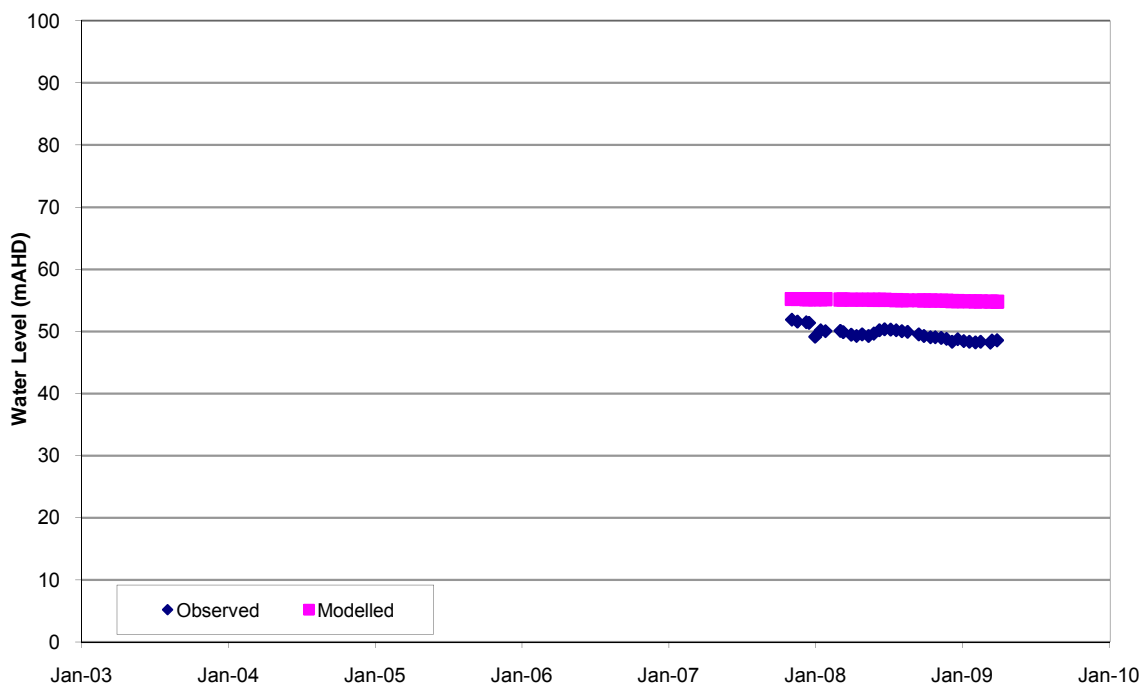




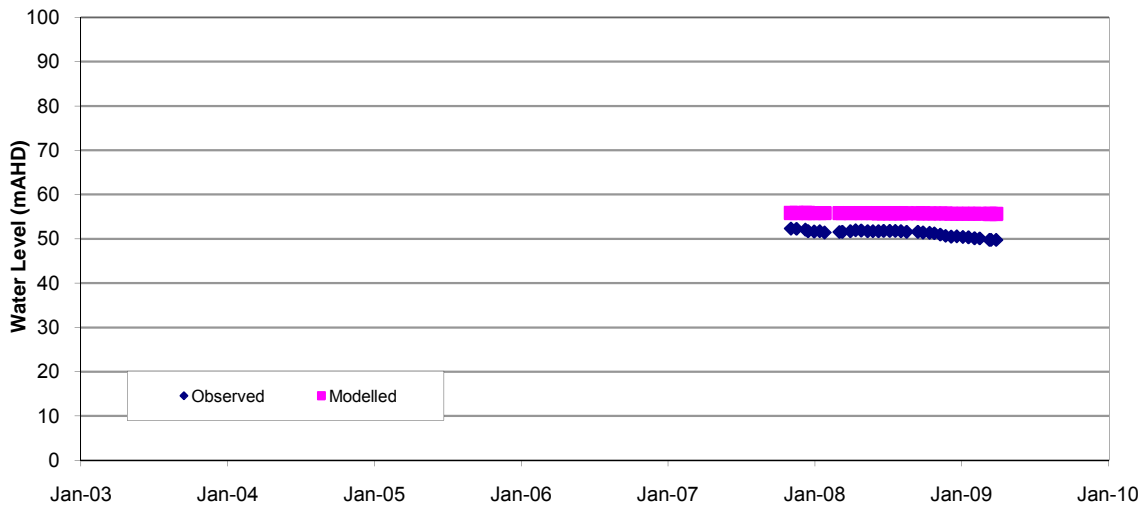
WML144A-32m - L11



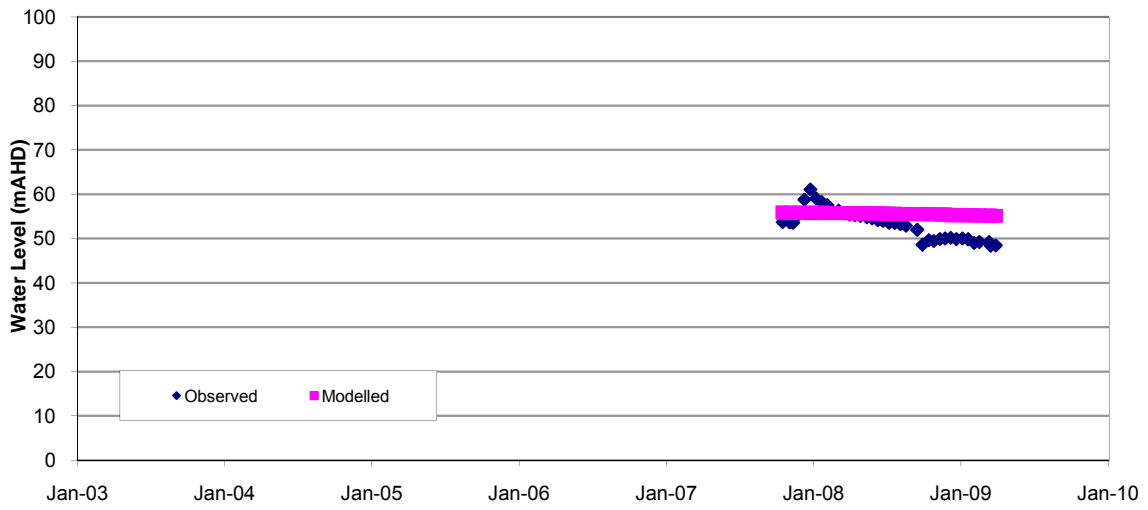
WML144A-45m - L11



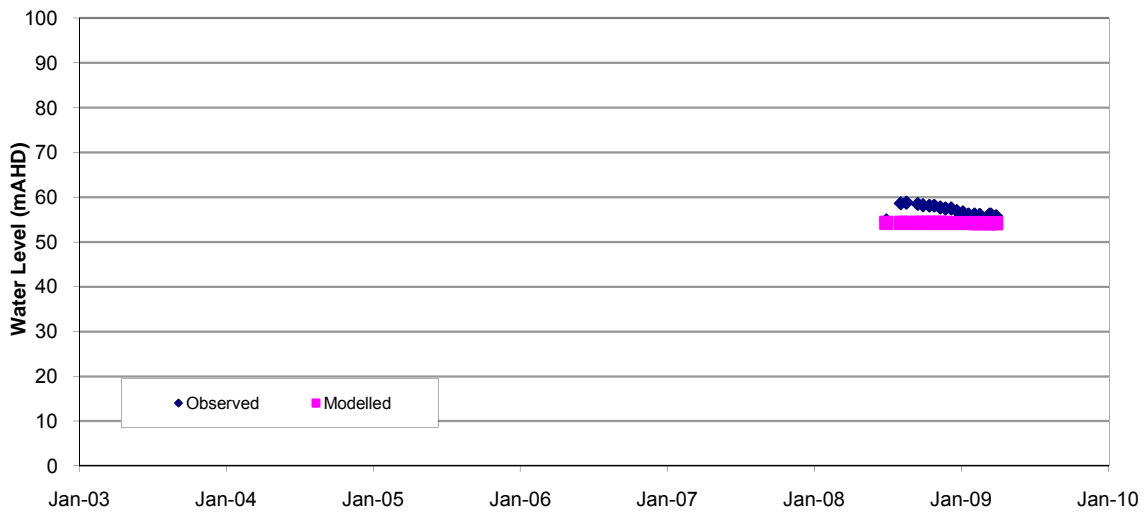
WML144A-50m - L12



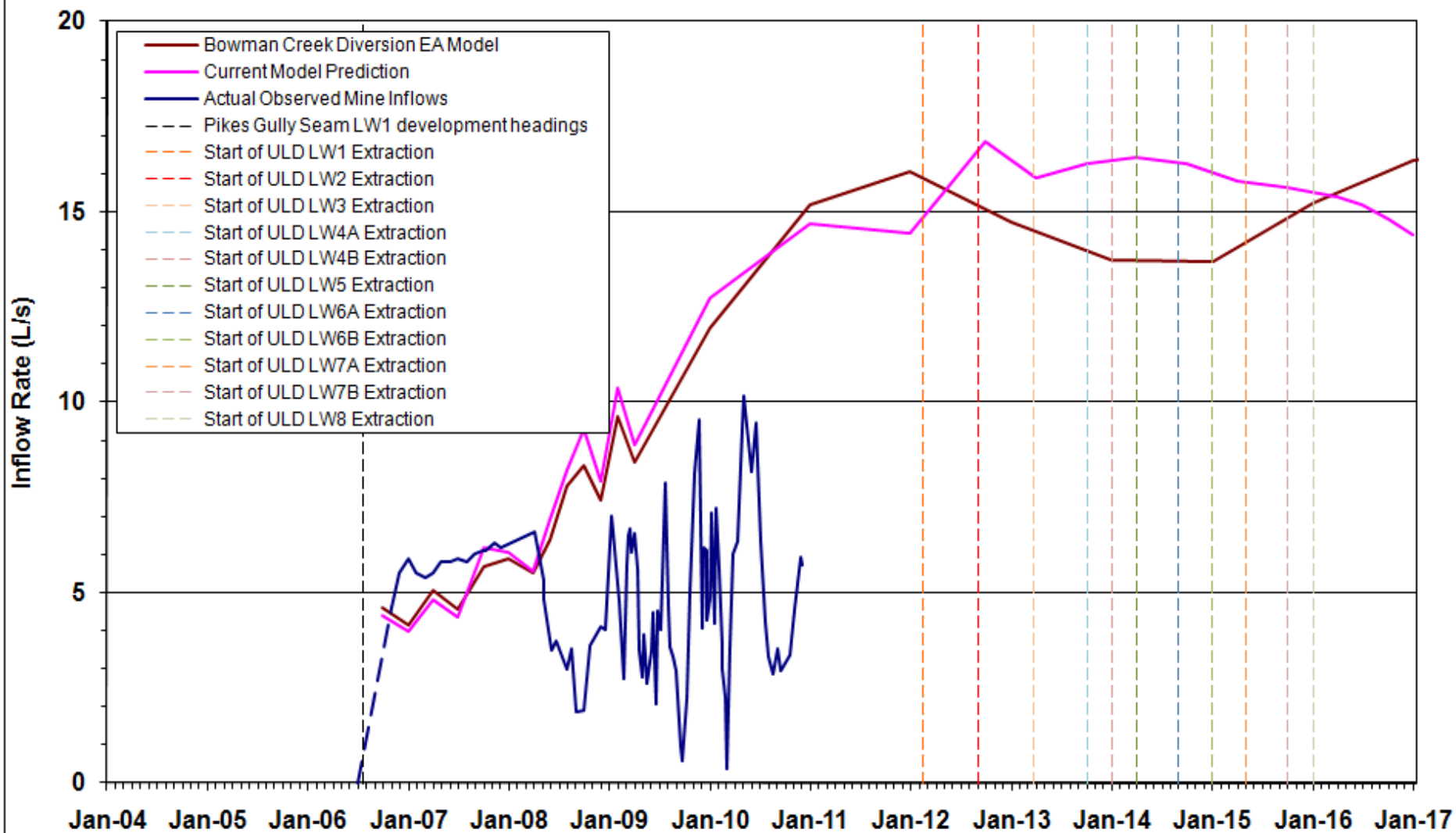
WML191-155m - L12



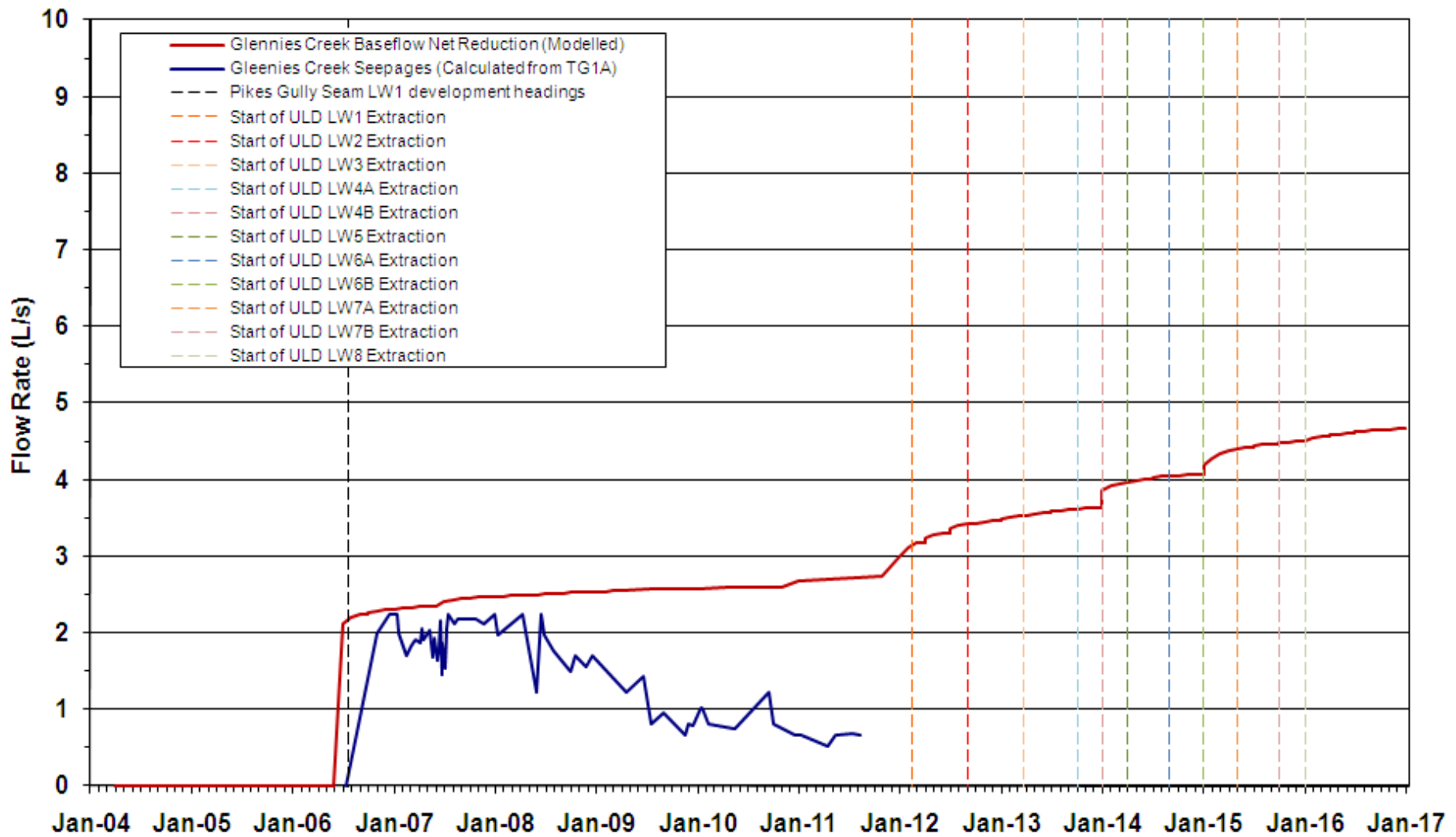
WML213-275m - L12



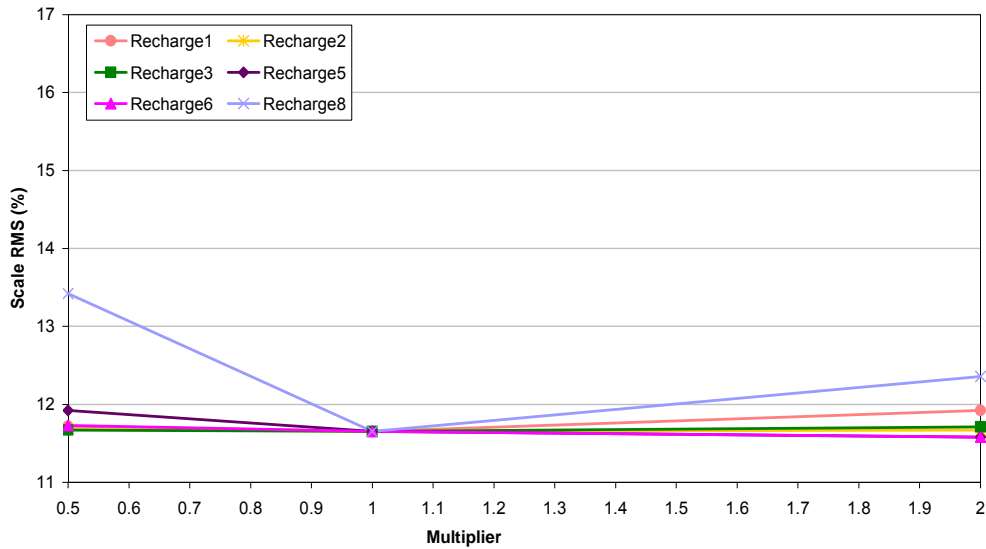
Total Underground Inflows



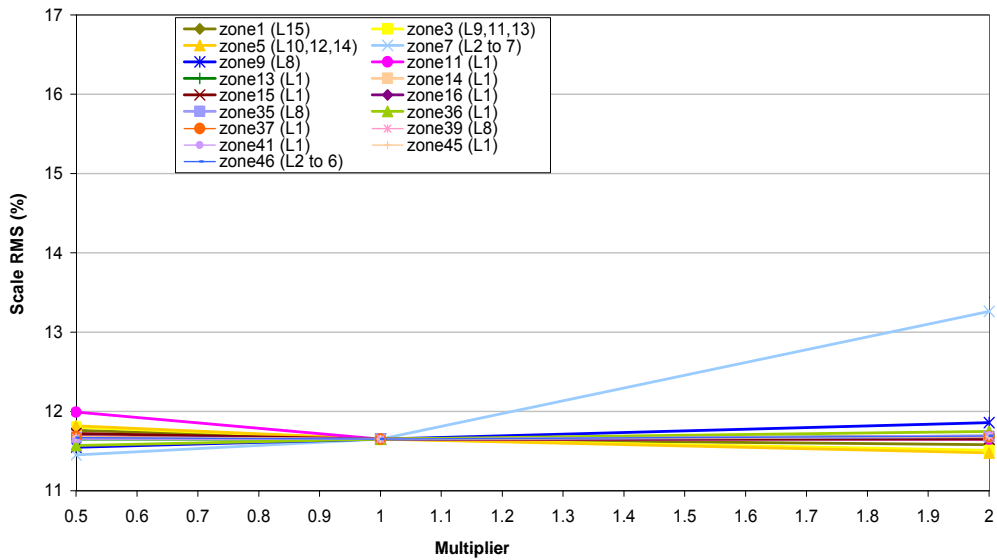
Seepage Losses from Glennies Creek



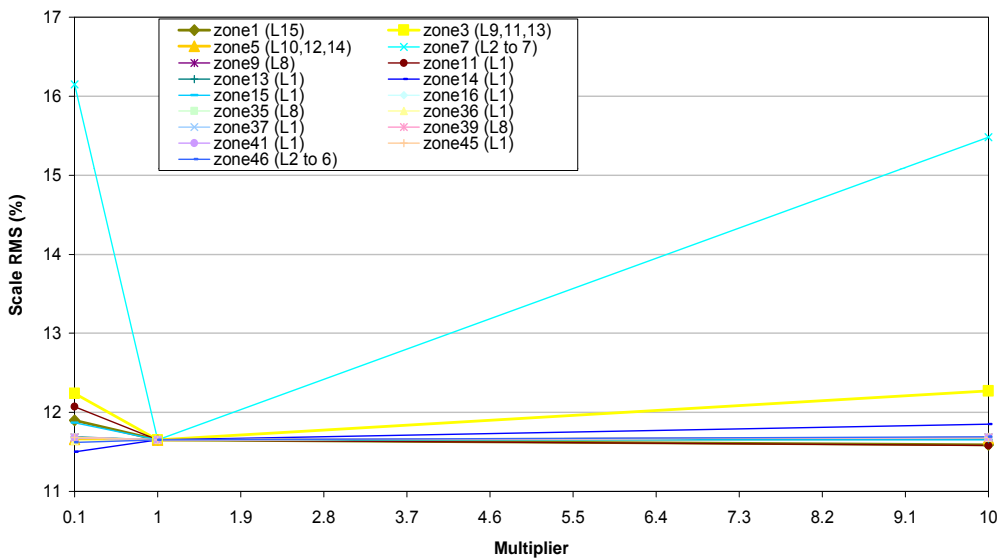
Sensitivity Analysis for Recharge



Sensitivity Analysis for Horizontal Conductivity



Sensitivity Analysis for Vertical Conductivity



Hunter River Baseflow / Recharge

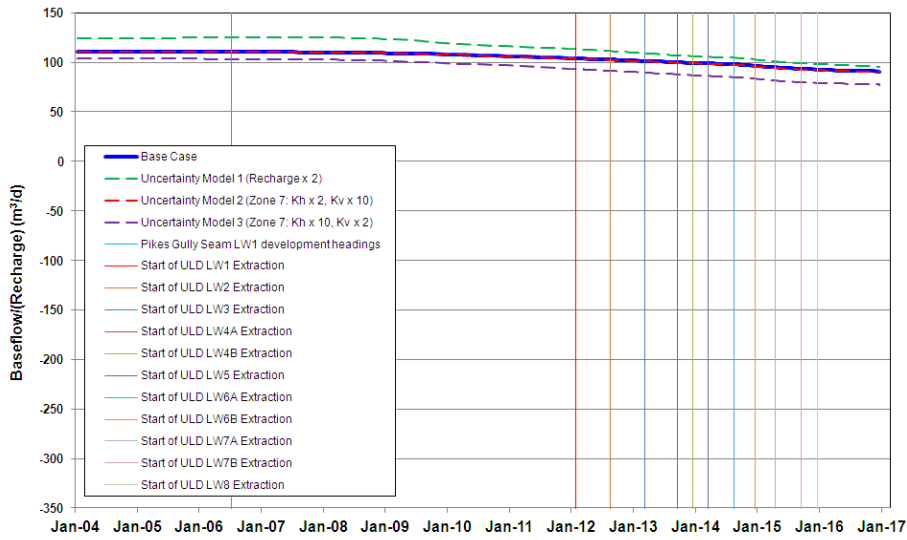


Figure 44a

Bowmans Creek Baseflow / Recharge

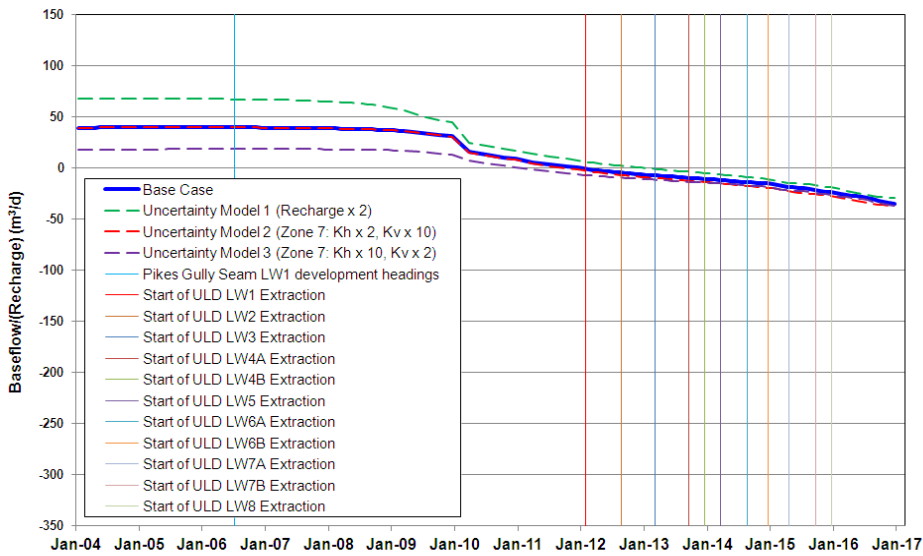


Figure 44b

Glennies Creek Baseflow / Recharge

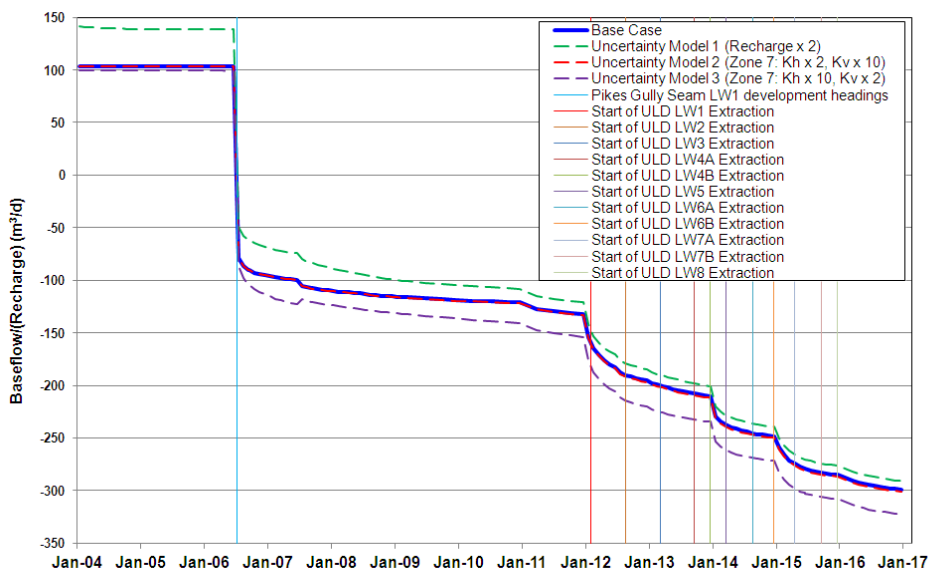


Figure 44c

Uncertainty Analysis Total Mine Inflow Rate

